Marine geomorphology study of post-glacial landscapes and the sea level implications; using multibeam bathymetry from Goletas Channel - Hardy Bay - Shusharti Bay, Northeast Vancouver Island, British Columbia, Canada

by

Byron James Molloy
B.Sc., Memorial University of Newfoundland, 2003

A Thesis Submitted in Partial Fulfillment
of the Requirements for the Degree of

MASTERS OF SCIENCE

in the School of Earth and Ocean Sciences

Marine geomorphology study of post-glacial landscapes and the sea level implications; using multibeam bathymetry from Goletas Channel - Hardy Bay - Shusharti Bay, Northeast Vancouver Island, British Columbia, Canada

by

Byron James Molloy
B.Sc., Memorial University of Newfoundland, 2003

Supervisory Committee

Dr. Vaughn Barrie, (School of Earth and Ocean Sciences, Geological Survey of Canada)
Supervisor

Dr. Vera Pospelova, (School of Earth and Ocean Sciences)
Member

Dr. Audrey Dallimore, (Royal Roads University, Geological Survey of Canada)
Additional Member

Supervisory Committee
Dr. Vaughn Barrie, (School of Earth and Ocean Sciences, Geological Survey of Canada)
Supervisor
Dr. Vera Pospelova, (School of Earth and Ocean Sciences)
Member
Dr. Audrey Dallimore, (Royal Roads University, Geological Survey of Canada)
Additional Member

Abstract

The submarine geomorphology of Goletas Channel - Hardy Bay - Shusharti Bay is a record of environmental change, defined by sediment deposition since the late Pleistocene draped over glacially sculpted physiography. Sea level change, contiguous with waning ice extent at the termination of the Fraser Glaciation, triggered an oceanographic transition within Goletas Channel from a low energy closed embayment to a higher energy open channel environment. Morphologic evidence of lower sea level position is observed from sequence stratigraphy in Hardy Bay and suggests regression to 74 m below present. Stratigraphy also shows a correlation between sea level transgression and turbidity current flows in northwest Goletas Channel, and although triggering mechanisms remain elusive, they are likely related to reworking of glacial sediments concomitant to initial open channel conditions. Holocene sediment accumulation has been highest in southeast Goletas Channel, represented by mud with interstitial gas, and has been reworked by tidal currents into contourite structures. A combination of high-resolution multibeam bathymetry, seismic and core samples are used to study the geomorphology of the region.

Table of Contents

List of Tables

List of Figures

Acknowledgments

I would like to thank my supervisors, Dr. Audrey Dallimore, Dr. Vaughn Barrie, and Dr. Vera Pospelova for giving me the opportunity to work on this project. My tenure at the University of Victoria has been very informative. For your generous feedback and patience, I am extremely grateful. Special thanks to the Kwakwaka'wakw (Kwakiutl) Nation for use of their traditional area for my research.

Many people have been a support network during this project. My family have been far away but close at heart, supporting my progress. Kind appreciation to Laura Sutherland for encouragement, and always believing this would be completed. Problem solving suggestions and constant comic relief was offered by students and alumni of University of Victoria. Intellectual contributions by Kim Conway, Dr. T. James and Dr. R. Thompson were extremely helpful. Thanks to Dave Spears, Greg Middleton, and Graham Standen for help with data collection and Dr. R. Hetherington for shell identification.

Special gratitude for funding contributions: Dr. A. Dallimore - NSERC Discovery Grant and Royal Roads University Internal Research and Scholarly Activity grants; Dr. V. Barrie - Geosciences for Ocean Management Program; Dr. S. Dallimore - GSC Gas Hydrates Program. In-kind contributions were vital for execution of this study, such as multibeam survey images provided by joint NRCan - CHS research cruises, and ship time collaboration provided by management of GSC - Pacific subdivision and executed by its helpful staff and DFO crews aboard the C.C.G.S. Vector.

Chapter 1 - Introduction

1.1 Overview

In this geomorphology study, general physiography and submarine sediment records are examined from Goletas Channel - Hardy Bay - Shusharti Bay, on the northeast coast of Vancouver Island, British Columbia, Canada (Figure 1.1). The study is set in Queen Charlotte Strait, in the constricted passages of Pacific Ocean waters between northern Vancouver Island and the Coast Mountains.

This geomorphology study examines three main landscape structures found within three respective locations: Goletas Channel, Hardy Bay, and Shusharti Bay (Figure 1.2). Goletas Channel is an elongate basin bound in the south by Vancouver Island and in the north by Hope Island and Nigel Island. The southeast portion of Goletas Channel opens into Queen Charlotte Strait. To the northwest, Goletas Channel is bounded by the shallow bathymetry of Cook Bank. It is considered the basin mouth in this study, marking the intersection between inner coast and less confined conditions of Queen Charlotte Sound waters. Hardy Bay and Shusharti Bay are submarine valleys forming part of the marginal coast between Goletas Channel and Vancouver Island, and provide additional information about glacial and post-glacial geomorphology of the coast from landforms identified within each.

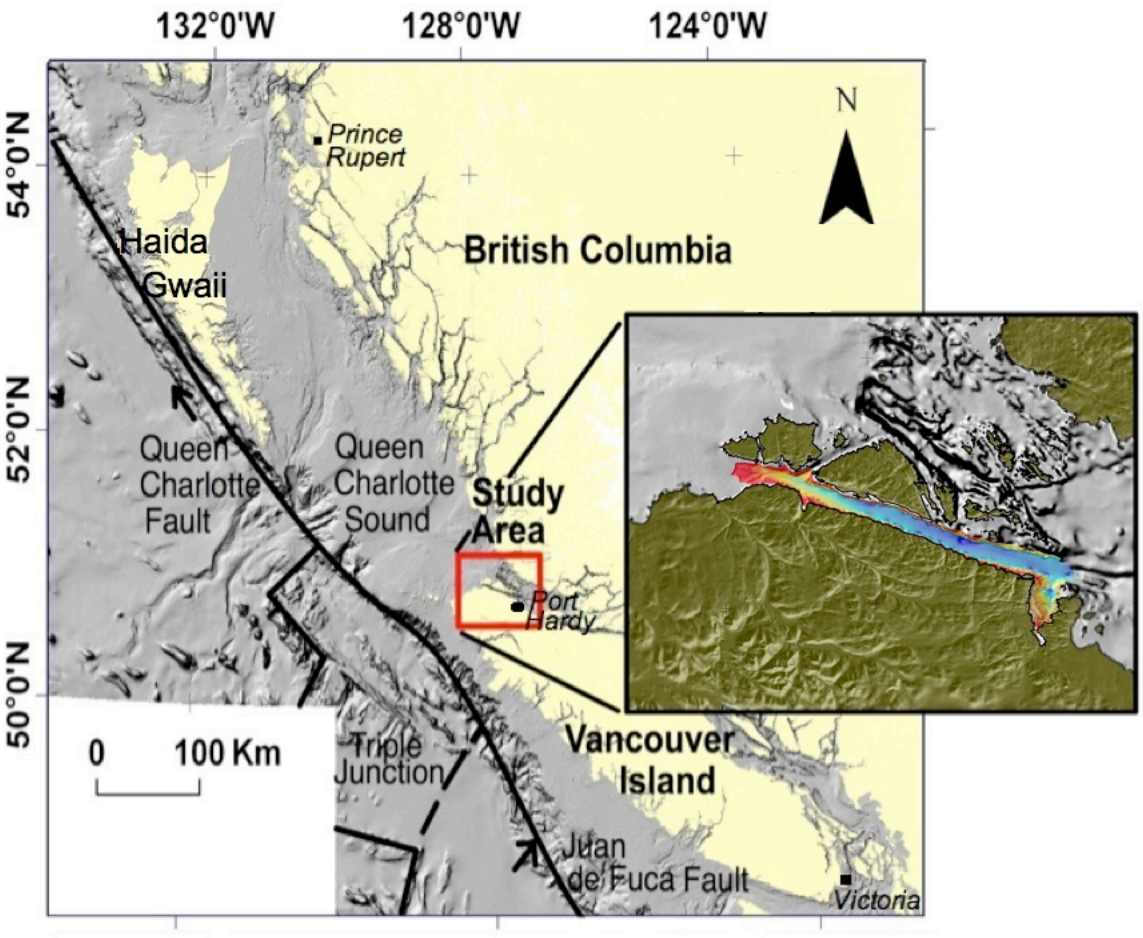

Figure 1.1 : Location of the study area in the Pacific Ocean between northeastern Vancouver Island and British Columbia mainland. Bathymetry is represented by grey shaded relief on map as well as color relief on inset box, which denotes the study area.

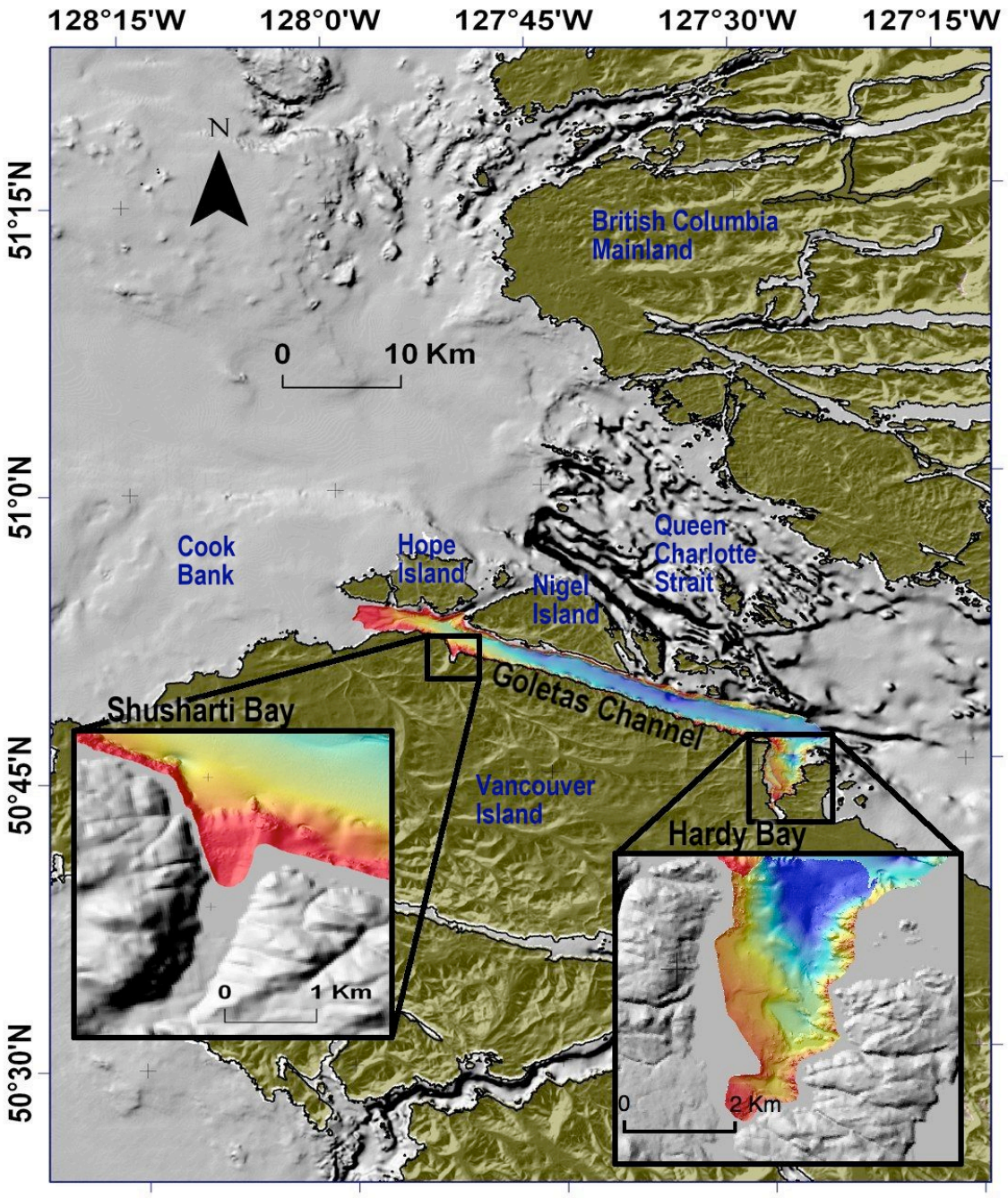

Figure 1.2 : Location map of Goletas Channel, Hardy Bay and Shusharti Bay on northern Vancouver Island. Bathymetry of the study area is shown in color shaded relief on the map.

The dominant physiographic features of the coast have largely resulted from plate tectonics, however cyclic glaciation has marred the Pacific Continental margin since Late Pliocene, resulting in submerged landscape structures such as fjords on the inner shelf (Shuster et al., 2005) and glacial troughs and banks on the outer shelf (Luternauer and Murray, 1983). Sediment records from the study region are dominantly constrained to deposition resulting from environmental changes since the last glacial cycle, referred to as the Fraser Glaciation (Luternauer et al., 1989b, Barrie and Conway, 2002).

Geomorphology is inferred from sedimentology, stratigraphy, and setting of marine landscapes and landforms within the study region. Previous studies of submarine sediment depositional sequences on other parts of the coast demonstrate environmental transitions since glacial retreat, represented by ice-contact to post-glacial sedimentation (Luternauer et al., 1989a, 1989b, Luternauer and Murray, 1983, Barrie and Conway, 2002) and are used as datum for analysing landform sedimentation within the study region.

By analysing geomorphology of each landform using high-resolution multibeam bathymetry, and by examining submarine sedimentation with respect to datum using Huntec seismic and piston core samples, we can infer possible mechanisms and timing of processes involved in the formation of each landform, contributing to knowledge of environmental change and sea level history on the central coast. Previous studies suggest a sea level transition on northern Vancouver Island exists between an area affected by pronounced glacial forebulge to an area where glacial forebulge is more subdued (Clague

et al., 1982). Relative to coastal regions of northern and southern British Columbia, there have been few geomorphology or sea level studies of central British Columbia and not enough data exists for a constrained sea level history curve.

This study is a marine geomorphology study, but it also has implications that reach further afield. Three direct implications of this study to other disciplines concern: 1) tectonic modeling, 2) resource sector hazard assessment and 3) archaeology. 1) The timing and elevation of sea level change allows quantification of total amount and rates of isostasy motion, both important parameters for crustal modelers in order to produce accurate depictions of crustal properties used to understand tectonic interactions for earthquake prediction. 2) Alternative energy initiatives in British Columbia implemented tidal current assessments near the boundary between northwest Goletas Channel and Cook Bank resulting in discovery of potential energy generation and may require geological hazard assessment in the near future. 3) In a previous study, important archaeological relics of ancient civilizations have been discovered near a relict subaerial shoreline in Hardy Bay (Bear Cove) dating back to 8,020 ^{14}C yrs BP (9000 Cal yrs BP), which is further than any other on Vancouver Island (Carlson, 1979). Constraining past sea level elevations is important to archaeological investigation, providing target information for archaeology sites occupied while lower sea level conditions existed that were subsequently inundated during sea level transgression in the late Pleistocene – early Holocene (e.g. Josenhans et al., 1995).

1.2 Thesis Outline

The approach for geomorphic analysis of Goletas Channel - Hardy Bay - Shusharti Bay involves identifying morphologic structures on multibeam imagery, deducing their properties using ground truth sampling methods, and creating conceptual models that explain genesis. This study is divided into four chapters in order to meet the aims of the research.

- Chapter 2 provides background information about processes that have impacted physiography of the study area, including tectonic setting, glaciation, sea-level changes, and modern oceanographic processes which have modified past sediments to produce a new suite of deposits and landforms.
- Chapter 3 explains methodology used for geological analysis, including multibeam bathymetry data, Huntec DTS seismic, and sediment samples from piston cores.
- Results are provided in Chapter 4 by characterizing observations from multibeam bathymetry data and describing lithology observed in Huntec DTS seismic profiles and sediment piston core samples.
- Chapter 5 is an interpretation and discussion of conceptual geomorphic processes involved in producing structures and stratigraphy identified in the data.
- Chapter 6 provides a list of conclusions that demonstrate the geomorphology of the study area.

Note that all age constraints come from background literature. Radiocarbon dates are referred to as "radiocarbon years before present" (^{14}C yrs BP), with the year 1950 used as a reference date. Where available calibrated dates are used, and referred to as calibrated years before present (Cal yrs BP). Further information on radiocarbon dating can be found in section 2.6.

Chapter 2– Background

2.1 Tectonic Setting

Tectonic assemblages and structural trends on northern Vancouver Island have formed along a northwest-southeast trending tectonic plate boundary within the western margin of the continental shelf. The region surrounding northern Vancouver Island is defined by three broad tectonic assemblages (Holland, 1964): the Insular Mountains of Haida Gwaii (previously named Queen Charlotte Islands) and Vancouver Island; the Coastal Trough in Hecate Strait (northern British Columbia), Queen Charlotte Sound (central British Columbia) and the Strait of Georgia (southern British Columbia); and the Coast Mountains of mainland British Columbia (Figure 2.1). The Insular Mountains developed on a convergent margin as Wrangellia, an island arc terrain, accreted to the North American plate in the late Paleozoic to Early Mesozoic, initiating formation of the Coast Mountains to the east (Jones and Silberling, 1977). A convergent plate boundary formed to the west of the amalgamated terrain, referred to as the Cascadia subduction zone, followed by mid-Tertiary transform fault development west of Haida Gwaii (refer to Figure 1.1 for fault locations).

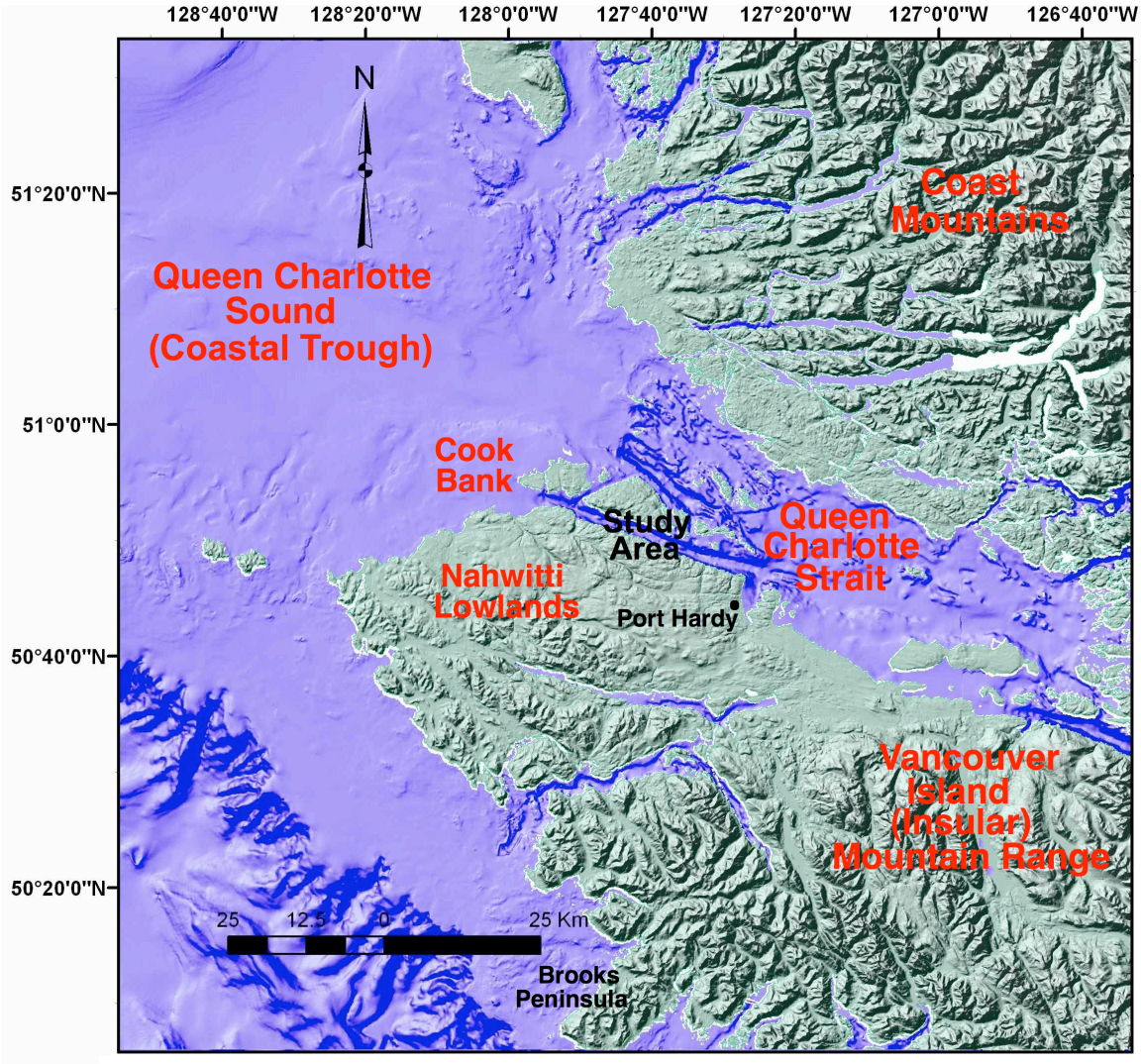

Figure 2.1 : Location map for the central coast of British Columbia.

Evolution of the continental shelf margin has resulted in a tectonic and structural transition located on northern Vancouver Island. The Queen Charlotte transform fault caused oblique extension and crustal thinning, accompanied by uplift and subsidence of fault blocks to the east. The effects of transtensional development are found within geology beneath Queen Charlotte Sound (Rohr and Currie, 1997), likely extending southeast as far as Brooks Peninsula (Lewis et al., 1997) (Figure 2.1). Fluck (2003) calculates crustal thickness based on magnetic anomalies, gravity and topography,

finding regional crustal thicknesses lessen from 30-40 km near Brooks Peninsula to 10-20 km in Queen Charlotte Basin, however this transition is not well defined. Structural grain on northern Vancouver Island has a northwest azimuth, produced by tectonics in the region. An example of this is seen in Goletas Channel where there is a geologic contact between the "Jurassic Island Intrusions", and "Vancouver and Bonanza Group", (Figure 2.2) which is mostly composed of volcanics (Armstrong et al., 1985).

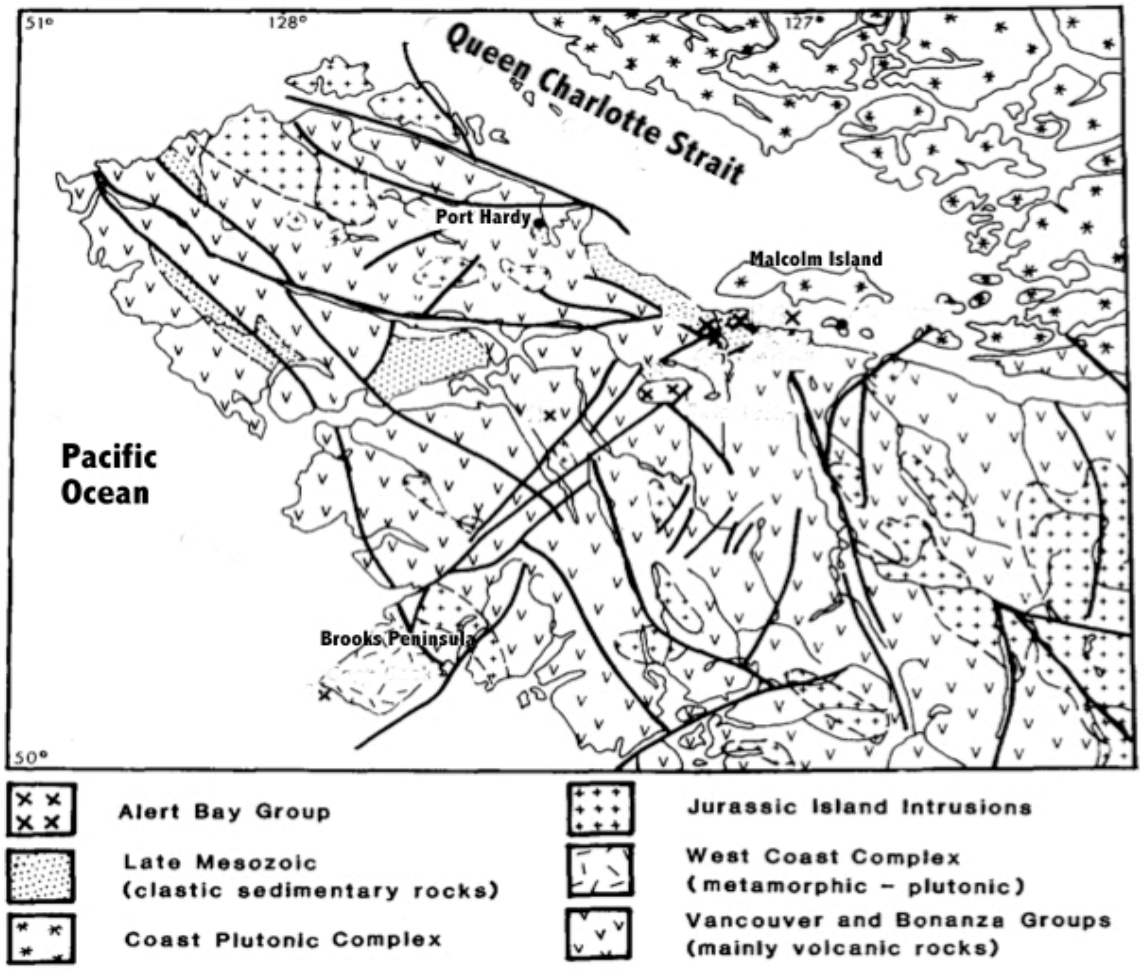

Figure 2.2 : Tectonic assemblages and structural trends oriented northwest and northeast on northern Vancouver Island and adjacent mainland (modified from Armstrong et al., 1985).

2.1.1 Earthquakes

Tectonic plate movements caused by subduction of the Juan de Fuca plate beneath the continental margin west of Vancouver Island in the Cascadia convergence zone, and transverse movements along the Queen Charlotte Fault located to the north result in earthquakes in British Columbia. Plates undergo cycles of locking and accumulation of strain causing most of Vancouver Island to experience vertical land motion with uplift in the range of ~ 4 mm/yr for northeast Vancouver Island (Thomson et al., 2008). Strain release from the subduction fault results in earthquake activity and rapid sea-level fluctuations in the range of 0.5 - 2 m (Thomson et al., 2008). The last great subduction earthquake happened in 1700, and there is 5-10% chance of another in the next 50 years (Mazzotti and Adams, 2004). The largest recorded earthquake happened along the transverse fault off Haida Gwaii in 1949 when an 8.1 magnitude event ruptured causing extensive damage.

There is no geological record of seismicity on northern Vancouver Island and major earthquakes have not been recorded since European settlement began in the late 18th century on the coast. Oral tradition by local native groups tell of tremors, flooding and subsidence on northern Vancouver Island in more ancient times (Ludwin et al., 2005), implying that the study area has not been seismically inactive.

2.2 Glacial progression

Since late Pliocene, glaciation of the Canadian Pacific Margin has introduced cycles of erosion and deposition to terrestrial and marine environments. Evidence of glaciation date back ~ 4 million years, preserved in volcanogenic flows on the British Columbia coast

(Souther et al., 1984), as well as indicated by deeply eroded landscape structure such as fjords and glacial troughs (Shuster et al., 2005; Luternauer et al., 1989b). However, stratigraphic evidence for reconstruction of glacial progression is possible for only the last major glaciation. The last main phase of glaciation is known as the Fraser Glaciation on the western Pacific Margin of Canada and correlates with the Wisconsinan Glaciation in eastern North America. Ice build up commenced in the late Pleistocene, about 29,000 ^{14}C yrs BP, and was largely completed by 11,500 ^{14}C yrs BP (Ryder et al., 1991). The Fraser glacial cycle was defined by Stumpf et al. (2000) as having three phases: *Ice Expansion, Ice Maximum* and *Late Glacial Phase* (retreat).

2.2.1 Ice Expansion

The Cordilleran Ice Sheet formed as merging mountain glaciers in British Columbia (Stumpf et al., 2000). Topography influenced its flow patterns and the Pacific Ocean provided sustenance for its growth and progression (Clague and James, 2002). The initial phase of glacial expansion began about 29,000 ^{14}C yrs BP (Ryder et al., 1991), which was marked by climate degradation related to the Fraser glaciation associated with cooler temperatures and increased precipitation (Clague and Bornhold, 1980; Clague and James, 2002). Ice flow proceeded from major ice centers in the high interior mountains of northern British Columbia. From these accumulation centers, extensive advance into valleys and fjords began sometime after 25,000 ^{14}C yrs BP (Clague, 1989; Stumpf et al., 2000).

Timing of initial glaciation on northern Vancouver Island was about 20,600 ^{14}C yrs BP, determined from terrestrial shell samples collected in silts deposited beneath glacial till

(Howes, 1981b). Ice on Vancouver Island was not extensive, and was likely isolated from the Coast Mountain glacial complexes, developing independently within the Vancouver Island Mountain Range (Howes, 1981b).

2.2.2 Ice Maximum

At maximum extent the Cordilleran ice sheet consisted of an interconnected system of mountain forming alpine and intermontane glaciers, and their converging lowland relative, piedmont glaciers. The ice sheet attained a minimum elevation of 2500m in interior British Columbia and covered much of the continental shelf (Stumpf et al., 2000).

In central British Columbia the Cordilleran Ice Sheet flowed westward from the mainland, across southern Queen Charlotte Strait and then toward the west and northwest (Dawson, 1886; Howes, 1997). Alpine and intermontane glaciers existed independently of the Cordilleran Ice sheet in Vancouver Island Mountain Range and coalesced as the ice sheet surged westward (Howes, 1997). Glacial striations on northern Vancouver Island indicate ice flowed northward and over Hope Island and Nigel Island (Dawson, 1886). Just south of Port Hardy, ice flow direction was toward the northwest, roughly parallel with the longitudinal axis of Goletas Channel.

At its maximum extent 15,000 ^{14}C yrs BP, the ice sheet had flowed northward out of Vancouver Island Mountains, extending over the islands northern limits (Howes, 1997). Ice thicknesses varied in the region and a possible localized refugium has been suggested on northern Vancouver Island. Ice possibly covered the entire northern lowland region and extended 5 km west onto the continental shelf from Brooks Peninsula (Howes, 1997).

2.2.3 Late Glacial Phase

The late glacial phase was a time of rapid glacial downwasting and retreat (Clague and James, 2002; Barrie and Conway, 2002). On northern Vancouver Island the Cordilleran ice sheet acted as a feeder system across Queen Charlotte Strait, rapid downwasting was initiated once sustenance was cut off (Howes, 1997). Vancouver Island was ice free earlier than parts of the Coastal Mountains where ice persisted until about 10,000 - 11,000 C^{14} yrs BP (Clague et al., 1982).

Dates of glacial retreat are similar for Queen Charlotte Sound and northern Vancouver Island, indicating rapid and widespread retreat. By 13,630 ^{14}C yrs BP (Hebda, 1983) ice had retreated from the Nahwitti Lowlands of northern Vancouver Island, a date obtained from initial organic growth (gyttja) on top glacial deposits near Bear Cove Bog, located adjacent Hardy Bay. In Queen Charlotte Sound ice was retreating between 13,630 ^{14}C yrs BP and 12,900 ^{14}C yrs BP (Luternauer et al., 1989b), dates obtained from shell samples in submarine sedimentation.

2.3 Marine Sedimentation

Commonalities between sediment sequences for a retreating ice margin have been studied and provide useful environmental datum for use in Goletas Channel. Syvitski (1991) defines five environments: Ice-contact, ice-proximal, ice-distal, paraglacial and post-glacial. In Queen Charlotte Sound, sediment deposition patterns during glacial retreat have been studied and ^{14}C dated (Luternauer et al., 1989b) and provide an analog for sequences from Goletas Channel in the absence of ^{14}C dates.

2.3.1 Ice-contact

Sediment that accumulates underneath the edge of an ice sheet (subglacial) and within close proximity of the edge is considered ice-contact (Eyles and Eyles, 1992). The primary facies found in the subglacial environment are till sheets and may be modified by glacial processes into various structures.

In Queen Charlotte Sound, ice contact phase is represented by a distribution of diamicton up to 50 m thick observed from seismostratigraphic investigations (Josenhans et al. 1995, Barrie and Conway, 2002). It is difficult to differentiate tills and massive diamicton facies from seismic alone, however the facies seen in Queen Charlotte Sound are considered associated with ice contact tills (Barrie and Conway, 2002).

2.3.2 Ice-proximal & Ice-distal

Ice-proximal environments are defined as direct sedimentation into the marine environment from the ice margin to several kilometers away (Eyles and Eyles, 1992). Diamicts of well-sorted and stratified gravel, sand and mud deposits, reflect the influence of strong meltwater flows from the ice-margin and increasing marine influence in contrast to ice-contact environment (Syvitski, 1991; Eyles and Eyles, 1992).

Sedimentation records of ice-distal environments occur on glacially influenced continental margins, characterized by glacimarine muds dispersed within several kilometers to several thousand kilometres of the glacier. The most dominant sedimentation is of extensive, blanket-like muddy sediment produced during settlement

of suspended plumes of mud that are released by melting icebergs (Eyles and Eyles, 1992).

In Queen Charlotte Sound, ice-proximal sediments are thin or absent, and overlain by up to 20 m of ice distal glaciomarine muds. The muds include equal parts, sand, silt and clay, as well as ice rafted debris and were deposited between 13,600 ^{14}C yrs BP and 12,900 ^{14}C yrs BP (Luternauer et al., 1989b; Barrie and Conway, 2002).

2.3.3 Paraglacial

Deposition in a paraglacial environment is caused by rapidly receding glacier margins and indicates a transition from glacial to fluvial environments. This episode is contiguous with recovery from isostatic loading, which is associated with sea level regression and, in response to high meltwater output, increased fluvial erosion (Syvitski, 1991). Larger sediment grain size and thick near shore successions are associated with higher yield river drainage during glacial retreat than at present. Buried channels, mass sediment gravity flow structures and hemipelagic deposits are commonly found in paraglacial sequences (Syvitski, 1991).

In Queen Charlotte Sound paraglacial sediment are represented by a stratified unit of sandy shelly mud deposited during a period of sea level regression and transgression, dating between 12,900 - 10,200 C^{14} yrs BP (Luternauer et al., 1989b). Thin interbedded sandy mud within this unit is interpreted as originating from submarine mass sediment transport caused by slope instability and exposure to a higher ocean energy regime during

sea level regression.

2.3.4 Post-glacial

The post-glacial environment is associated with establishment of modern marine conditions marking initiation of oceanography processes similar to today, referred to as beginning of the Holocene (Eyles and Eyles, 1992). An influx of organic rich muds associated with hemipelagic sedimentation drape the ocean floor while hydrodynamic processes, tectonic events, and biological disturbances cause reworking of sediments (Syvitski, 1991).

In Queen Charlotte Sound, an organic rich olive mud ranging from <1 m to >7 m thick overlies the ice-distal sediments, interpreted as being deposited in a post-glacial sedimentary environment (Luternauer et al., 1989b). The hemipelagic sediments mark initiation of post-glacial conditions ~ 9000 ^{14}C yrs BP in Queen Charlotte Sound (Luternauer et al., 1989b; Barrie, 1991).

2.4 Central British Columbia Sea Level Change

A combination of marine and terrestrial sedimentation studies from central British Columbia show trends in spatial variation of sea level change after glacial retreat, which have implications to environments of Goletas Channel. Complex variations were initially characterized by localized isostatic recovery from glacial loads, followed by a slower response resulting from eustasy and vertical displacement of the crust caused by plate tectonics. Also, some areas of the outer continental margin, including Queen Charlotte Sound and Cook Bank experienced glacial forebulge subsequent to isostatic recovery

(Clague et al., 1982; Luternauer et al., 1989a,b; Hetherington and Barrie, 2004; Hetherington et al., 2004).

2.4.1 Isostasy

The lithosphere and asthenosphere response to a glacial load, referred to as isostasy, contributed significantly to sea level change on the British Columbia coast during the last glacial cycle. Development of thick ice sheet complexes on the western Pacific Margin during the Fraser Glaciation resulted in localized examples of vertical subsidence of topography by over 200 m along the western margin of the Coast Mountains (Clague et al., 1982; Barrie and Conway, 2002). The magnitude of lithosphere and asthenosphere response depends on size and duration of the applied load as well as lithosphere and asthenosphere characteristics, such as local and regional rheology, thickness and flexural ridgidity (Turcott and Schubert, 1982).

Glacial forebulge is a lateral variation resulting from glacial isostasy. The effect is characterized by displacement of the underlying asthenosphere from the region of applied load and resulting in a glacial forebulge forming in adjacent landscapes, and notable for parts of British Columbia are relict sediment evidence of sea level regression (Clague et al., 1982). During glacial retreat, the glacial load diminishes causing forebulge collapse when the asthenosphere and lithosphere return to previous conditions (Ryder et al., 1991). The wavelength of forebulge is also dependant on lithosphere and asthenosphere characteristics, and can produce varying dynamics according to its properties (Turcott and Schubert, 1982).

2.4.2 Eustasy

Eustatic sea level change refers to ocean volume changes. During glacial episodes most eustatic change was caused by water transfer when large amounts of water were removed from the oceans and stored in the form of continental ice masses. Profiles representing sea level change since the last glacial maximum have been created by collecting data removed of vertical inaccuracies caused by isostasy and vertical plate tectonic motions producing a long-term global sea level curve such as the example in Figure 2.3 (Lambeck and Chappell, 2001; Stanley, 1995; IPCC, 2007).

The sea level curve exhibits greatest water volume changes during initial stages of continental ice melting in the late Pleistocene, then shows slower sea level changes during the Holocene. During the last glacial maximum global sea levels were about 121 m lower than present. By about 5 - 6 Cal yrs BP, the melting of the great high-latitude ice masses was essentially completed resulting in little eustatic sea level change thereafter (Fairbanks, 1989).

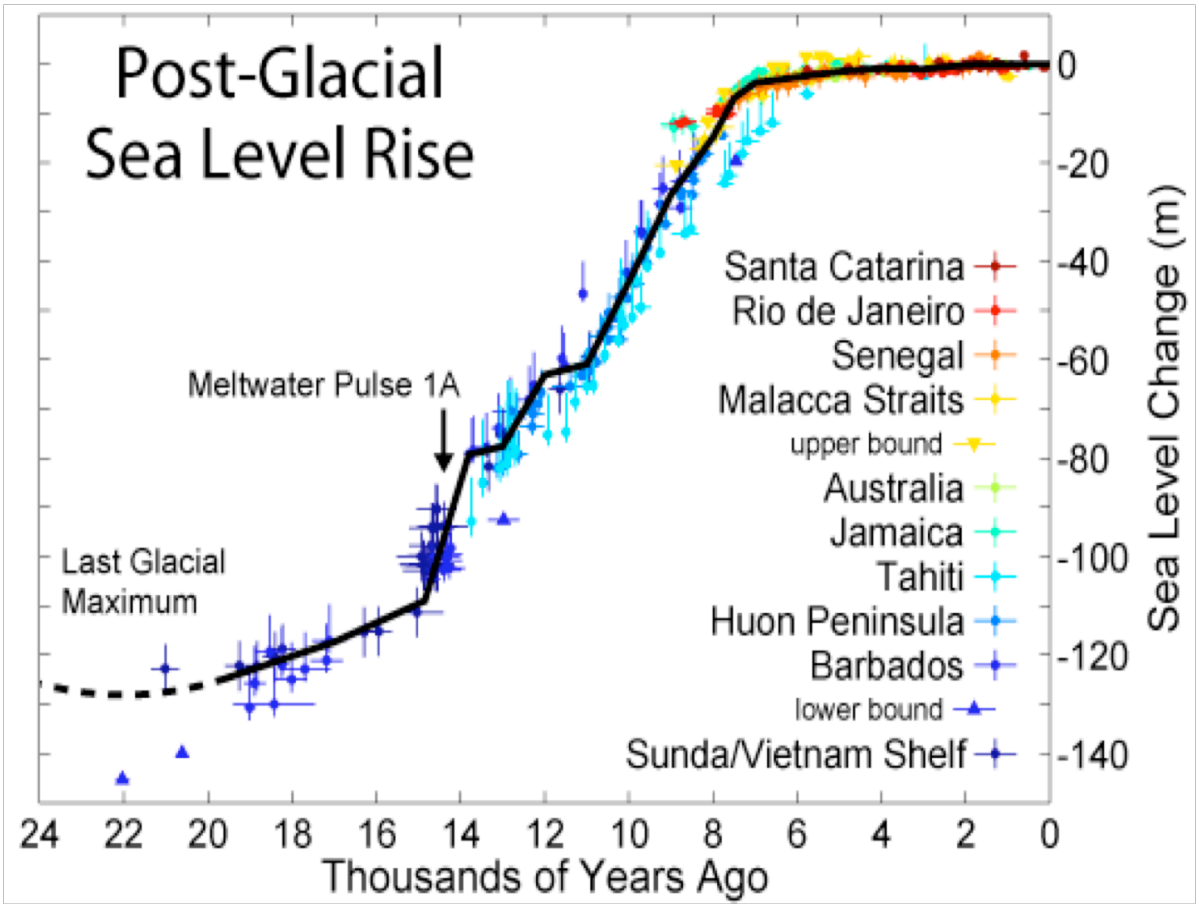

Figure 2.3 : Eustatic sea level data accumulated from multiple locations considered to have been in stable isostatic environments since last glacial maximum (IPCC, 2007).

2.4.3 Northwest Goletas Channel

Previous terrestrial and marine studies provide evidence for sea level change dynamics near the basin mouth in northwest Goletas Channel. Subsequent to glacial retreat, isostatic rebound of Cook Bank resulted in sea level regression 95 - 105 m below present (Luternauer et al., 1989a; Barrie, 1991). An in-situ wood sample from Cook Bank, taken ~ 20 km away from northwest Goletas Channel, corresponds with > 95 m sea level low stand ~ 10,500 ^{14}C yrs BP . Figure 2.4 exemplifies a possibly genetic relationship with synchronous sea level rise between Coast Mountains and Cook Bank, suggesting

forebulge collapse has contributed to vertical displacement during sea level rise to present (Luternauer et al., 1989a). As can be observed from the eustatic sea level curve in Figure 2.3, eustatic sea level has risen ~ 60 m since ~ 10,500 ^{14}C yrs BP, mostly before 7,500 ^{14}C yrs BP. About 40m of sea level change is unaccounted for by eustatic sea level rise, and was likely generated by lithosphere displacement during forebulge collapse. Also, plate tectonic processes may have resulted in a smaller contribution of vertical displacement in the area. Sea level fell ~ 3 m in the southeast portion of the study area since 8,020 ^{14}C yrs BP, suggesting sea level regression of 1 - 2 mm/yr during mid-late Holocene resulting from tectonic uplift (Howes, 1997).

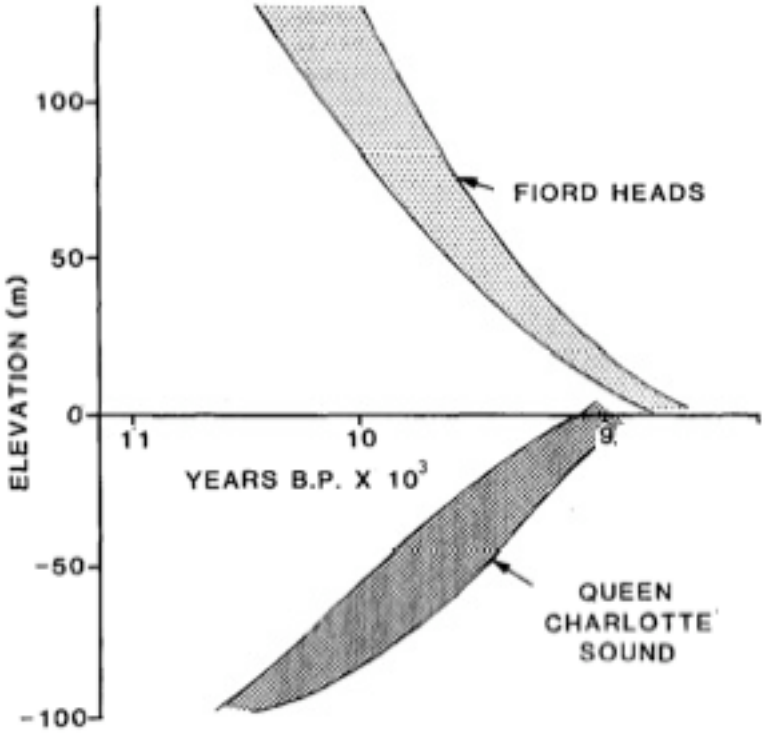

Figure 2.4 : Relative sea level curves of northern Vancouver Island and fjords from the east and northeast mainland coast of British Columbia (modified from Luternauer et al., 1989a).

A forebulge hinge line extending along the mainland coast has been suggested from previous research (i.e. McLaren, 2008), representing a zone between isostatically depressed inner coast and forebulged outer coast, however sea level models are poorly confined for the central mainland coast. Previous research shows a trend where relative sea level near fjord mouths regressed to near present elevations approximately 11,800 ^{14}C yrs BP (14,500 Cal yrs BP) (Galloway et al., 2007), which is a few thousand years before sea level regression near fjord heads. Also, evidence of a sea level regression to lower elevations than present, followed by a slower transgression to present about 7,500 ^{14}C yrs BP have been argued for the outer mainland coast (Andrews and Retherford, 1978; Cannon, 2000). A hinge line may have existed along the outer mainland coast of central British Columbia, however more data is needed in order to suggest its location. Figure 2.5 demonstrates the relationship between isostatically depressed Coast Mountains on the mainland coast concomitant with a dominant isostatic forebulge in Queen Charlotte Sound and Cook Bank. Note that the lateral extent of forebulge past Cook Bank to the southeast is poorly constrained.

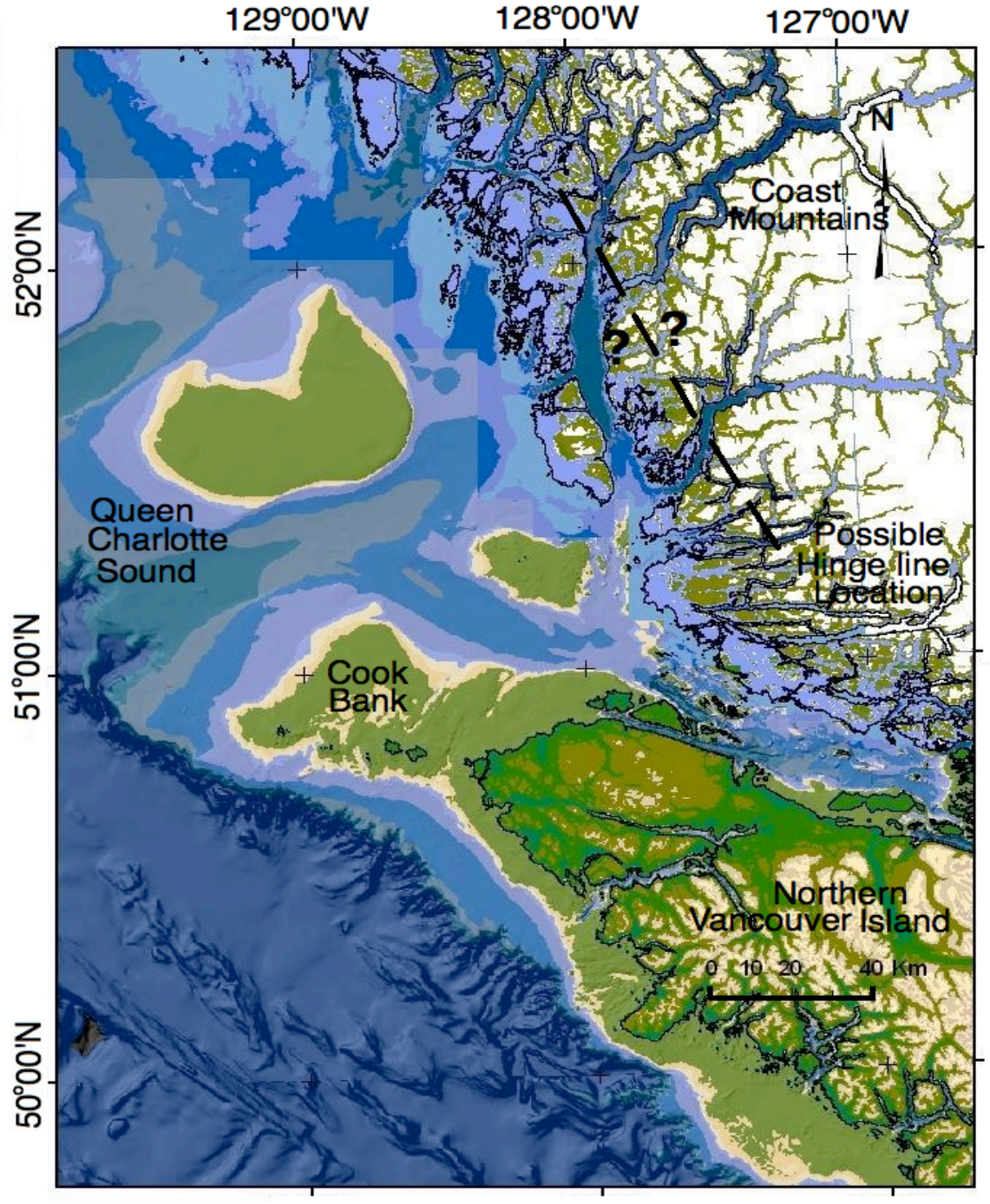

Figure 2.5 : Model of relationship between forebulged outer coast, including Queen Charlotte Sound and Cook Bank, and isostatically depressed mainland coast ~ 10,500 ^{14}C yrs BP.

2.4.4 Hardy Bay

Port Hardy, located adjacent Hardy Bay (Figure 2.1), has been previously studied for terrestrial evidence of sea level change. Glacier retreat prior to 13,630 ^{14}C yrs BP had induced isostatic suppression of landscapes, and resulted in relative sea level 30 m above modern sea level elevation (Hebda, 1983). Global eustatic sea level was ~ 80 m lower at the time (Figure 2.3), implying that the crust was isostatically depressed ~ 110 m.

Initial stages of isostatic rebound may have been very rapid near Port Hardy. Evidence shows most isostatic uplift occurs in < 2000 years in British Columbia, and possibly within a few hundred years, with rates commonly exceeding 10 cm/yr (Mathews et al., 1970; Clague et al., 1982, Clague and James, 2002). By 8,020 ^{14}C yrs BP (9,000 Cal yrs BP) sea level was 3 m above present on the shores of Port Hardy (Carlson, 1979) and was followed by slower sea level regression caused by tectonic uplift which continues today (Howes, 1997; Thomson et al., 2008).

2.5 Oceanography

Oceanography varies through the study region dependant on tidal energy interaction with physiography and vulnerability to wind-generated wave energy (Thomson, 1981). Tidal current measurements have not been made from Hardy Bay or Shusharti Bay, however the entrance to Hardy Bay and Shusharti Bay are both absent of barriers, which tend to amplify tidal current velocity, thus low velocity currents are thought to prevail in these areas (Thomson, R., personal communication, 2009). Physiography modifies tidal currents as a result of frictional dampening, landward constriction of the channel (convergence), and reflection from physiographic boundaries such as banks, shoals and long, narrow embayments.

Tidal currents are strong in northwest Goletas Channel in the location of a shallow constricted passage between Queen Charlotte Sound and Goletas Channel, referred to as the Nahwitti Bar. The Nahwitti Bar forms a bathymetric high at ~ 9 m water depth across the northeast boundary of Goletas Channel where currents average 5.5 m/s during ebb and flood tidal cycles (Triton Consultants Ltd., 2002).

Winds along the coast are dominantly southeasterly in the winter and northwesterly in the summer (Cherniawsky and Crawford, 1996). The influence of wind-generated wave energy in Goletas Channel is thought to be shallow and weak, losing energy because of destructive interference on cliffs along the narrow channel (Thomson, R., personal communication, 2009). Winds may be influential in northeast Goletas Channel where storm waves cross southward onto Cook Bank from Queen Charlotte Sound. Hardy Bay and Shusharti Bay experience minimal effects from wind-generated wave conditions because of the shelter from dominant wind directions.

2.6 Radiocarbon Dating

Radiocarbon dating methods were not implemented for samples recovered from Goletas Channel study area, however sediment records in previous research use radiocarbon dating extensively to constrain events. Formation of radioactive isotope Carbon-14 (^{14}C) occurs in the upper atmosphere when cosmic radiation forces neutrons out of atomic nuclei. Carbon, with six protons and six neutrons, capture two extra neutrons from nitrogen becoming ^{14}C, an isotope of carbon (Libby, 1946). They then proceed to mix throughout the troposphere and exchange with the reactive carbon reservoirs of the oceans and biosphere (Stuiver et al., 1986).

Throughout the troposphere carbon dioxide contains the same proportion of radioactive ^{14}C and stable isotope Carbon-12 (^{12}C). Plants use carbon dioxide from the atmosphere for photosynthesis. Animals eat plants or other animals, which ultimately eat plants. ^{14}C and ^{12}C exist in plants and animals in the same proportion as in the atmosphere, until they die. At which point radioactive ^{14}C begins to decay, losing its two neutrons and gassing off. This decay, or loss of energy, results in an atom of one type, called the parent nuclide transforming to an atom of a different type, called the daughter nuclide. The ^{14}C dating technique measures ratios of the isotope ^{14}C with respect to stable ^{12}C in order to date samples.

Any material that once lived can be measured for ^{14}C. Wood, wood fragments, gyttja, peat and shells have popularly been used for sea level reconstructions. ^{14}C decays with a half-life of 5,730 +/-40 years, and is practical when testing samples up to 50,000 years of age, thereafter very little carbon remains. Thus, the half-life of ^{14}C is beneficial to accuracy for dating carbon created during late Pleistocene until up to ~ 700 yrs before present, which is the upper limit of the technique.

The radiocarbon technique employed for quantitatively dating materials was initially based on the assumption of stability for ^{14}C and ^{12}C ratios in ocean and land reservoirs over time. For the past 11,000 years fluctuations in ^{14}C have been noted due to changes in the solar output (Stuiver and Quay, 1980). Also, carbon cycle changes tied to deep ocean circulation are a significant cause of atmospheric ^{14}C fluctuations (Stocker and Wright,

1996). In each case the ratio of ^{12}C to ^{14}C changes causing a discrepancy between radiocarbon dates and calendar dates. Radiocarbon measurements and a chronology of counted annual growth rings of overlapping dated trees have been compared and are used as a calibration curve to align dates up to nearly 12,000 yrs BP (Friedrich et al., 1999).

2.6.1 Reservoir Correction

In the ocean the issue of ^{14}C dating accuracy is compounded. Calibration of dates from shell samples must be corrected for the difference in ^{14}C activity between ocean surface water and the atmosphere. There are two main interactions that combine to deplete ^{14}C in ocean waters (Robinson and Thompson, 1981). First, ocean mixing is not as rapid or effective at the ocean-atmosphere boundary as in the atmosphere, taking an average of 400 years to mix. Secondly, on a localized coastal scale carbon upwelling varies, and when this old water mixes it causes regional contrasts in water ages in comparison with global ocean water ages on the scale of a couple hundred years. Thus, ages vary by location, in response to upwelling and mixing of ocean waters. For example, nine samples taken from a 3 cm interval within a core sample from Effingham Inlet on the outer coast of Vancouver Island have a scattered age range of 3,650 years in a result that should have shown nearly contemporaneous deposition (Dallimore et al., 2008).

The depleted ^{14}C in water is transferred to marine organisms. Similar to dendrochronological calibration of terrestrial radiocarbon dates, ocean samples are calibrated by comparison to terrestrial organics found in the same stratigraphic unit. In vicinity of Queen Charlotte Strait the nearest regional reservoir correction value

calculated is 950+/-50 years from southwestern British Columbia (Hutchinson et al., 2004b). Shell ages from northern Vancouver Island may be inaccurate by up to a thousand years for uncalibrated dates depending on upwelling and ocean mixing in the area.

Chapter 3- Methodology

The study location of Goletas Channel - Hardy Bay - Shusharti Bay was chosen based on initial qualitative analysis of bathymetry maps in search of potential sea level terraces. Most potential terraces, defined by a linear shelf and shelf break profile, were noticed in harbors along the coast of Vancouver Island. From the in-stock multibeam at NRCan, five unstudied potential sea level terraces were observed, however none were in locations where Huntec seismic data or sediment piston cores had been previously collected. Goletas Channel offered the best potential for a geomorphology study for a number of reasons: 1) Two potential marine terraces were discovered in close vicinity along harbors flanking Goletas Channel, an area with continuous multibeam bathymetry coverage; 2) Our research team planned to be nearby Goletas Channel in the fall of 2007 and summer of 2009 with all necessary equipment aboard the ship for Huntec seismic and sediment piston core collection; 3) A number of other marine landforms were noticed from multibeam bathymetry of Goletas Channel and provided supplementary information for a more thorough geomorphology investigation.

It should be noted that an initial attempt to focus on collecting subaerial sea level data was discontinued because of logistics. Data collection for the endeavor was attempted by way of scheduling land party excusions during on-going ocean research within the mainland fjords of central British Columbia. Because of time constraints and difficulties of bushwacking through uncharted forest only a few data points were attempted. After much consideration, this marine geomorphology study of Goletas Channel was proposed.

3.1 Multibeam bathymetric mapping

Multibeam imagery is utilized in this geological analysis for identification of morphologic seafloor structures. Detail can be examined from large contiguous regions of the seafloor in the range of 1 - 3 m using this method, which is beneficial for ascertaining spatial relationships between structures. The study uses multibeam bathymetric mapping data collected in 2006 and 2008 aboard the Canadian Coast Guard Ship (CCGS) Vector and CCGS Otter Bay. The data was collected during collaborative research cruises between Canadian Hydrographic Survey (CHS) and the Natural Resources Canada (NRCan) in pursuit of complete seafloor coverage of the Strait of Georgia and parts of Queen Charlotte Sound.

Surveys were undertaken from the CCGS Otter Bay for shallow water depths <50 m in Hardy Bay, using a hull-mounted Kongsberg-Simrad EM3002 system, which operates at a frequency of 300 kHz utilizing 121 - 135 beams and from the CCGS Vector in water depths >50 m, using a hull mounted Kongsberg-Simrad EM1002 system operating at a frequency of 95 kHz with 127 beams. Using hull-mounted transducers cone-shaped swaths of acoustic beams are projected perpendicular to the vessel direction and toward the seabed. Reflected swaths are collected with a receiver array, recording two-way travel time from the seafloor. Using sound velocity in water the collected data can then be converted to water depth to create a bathymetry map. Scientists orient cruise track lines with 100% swath overlap for complete coverage of the seafloor. Appropriate survey speeds are in the range of 6 knots or less.

Multibeam images are displayed with a cell size of 5 m, which is above spatial accuracy limitations. The range of vertical error is approximately 1% of water depth. Sound velocity of the ocean is measured every 30 - 60 minutes to reduce error by ensuring the path of each acoustic beam is measured correctly. Location is determined using Differential Global Positioning System (DGPS). Data are adjusted for tidal variations using tide prediction charts from the Canadian Hydrographic Service. Any erroneous information can be filtered in real-time during the acquisition process.

3.1.1 Multibeam Classification

A geomorphological classification system for high resolution multibeam imagery is in the beginning stages of development. Currently, consistent genetic terminology is lacking for marine geological classification. The simple classification system used in this study is adapted from NiN classification (Thorsnes et al., 2009), comprising “landscapes” and “landforms” based on morphologic elements that define them. Using this system landscapes and landforms are defined within terminology limitations.

Morphology elements that make up “landscapes” combine to describe the entire study area and do not overlap. They have a characteristic distribution of morphologic elements that describe basic geometrical attributes. For example, a study area may contain “landscapes” such as a fjord and glacial trough, and can be discriminated from each other by morphological elements that describe their properties.

“Landforms” can be in multiple “landscapes”, and overlap each other. They are of any

size smaller than the landscape they are confined and are also defined by morphology elements. For example: the shelf, shelf break, and slope make up morphologic elements that define a terrace in a landform category.

3.2 Seismic

During the fall of 2007 and summer of 2009 (cruise #'s -PGC2007007, PGC2009003), during collaborative research between NRCan-DFO-NSERC, seismic surveys were conducted to gather information of subsurface morphologies for better understanding of landforms observed in high-resolution multibeam bathymetry imagery. To carry out these studies a Huntec Deep-Tow Seismic (HDTS) system was used aboard the CCGS Vector to characterize sub-bottom geological properties.

The HDTS system is a high resolution seismic profiling system intended for use in water depths generally found on continental shelves and margins. It is designed to collect high-resolution acoustic data with vertical resolution of 10-30 cm with as much as 50 m sub-bottom penetration (McKeown, 1975). The electronics for the transmitting and receiving systems are mounted within the body of a towed 'fish' (Figure 3.1), which can be towed behind a surface vessel at depths from 6 - 160 m, at speeds up to 8 knots. The HDTS system generates energy from .5 kHz, for better penetration, to 6.5 kHz, for the high-resolution required in most surficial geological profiling.

Figure 3.1 : A deep-tow Huntec seismic system as it goes in the water in preparation for surveying. Picture taken aboard the CCGS Vector (November, 2007).

The HDTS system uses an electro-dynamic plate, often referred to as a 'boomer', to generate an acoustic pulse, a receiver consisting of an internal hydrophone mounted within the body of the 'fish', and an external hydrophone streamer towed behind it (McKeown, 1975). A sequence of transmitted acoustic waves penetrate the seafloor, partially reflect off subsurface acoustic boundaries and are collected by the towed hydrophone. The amount of reflection across a boundary is proportional to acoustic impedance contrasts, which is a product of sonic velocity and density. Collected acoustic information, organized into reflection profiles, indicate acoustic boundaries defined by materials with contrasting acoustic impedance. Certain reflection configurations correlate with distinct rock types, which is useful for geologic evaluations. The electro-dynamic 'boomer' has the advantage of high peak frequencies and large bandwidths, which are

sought from relatively low energy sources for high-resolution geophysics (Mosher and Simpkin, 1999). Though high frequency sound incurs greater energy losses with depth, it has higher resolution in small impedance contrast sediment stratigraphy than when a low frequency source is applied.

3.2.1 Seismic Classification

Seismic facies are generally classified based on reflection configuration, including amplitude, frequency and continuity (Stoker et al., 1997). The expected response for a glacial sedimentation sequence is shown in Table 3.1.

Table 3.1 : Character of seismic reflection in a glacial sequence (modified from Shipp et al., 1991).

Unit	Reflection Intensity	Reflection Geometry	Interpreted Lithology
Mud	Very Subdued	Few internal reflections	Modern marine mud
Natural Gas	Intermediate	Convex-upward turbid signature, acoustic wipeout below	Natural gas in sediments
Sand & Gravel	Intense	Conformable (draped) to Ponded	Paraglacial sand and gravel
Glacio-Marine	Subdued to Intense	Conformable (draped) to ponded	Glaciomarine mud, some sand
Diamict	Intense	Massive unit, turbid signature	Glacial diamicton
Bedrock	Very intense	Few internal reflections, turbid signature is common	Crystalline bedrock

The reflection amplitude is determined by acoustic impedance contrast between strata and described as low, medium or high. Lateral changes in amplitude may also provide facies information, however interference effects may also cause changes. Reflection frequency within facies is dependant on bed thickness and described as broad, moderate

or narrow. Vertical thickness variations help identify sequence boundaries, lateral changes provide facies continuity information. All depths on seismic profiles in Chapter 4 (Results) are estimates based on seismic velocity through water saturated sand, using a seismic wave velocity of 1500m/s (Keary and Brooks, 1991).

Geometry of seismic facies sequences provide information on depositional environments, sediment sources and geological setting, (Stoker et al., 1997). Examples of sequence patterns are shown in Figure 3.2 and some important definitions are provided below.

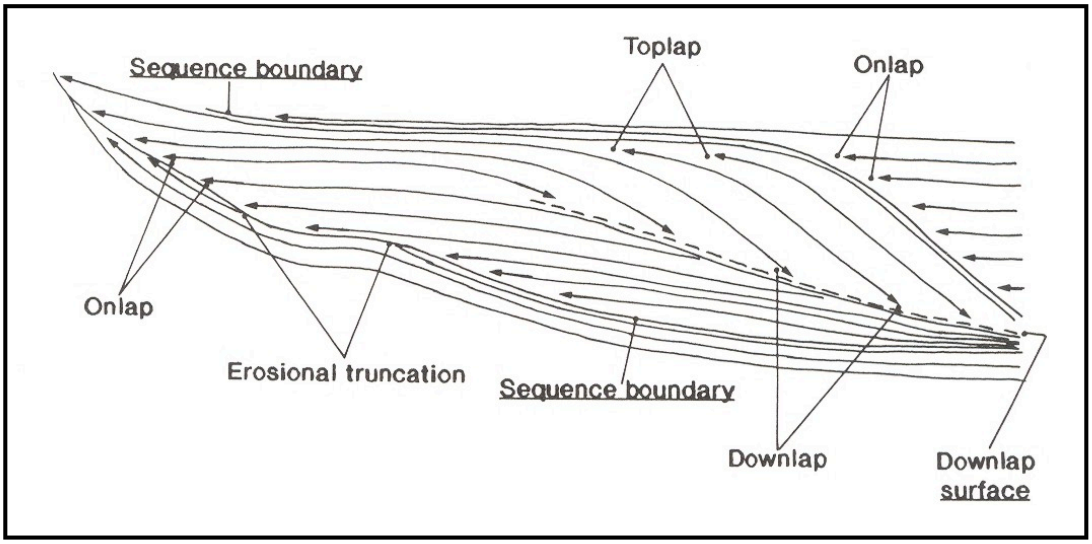

Figure 3.2 : Examples of sedimentation sequence patterns often seen in seismic reflection profiles (from Stoker et al., 1997).

Onlap - the successive deposition of stratal packages toward the shoreline, often progressively covering an erosional surface. Onlap occurs during transgression as depositional environments backstep shoreward.

Downlap - the successive depositon of stratal packages over underlying strata toward the basin center. This is generally a progradational pattern, occurring during relative sea level fall as sediment packages build farther out into the basin.

Toplap - the pattern made by the deposition of a horizontal strong reflector above a succession of downlapped or inclined packages of strata.

Erosional truncation and unconformities - these do not create reflectors themselves, rather, they are revealed by reflector terminations. Generally, some angular discordance is needed between the reflectors and the unconformity for the unconformity to be resolved. Minor episodes of erosion and unconformity generation may not show up on a seismic profile unless the relief of erosion exceeds the resolution depth of seismic imaging.

Continuous reflectors - suggest sedimentary strata deposited in a relatively stable environment that changes periodically through time.

Discontinuous reflectors - suggest sedimentary strata deposited in regionally heterogeneous environments.

Turbid reflectors – produced by scattering of acoustic energy, and may be related to crystalline rock, interstitial gas, or poorly sorted sedimentation such as diamict or till.

3.3 Grab Sample

Grab samples were collected during this study for an initial evaluation of seafloor bottom sediment composition before piston coring. This practice reduces the hazard of piston coring into an impenetrable surface and causing damage to equipment on the coring assembly. In this study a Petersen grab sampler (Figure 3.3) was used. This sampler is

about 70 lbs, consisting of a set of jaws that are locked by way of a lever system that releases under its own weight after settling on the ocean floor. Equipment set up involves attachment of sampler to a cable spool, cocking the jaws of the grab sampler and leveraging the assembly over the side. The sampling method can be performed in approximately 30 minutes, depending on water depth.

Figure 3.3 : Petersen Grab sampler operates on a lever system whereby the jaws release under its own weight and close upon sediments on the seafloor.

3.4 Marine Piston Coring

During the fall of 2007 and summer of 2009 (cruise #'s -PGC2007007, PGC2009003), during collaborative research between NRCan-DFO-NSERC, marine piston core samples were collected to gather information of subsurface morphologies for better understanding of sedimentation comprising landforms observed in high-resolution multibeam imagery and facies observed seismic profiles. To carry out these studies samples were attained

aboard the CCGS Vector and brought back to the GSC-Pacific at the Institute of Ocean Science in Sidney, British Columbia for analysis.

Sediment sampling with the piston corer involves assembly and operation aboard the ship. The piston corer is configured so that the pilot gravity corer hangs in the water below the piston corer. The pilot gravity corer and piston corer are connected to the trip arm assembly (Figure 3.). There are extra loops of cable attached between the trip arm

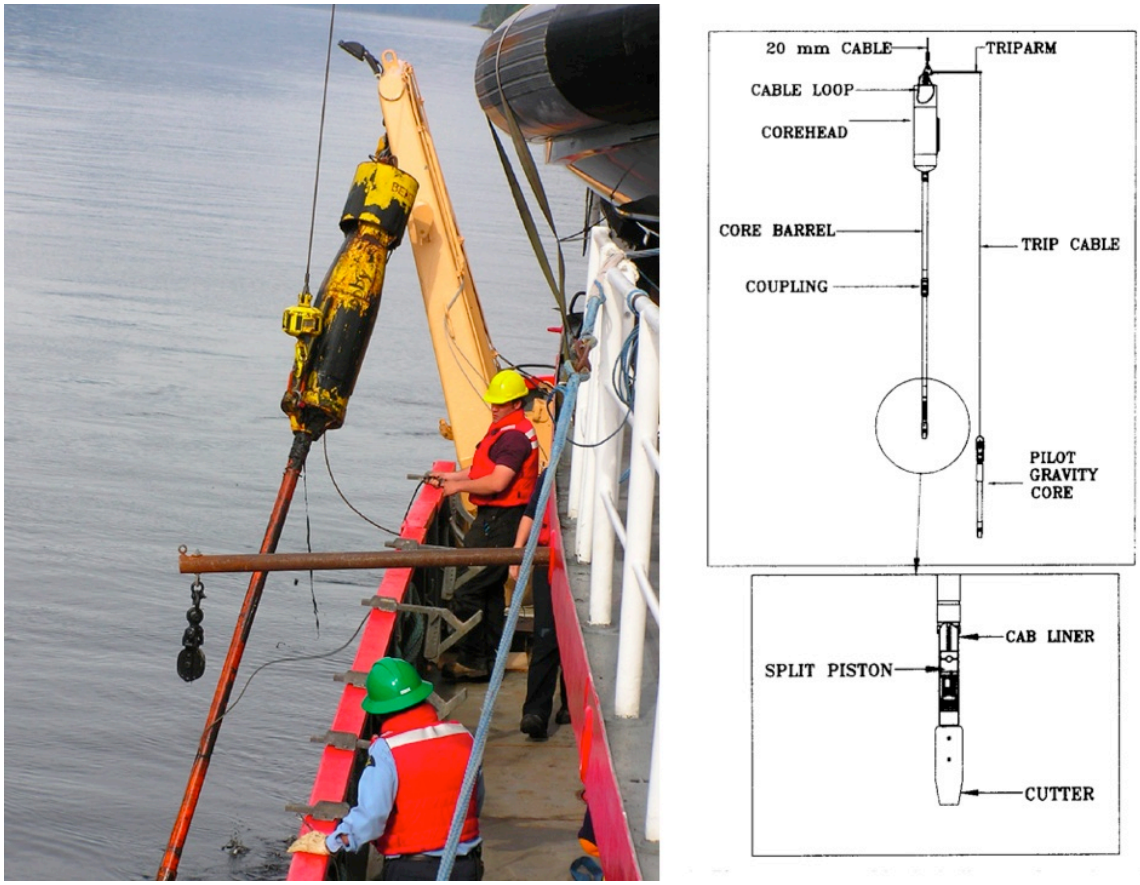

Figure 3.4 : Left- Piston coring aboard CCGS Vector (photograph taken in April, 2009). Right- Piston core assembly including piston core barrel, trip arm assembly, and pilot gravity core (from Buckley et al., 1994).

assembly and the piston core, which is also connected by wire to the winch on board the ship. The whole assembly is lowered into the water in the location where the core is to be taken. As the pilot gravity core touches the seafloor it triggers the release of the core barrel and extra loops of wire, causing them to freefall. A 600 kilogram core head weight provides added inertia as the piston corer penetrates the ocean floor. A piston inside core tubes, housed by the piston core barrel, is attached to the trawl wire, which becomes fully extended during sediment penetration. The piston slides upward through the core barrel causing vacuum suction, also encouraging penetration and collection of undisturbed sediment inside the core tubes. Maximum penetration with this coring device is 15 m (50 ft).

Piston coring sometimes has problems that result non representative sampling of the sediment column and are often difficult to recognize by observation alone (Buckley et al., 1994). The primary source of error is pressure acceleration changes inside the core barrel during coring. This happens after tripping the core into freefall. The piston should be hauled taut by the cable attached to the winch on board the ship and decelerate evenly as the piston core barrel enters the subsurface. However, variable accelerations in the lowering cable are common and cause cavity pressure variations inside the core barrel. Another source of error is caused when a hydrodynamic pressure front is created by piston core displacing water in front of the cutter, creating a turbulent head during penetration into the sediment column, which results in displacement of sediment instead of collection. Non-representative collection often results in more than 1m of missing strata from below the subsurface interface.

3.4.1 Piston Core Logging

Once the assembly is back on board the ship, the piston core sample is removed from the core barrel and cut into more manageable lengths. These core segments are brought back to the labratories of GSC Pacific where detailed analysis of core samples are conducted. The process initially involves cutting the core in half lengthwise using a core splitter before being photographed (see appendix for examples). One half of the core is plastic wrapped to hold the sediment in place, then archived in a D-tube and placed in a cooler for preservation, and the other is analyized. After analysis has been transcribed, the core is plastic wrapped then stored in a D-tube and placed in a cooler for preservation.

Lithologic description involves textural analysis and providing grain size qualifiers at 0.05 m intervals along the core. Grain size analysis in this study adhere to the Wentworth size class scheme for clastic sediments (Wentworth, 1922). Grain size distribution is a fundamental characteristic of any collected sediment. It can provide valuable insight into environmental contexts and is especially useful in the characterization of sedimentary sequences, such as establishing changes in the energy of the depositional environment. Grain size boundaries are marked to define intervals of similar grain size where bedding (single bed thickness > 2 cm) and sharp or gradational contacts occur. The degree of sorting of the core is also noted as poorly sorted, moderately sorted, or well sorted.

Also noted in description:

- Stratification: The degree (or intensity), the scale and the type of bedding features.
- Colour: Munsell notation and name.
- Additional texture and compositional notes, sedimentary structures, and fossils.

3.5 Malacological Evaluation

Malacological (shell) datum was obtained from core PGC2007007-005 in Goletas Channel for analysis of ocean environment and historical habitation record of the fossils within the sediment column. The underpinnings of this method involve knowledge of the varying sensitivities and diverse environmental domains of malacological taxonomy. Shells discovered from a core collected for this study were sent to expert Dr. Renee Hetherington for analysis.

Though a complete understanding of malacological habitat is not available, there is understanding of basic habitat information for many shallow water species. Various assemblages inhabit specific depths of the ocean and by identifying a mollusc species valuable paleo environment information for the sediment record can be attained. (e.g. Hetherington and Reid, 2003; Hetherington et al., 2003, Hetherington et al., 2004, Hetherington and Barrie, 2004).

A number of considerations must be made for each shell upon analysis. Displacement from “life position”, defined as the environment the mollusc habituated, is examined by observing fragmentation status of the sample. Transport often results in fractures and breaks, whereas samples from a stable environment are usually more complete. Background knowledge of regional sediment and ocean dynamics can help determine possible displacement history.

Chapter 4 – Results

4.1 Goletas Channel

Large-scale geometric trends in multibeam bathymetry data are used to characterize Goletas Channel and to classify properties of its landscape structures. Locations of longitudinal and transverse bathymetry transects in Goletas Channel are shown Figure 4.1 with profiles of the transects in Figure 4.2. Longitudinal Profile (a-a') is shown in Figure 4.2 (a), note that the deepest bathymetry in the study region is located on the basin floor to the southeast, which inclines toward Cook Bank in the northwest. The basin is oriented northwest-southeast stretching longitudinally ~ 45 km along the coast. It is over 300 m in depth through most of the profile and reaching a maximum depth of 500 m. Secondary features such as smaller undulation patterns are noticeable within the profile as well and are discussed in relation to landforms in section 4.2 and section 4.3.

The transverse profiles of Goletas Channel in Figure 4.2 have an asymmetric u-shape and a consistent diameter of ~ 2 km. In general, the south facing basin wall, adjacent Hope and Nigel Islands, has a steeper profile in contrast to the north facing basin wall, adjacent Vancouver Island. A transverse profile from the basin floor in the northwest, shown in Figure 4.2 (b), exhibits a bathymetric high in the center of the basin. Also, deeper bathymetry is recognized on the basin floor adjacent the south facing basin wall in profile 4.2 (c) and 4.2 (d).

Geomorphology of landscape structures found in the study area is discussed further in Chapter 5 (section 5.1). By taking a closer look at multibeam bathymetry, smaller scale

secondary patterns representing landform structures can be examined. Goletas Channel is subdivided in this study based on contrasting landforms: southeast Goletas Channel (section 4.2) and northwest Goletas Channel (section 4.3).

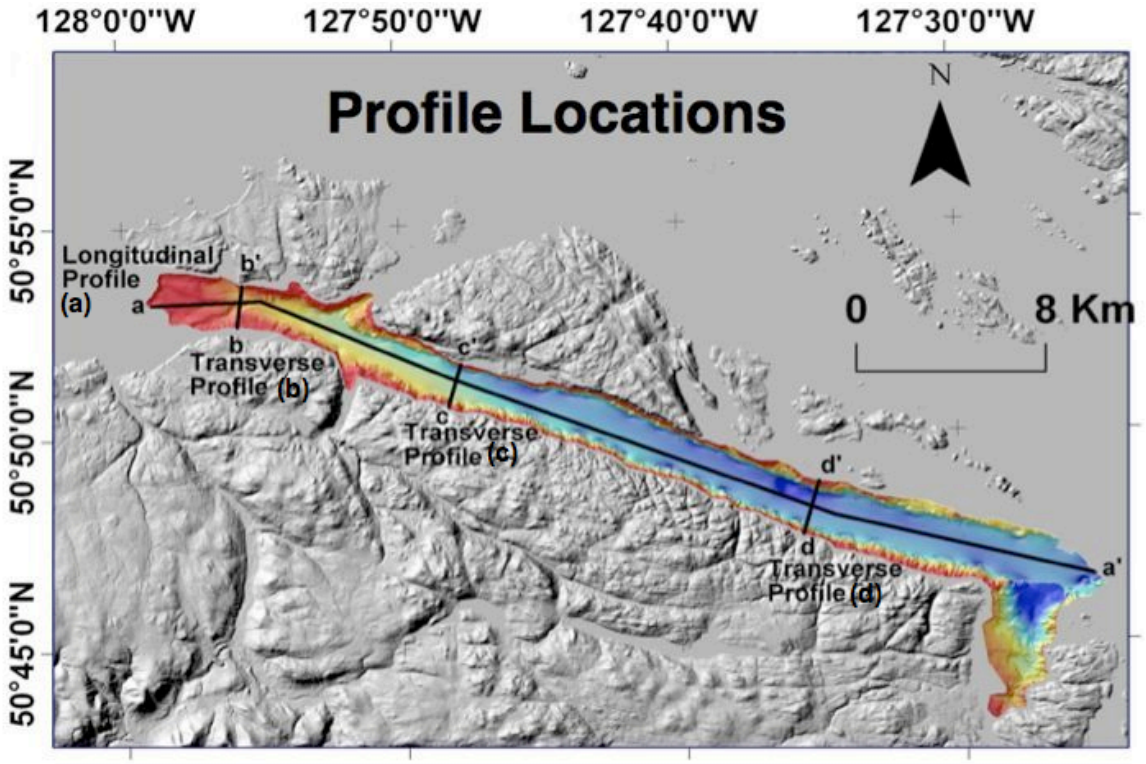

Figure 4.1 : **Location map of bathymetry profiles through the basin of Goletas Channel for Longitudinal profile (a - a') and Transverse profiles (b - b'), (c - c'), (d - d') of Figure 4.2.**

(a)

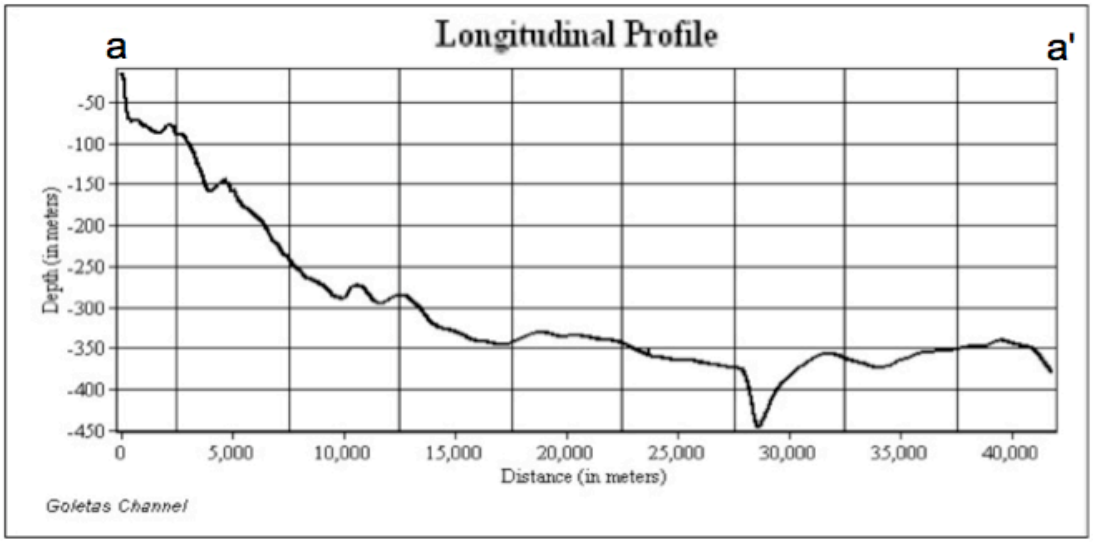
Longitudinal Profile
a
a'
-50
-100
-150
-200
-250
-300
-350
-400
-450
Depth (in meters)
0
5,000
10,000
15,000
20,000
25,000
30,000
35,000
40,000
Distance (in meters)
Goletas Channel

(b)

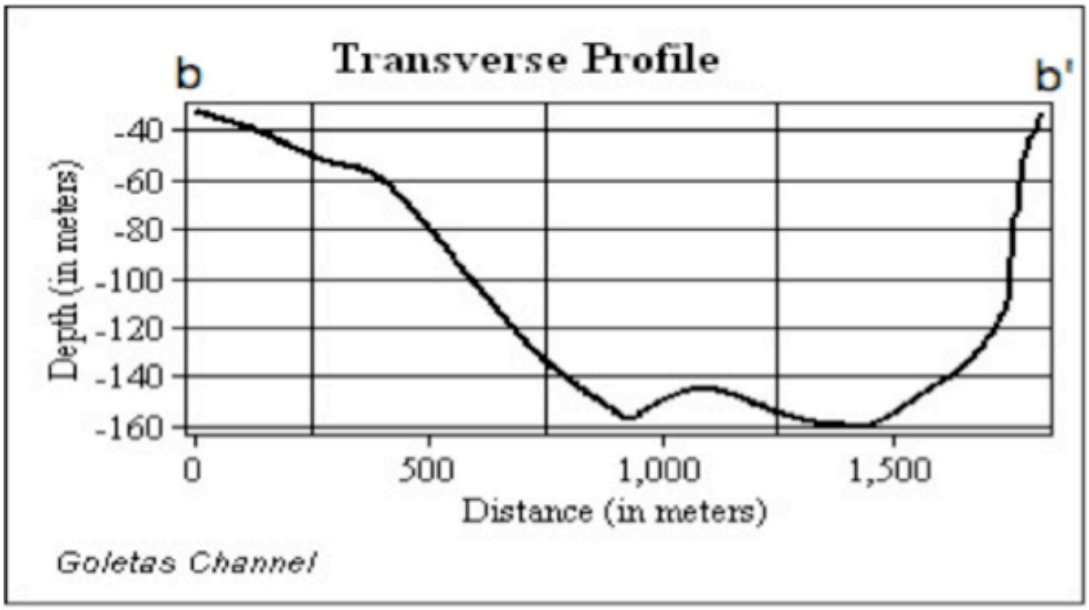
Transverse Profile
b
b'
-40
-60
-80
-100
-120
-140
-160
Depth (in meters)
0
500
1,000
1,500
Distance (in meters)
Goletas Channel

(c)

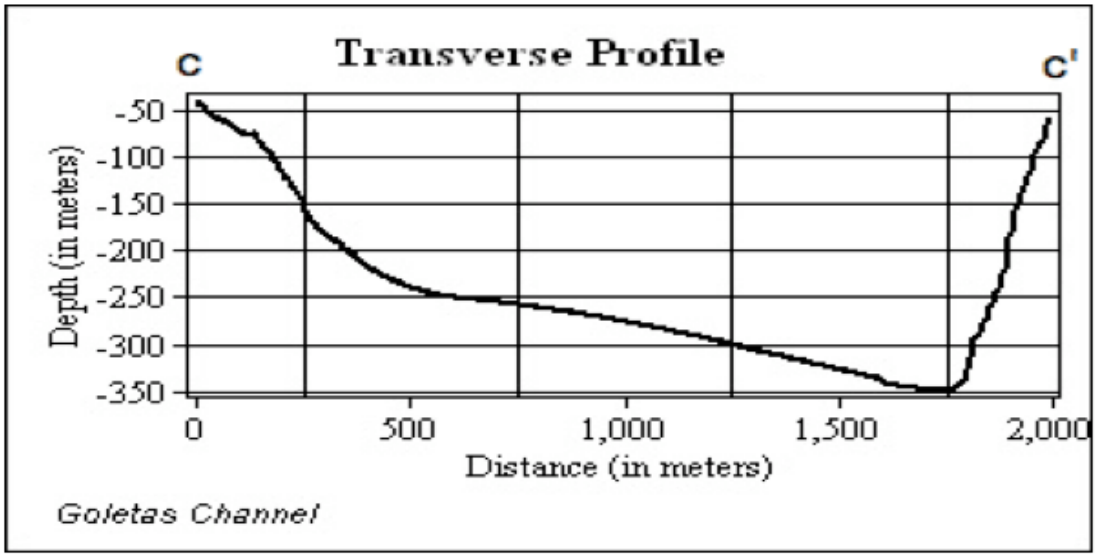
Transverse Profile
c
c'
-50
-100
-150
-200
-250
-300
-350
Depth (in meters)
0
500
1,000
1,500
2,000
Distance (in meters)
Goletas Channel

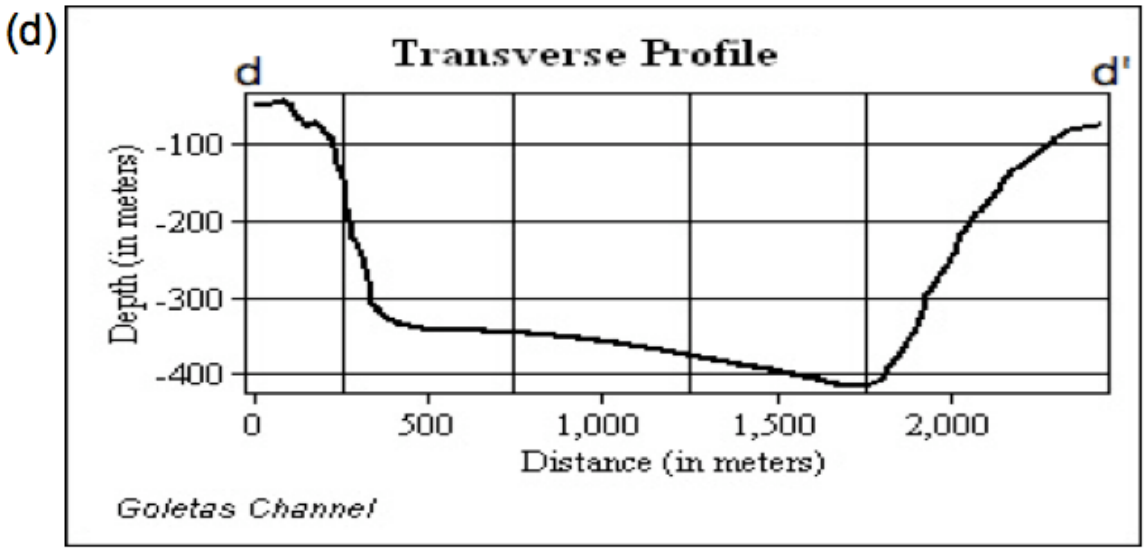

Figure 4.2 : (a) Longitudinal profile (a - a'), (b) Transverse profile (b - b') of Northwest Goletas Channel, (c) Transverse profile (c - c') of central Goletas Channel, (d) Transverse profile (d - d') through southeast Goletas Channel. Note deep basin of Longitudinal Profile (a) that shallows toward basin mouth on Cook Bank as well as it's the u-shape demonstrated by each of the Transverse Profiles.

4.2 Southeast Goletas Channel

Most of the basin, ~ 30 km of southeast Goletas Channel, has basin slopes with angular surfaces and a relatively smooth basin floor with undulating surface sedimentation, as illustrated in the multibeam imagery of Figure 4.3. Angular geometric patterns, such as 100 - 500 m wide vertical ridges extend from upper to lower basin walls. The multibeam bathymetric survey shows smaller angular variations on the surface of the ridges that are consistent with rough surface texture. Smoother surfaces are located above ridges on the upper basin wall and within small valleys located between ridges.

The basin floor is ubiquitously smooth and featureless, with only slightly dipping gradients associated with its bathymetry. The gradual slopes form mound structures with

a concave dome-like shape often as wide as 1 - 2 km on the basin floor and meld with the basin walls. These contrast with moat shaped structures, which are convex trough-like shapes, strictly located where basin wall ridges intersect the basin floor. Moats are distinguished by elongate depressions 500 - 2000 m in length, 100 - 200 m wide, and relief on the scale of 10's of meters from the basin floor.

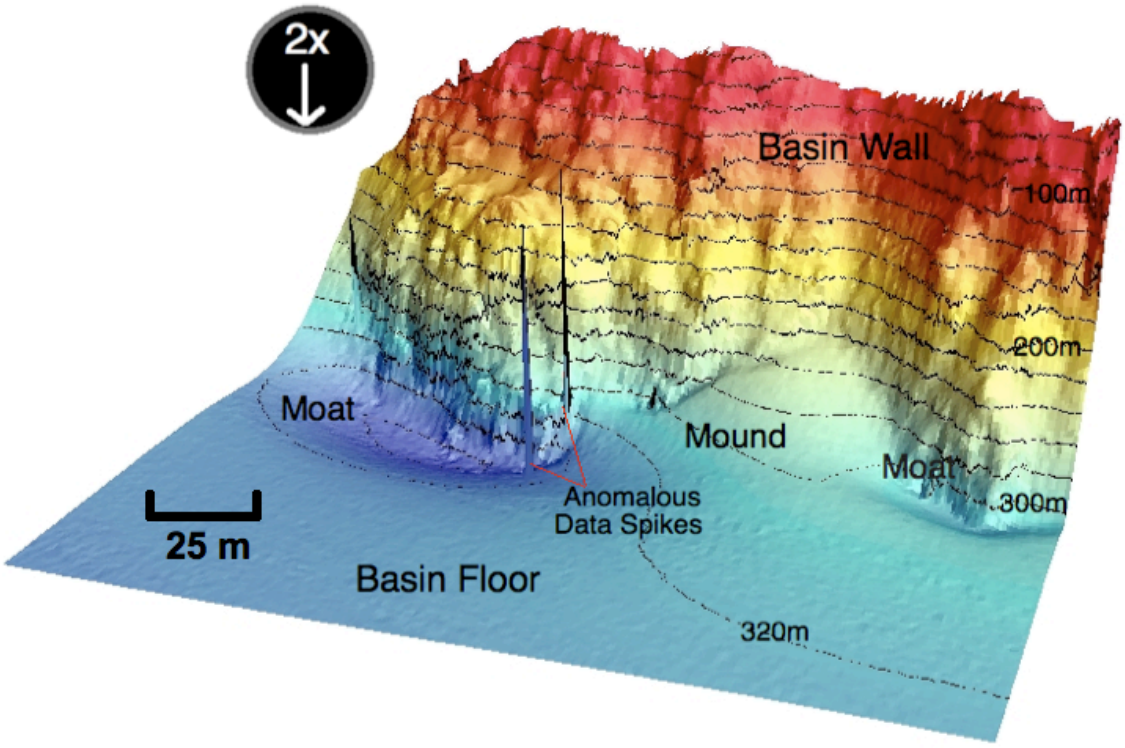

Figure 4.3 : Example of angular basin walls, as well as moat and mound structures from 3-dimensional color shaded relief of multibeam bathymetry in southeast Goletas Channel located near profile d-d' in Figure 4.1 (isobaths are 20 m apart). Wheel diagram in upper left shows vertical exaggeration and view azimuth.

4.2.1 Shallow sediment architecture

A Huntec DTS seismic survey of the basin floor was conducted along its length and a representative section of the survey was selected for seismic profile analysis (location shown in Figure 4.4). The facies described for seismic profile a - a' are shown in Figure 4.5, and have a lateral continuity that extends along most of the basin except in the vicinity of the basin mouth in northwest Goletas Channel (Section 4.3). Facies A is the lower unit in the sequence and is acoustically turbid, with an absence of internal structure throughout. Facies B overlies facies A, with an undulating, poorly defined interface. Facies B has thicknesses in the range of 4 - 8 m, and consists of a low amplitude internal reflection. Also, throughout facies B intermittent discontinuous bedding of higher acoustic intensity are observed. In places the discontinuous bedding appears to truncate within facies A.

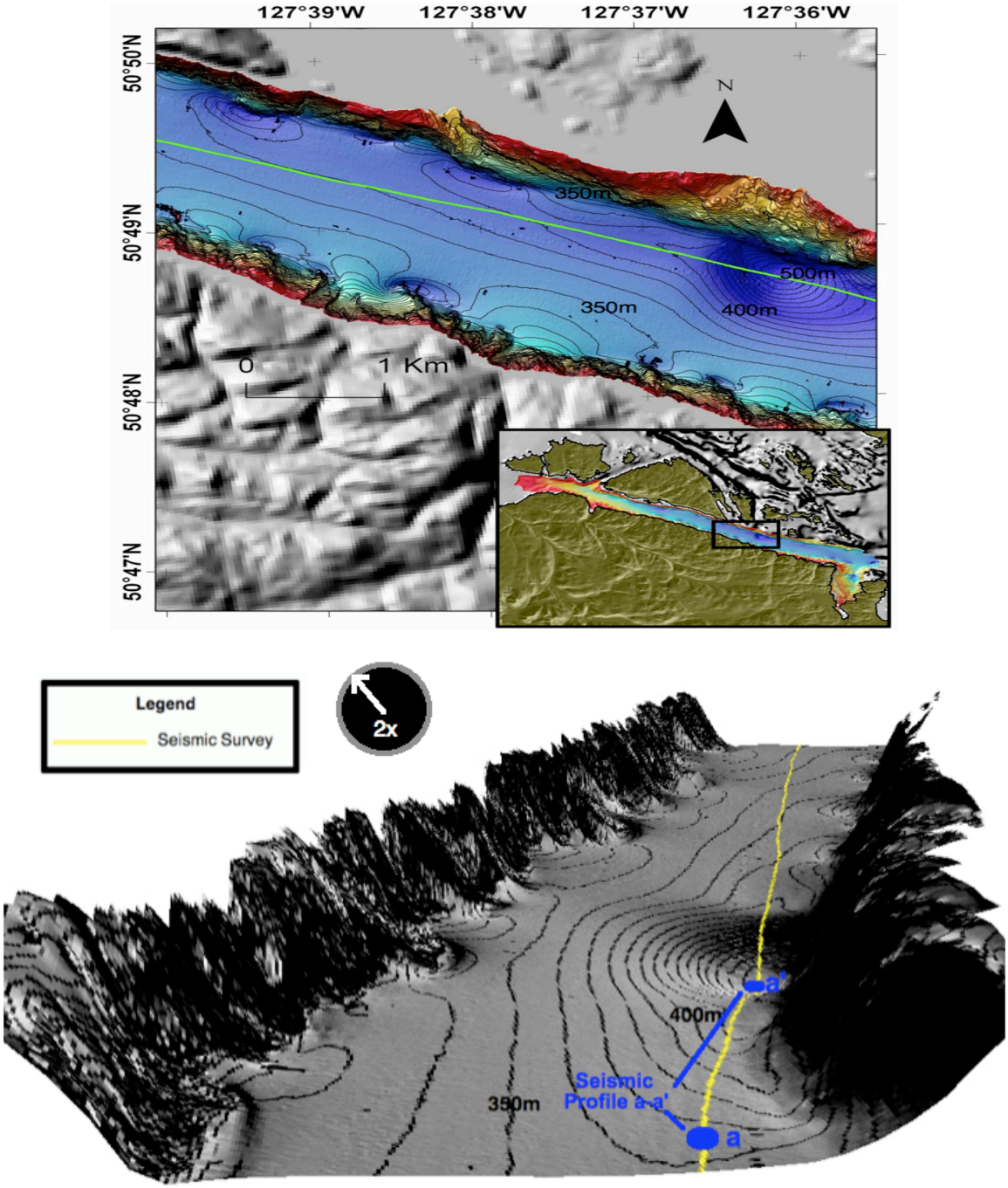

Figure 4.4 : Top - Color shaded relief bathymetry location map of southeast Goletas Channel (isobaths are 10 m apart). Bottom - Shaded relief 3-dimensional representation of multibeam bathymetry showing location of seismic for profile a - a' in Figure 4.5 (isobaths are 20 m apart). Wheel diagram in upper left has vertical exaggeration and view azimuth.

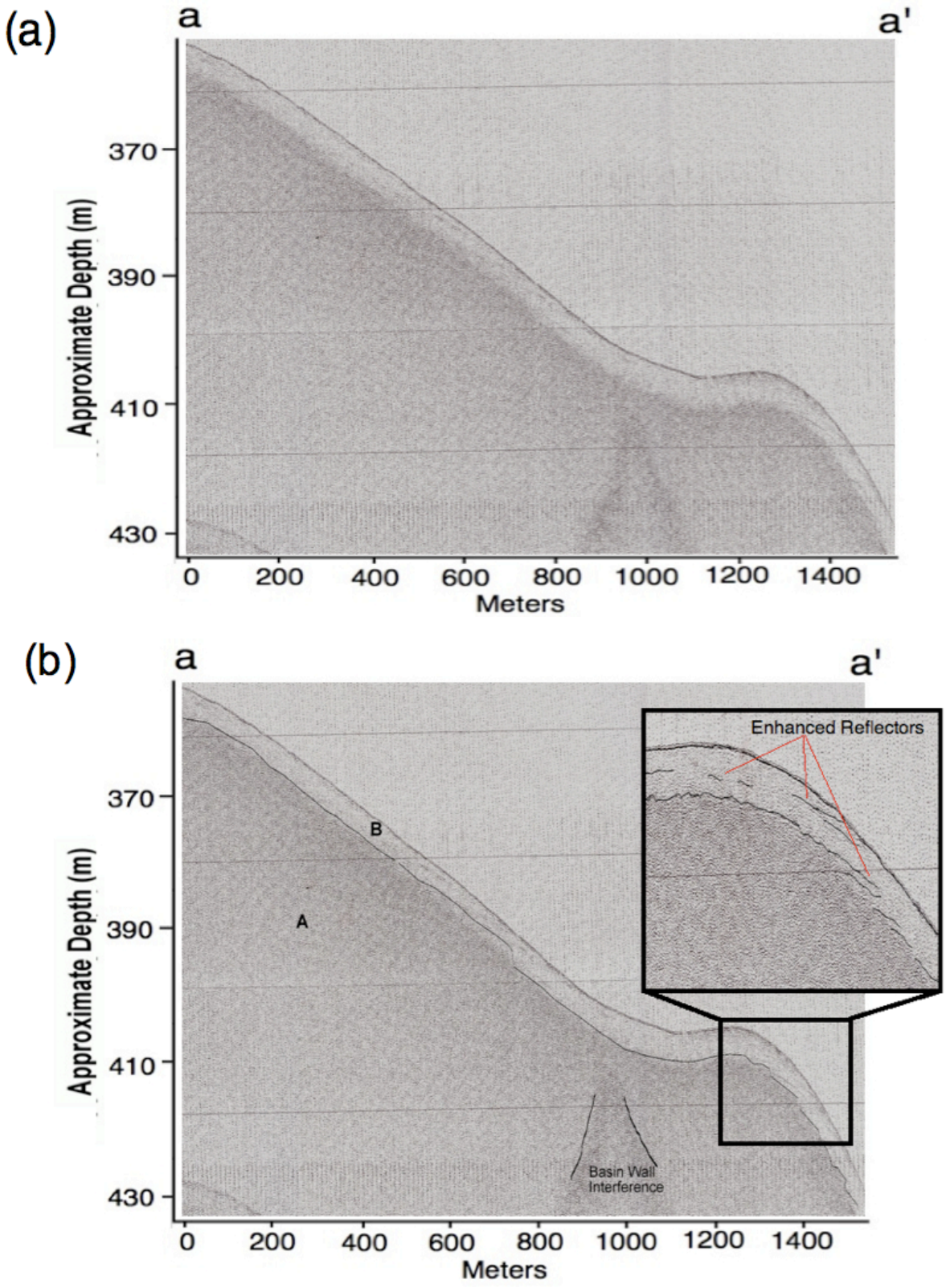

Figure 4.5 : (a) Uninterpreted Huntec seismic profile a - a' (b) Interpreted Huntec seismic profile a - a' from the basin floor of Goletas Channel. For location refer to Figure 4.4.

4.3 Northwest Goletas Channel

The bathymetry of northwest Goletas Channel is much different than bathymetry of southeast Goletas Channel. Basin walls of northwest Goletas Channel are generally smooth textured, however directly adjacent the basin mouth, smooth architecture of the basin wall is cut vertically by linear v-shaped incisions (Figure 4.6). Most of the heads of the incisions cannot be inspected because of shallow water depth locations above multibeam collection limits. On north-facing basin walls near the basin mouth, v-shape incisions terminate directly above the flank of channel 1 at depths ranging between 60 m and 100 m. Basin walls gradually become more angular ~ 15 km south of the basin mouth.

The basin mouth, located on the edge of Cook Bank, is characterized by large angular arcuate indentations 500 - 800 m in width, each of which contains a channel that meanders downslope toward the basin floor. The arcuate indentations are characteristic of scarps, marking the upper limit of the channel heads in the multibeam bathymetry data. Scarps of channel 1 and 2 are poorly defined appearing rounded and deeply set into the shelf, in comparison to well-defined angular qualities of channels 3 and 4 (Figure 4.6).

Channel Development

Four main channels are recognized from multibeam imagery of the basin mouth. Channel positions are indicated in Figure 4.6, with the thalweg (center line of a channel) of each demonstrating variations. Thalweg bathymetry profiles for each of the four channels are observed in Figure 4.7. Channel 1 is the longest, with a thalweg extending 6.5 km from the channel head to the basin floor. Channels 2, 3, and 4 appear to intersect and

discontinue downslope within 2.5 km of their head locations on the basin mouth, forming a large fan-shaped tributary head.

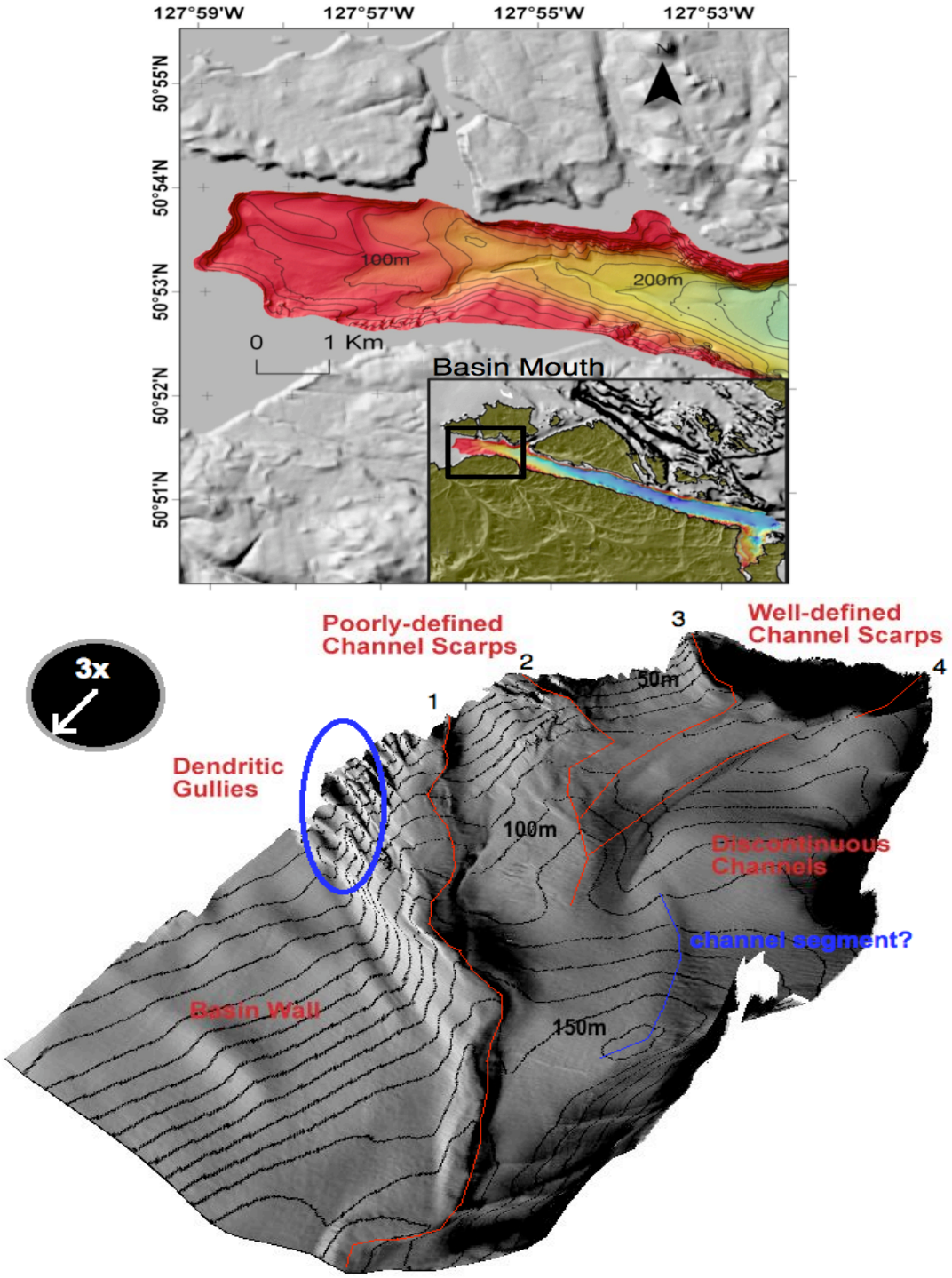

Figure 4.6 : Above - Color shaded relief bathymetry of the basin mouth in northwest Goletas Channel (isobaths are 20 m apart). Below - Shaded relief 3-dimensional multibeam bathymetry (isobaths are 10 m apart). The red lines indicate the location of each channel

thalweg, numbered 1 - 4 above each respective scarp. The profiles of each channel thalweg are shown in Figure 4.7. Wheel diagram in upper left has vertical exaggeration and view azimuth.

(a)

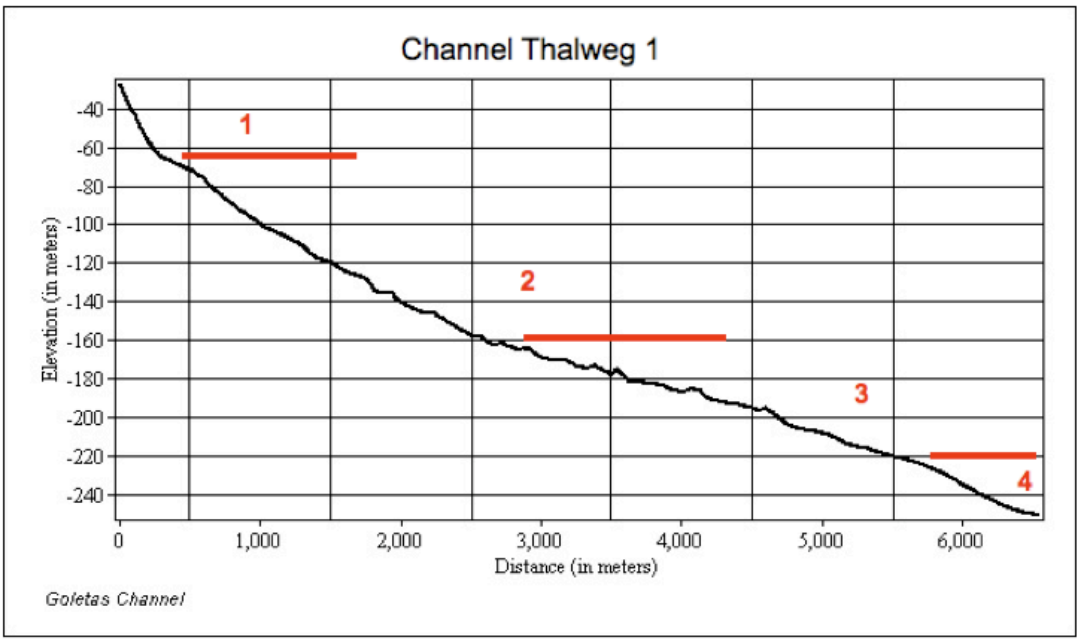

(b)

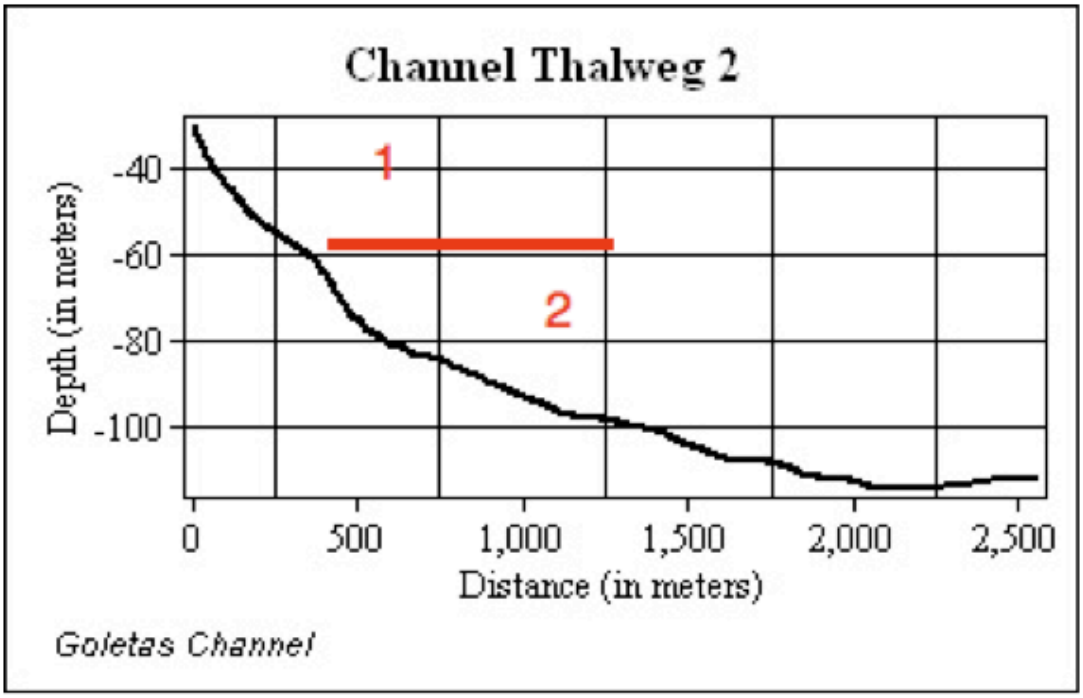

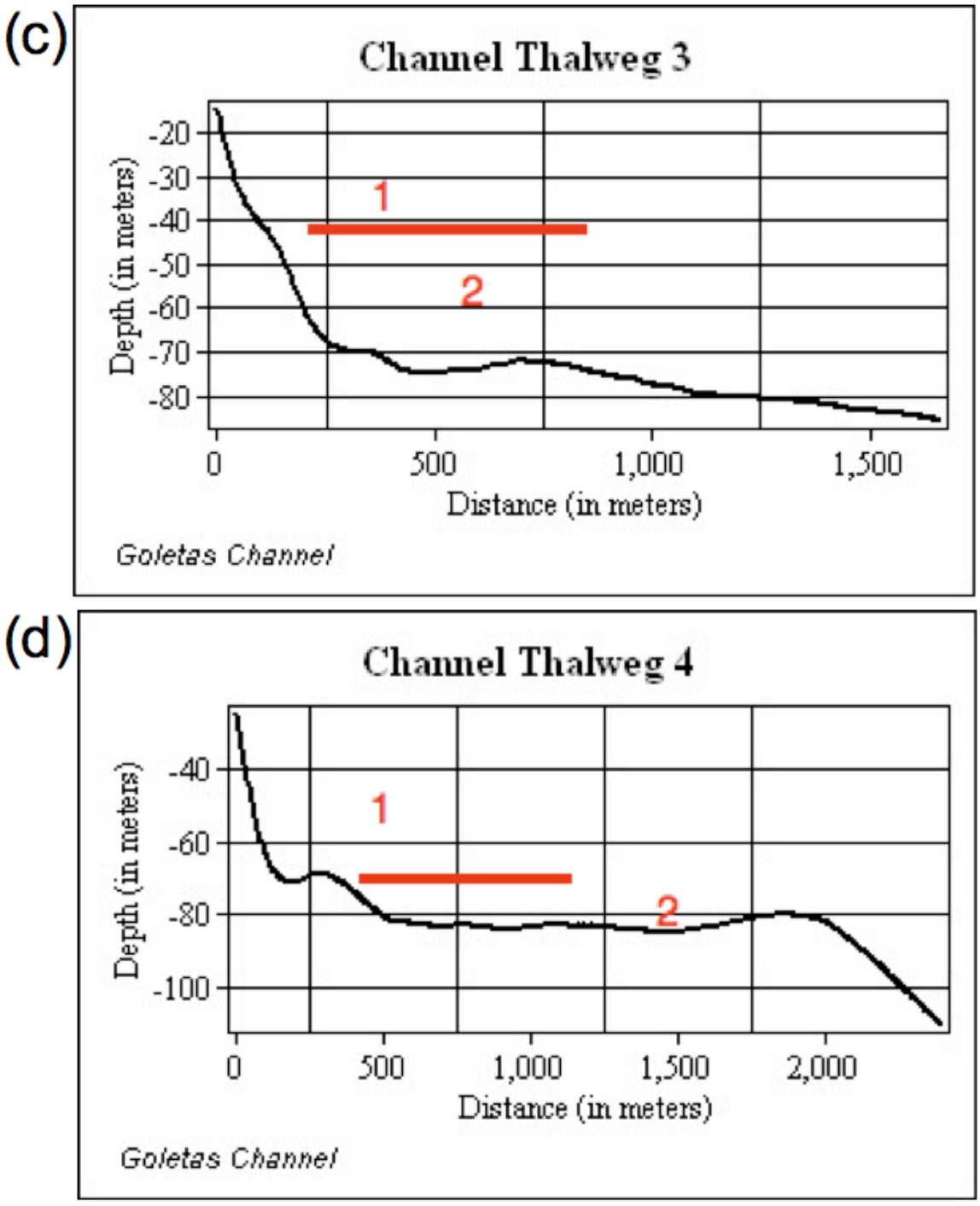

Figure 4.7 : Four bathymetric profiles of Channel Thalwegs for channels 1 - 4 (Figure 4.6), across the basin mouth of Goletas Channel. Profile transitions are demarcated in red; note common slope break at the transition between sections 1 and 2 for each of the channel profiles.

Channel thalweg 1 (Figure 4.7a) is the longest channel in the basin and has been subdivided into sections based on four main slope gradient changes and each analyzed for sinuosity. Sinuosity index is defined as ratio of straight-line length of the channel to length along the meandering channel. Therefore, low sinuosity correlates with channel wander. The gradients of the segments range from 3.60° in section 1 (35 - 70 m depth), 2.52° in section 2 (70 - 160 m depth), 1.22° in section 3 (160 - 220 m depth) and 2.11° in section 4 (220-250 m depth). The sinuosity index is 0.882 for the entire channel, generally being lower at the higher elevations and increasing with depth, except in the case of section 3 (160 - 220 m). Sinuosity index through section 1 (35 - 70 m depth) is 0.882, section 2 (70 - 160 m depth) is 0.91, section 3 (160 - 220 m depth) is 0.88 and section 4 (220 - 250 m depth) is 0.98.

Headwall development

Well-defined headwall locations for the each of the four channels indicated in Figure 4.6 are recognized in bathymetry profiles of their respective thalwegs. An upward inflection exists between 60 - 70 m in each of the profiles. Channel thalwegs 3 and 4 (Figure 4.7c and 4.7d) each have steep headwalls of ~ 12° (section 1 in profiles) and contrast with channel thalweg profiles 1 and 2 (Figure 4.7a and 4.7b), which are ~ 4°.

4.3.1 Shallow sediment architecture

The location of a Huntec seismic survey crosses through channel 1 multiple times in an upslope direction toward the basin mouth, as shown in Figure 4.8. Seismic profile b - b', shown in Figure 4.9, is used to explore stratigraphy in the area. Facies A is reflection

free, and only appears ~ 10 m below the surface on the upper slope in the reflection profile. A sharply defined horizon is recognizable in the interface between facies A and B. Facies B has a thickness of 6 - 8 m at its most narrow section on the slope where it is capped by facies C, with an undulating discontinuous contact interface. Facies B is thicker upslope and exposed on the seafloor. Facies B has a low amplitude to reflection free appearance and is absent of bedding reflectors. At the center of each valley thalweg, where channels are suspected, a high amplitude discontinuous bed is noticeable. Facies C is located on the channel margin and has bedding with high amplitude, discontinuous, non parallel reflections, though bedding is not recognisable in all channel margin locations (i.e. location marked “C?” on Figure 4.9).

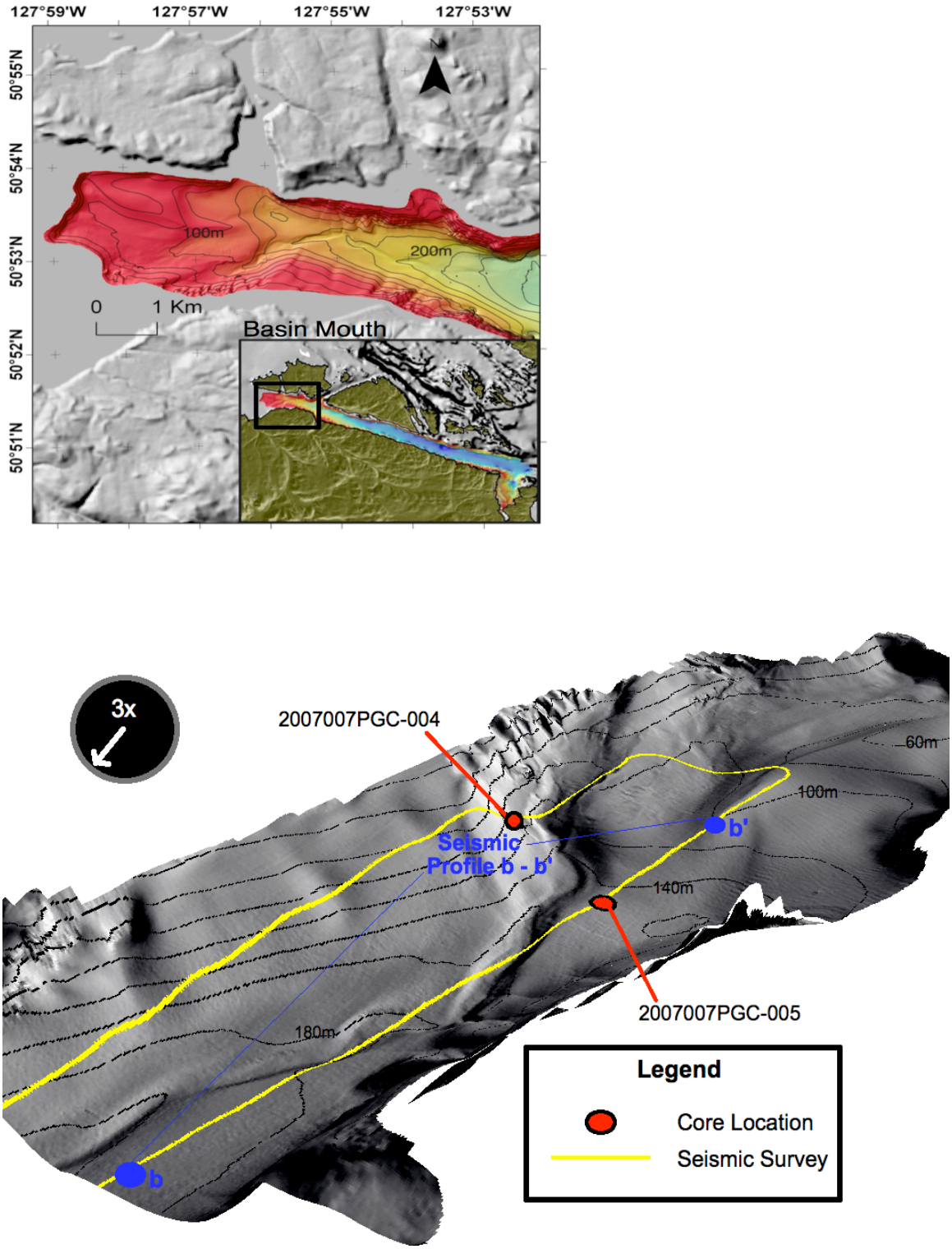

Figure 4.8 : Above - Color shaded relief bathymetry of the basin mouth in northwest Goletas Channel. Below - Shaded relief 3-dimensional bathymetry map with piston core and Huntec seismic survey location for northwest Goletas Channel (isobaths are 20 m apart). Wheel diagram in upper left shows vertical exaggeration and view azimuth.

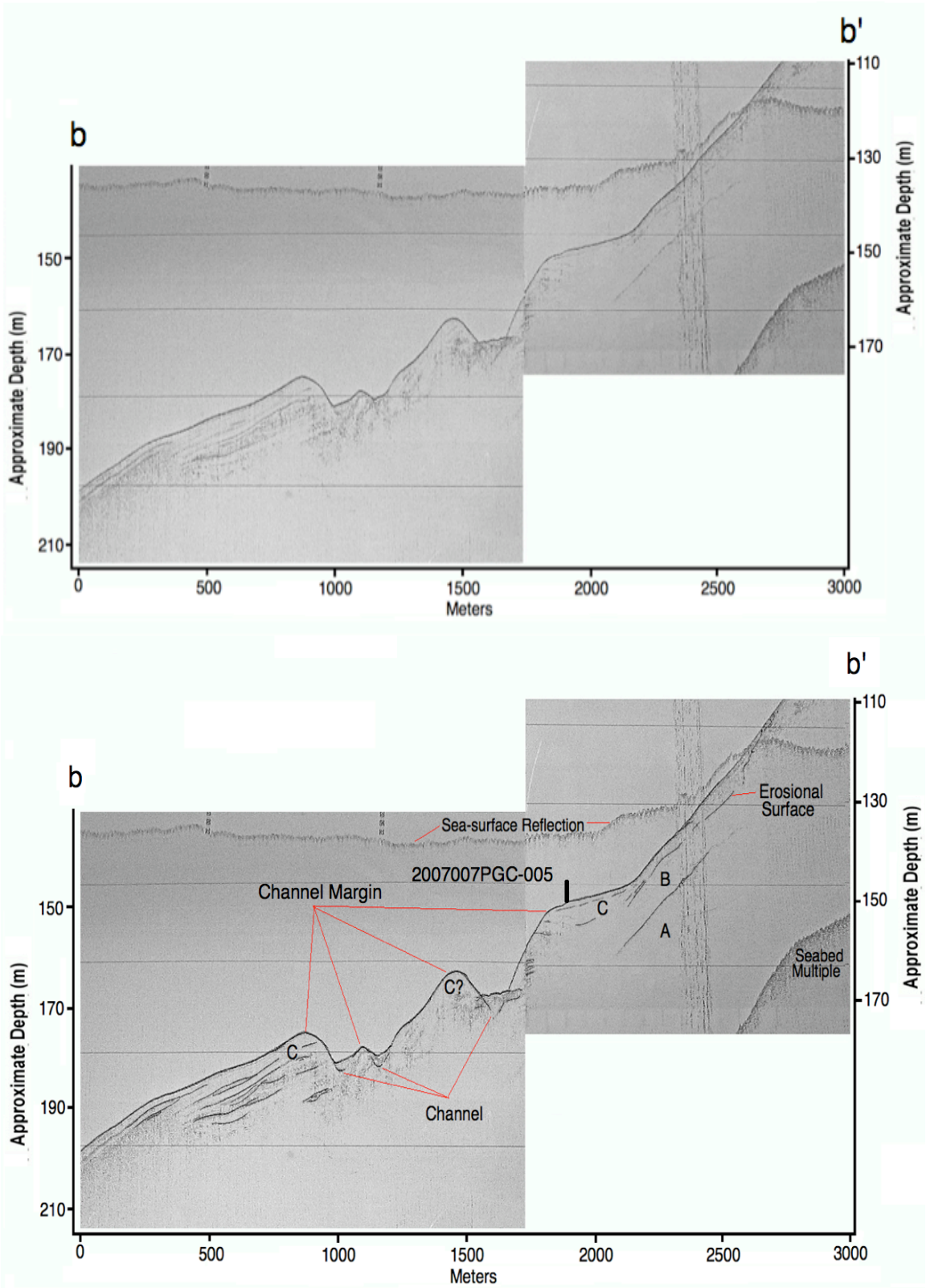

Figure 4.9 : Uninterpreted (top) and interpreted (bottom) Huntec seismic profile b - b' in northwest Goletas Channel. For location see Figure 4.8.

4.3.2 Shallow sediment lithology

Piston cores 2007007PGC-004 and 2007007PGC-005 were recovered in November, 2007 (cruise # - PGC2007007), during collaborative research between NRCan-DFO-NSERC. Figure 4.8 shows locations where each core was collected.

Core 2007007PGC-004

Piston core 2007007PGC-004 recovered 5.1 m of sediment core from 109 m water depth adjacent the north-facing basin wall. The core exhibits fine to medium grained, well sorted, olive grey, moderately consolidated sands throughout with no obvious indication of a stratigraphic boundary. Shell fragments ranging from 0.25 - 3 mm are found throughout the core with quantities of <1%. Homogeneity of the sediment indicates the piston core is possibly a sucked core. Sucked cores occur in many cases when the core barrel does not penetrate to its fullest extent. The piston will be pulled up as the coring device is pulled out, consequently material around the core nose flow into the pipe.

Core 2007007PGC-005

Piston core 2007007PGC-005 recovered 1.2 m of sediment core from 151 m water depth adjacent to a channel in the basin mouth. A Pilot core also collected 0.85 m of sediment core from the same location. Differing upper core (near surface) sedimentation records can be observed between the piston core and pilot gravity core. Near surface sediment is missing from the piston core and indicates a hydrodynamic pressure front forced surface sediment to be displaced during initial penetration of the coring device (see section 3.4).

Piston core 2007007PGC-005 (see figure 4.10) exhibits sharply bound laminae of olive grey clayey silt, with thicknesses of 0.25 cm to 5 cm, ranging from 5 cm to 20 cm apart

throughout the core, occurring within normal graded (fining upward) sediment. At the bottom of the core the normal graded sediment contains medium to coarse grained, well-sorted, olive grey sand with small quantities (<1%) of shell fragments. There is a fining upward progression from the bottom of the core to well sorted, olive grey silt, then dark olive gray mud at the top of the core, and is a continuous transitional unit broken only by the interlayered laminae of clayey silt. The laminae of clayey silt are poorly sorted, containing pebbles as well as organics, such as tree needles, whole shells and fragments. The base of the core sample contains 80 - 90% whole shells and fragments, and a matrix of poorly sorted, medium sand to gravel grain size. Shells were obtained from a basal layer as well as a clayey silt laminae at 99 cm and used for malacological (shell) assessment, results of which are shown in Table 4.1.

The malacological assessment of core 2007007PGC-005 (Table 4.1) provides shell assemblage life-position environmental characteristics from two depths in the piston core (assessment performed by Hetherington, 2009). Both shell types analyzed from the 99cm horizon suggest development in an intertidal protected shallow beach environment. Shells observed in the 119 cm horizon develop in varying environments, accommodating a greater depth range and environment conditions. Many of the shells were fragmented beyond recognition, indicating dynamic environment conditions prior to final deposition at the site location, though samples up to 3 cm in diameter were also found at the 119 cm boundary, indicating that dynamic conditions were either not capable of destroying all transported shells, or that some shells had travelled less prior to deposition.

Table 4.1 : Malacological assessment results

Core sample depth	Species name	Depth Tolerance	Habitat
99cm	Margarites pupilus	Intertidal to -90m	Sheltered beaches, sand, mud & rubble
99cm	Olivella baetica	Intertidal	Sand flats, sandy beaches, protected waters
119cm	Alia gausapata	Subtidal to -200m	On rocks
119cm	Bittium attenuatum	Intertidal to -70m	Eelgrass, rocky beaches
119cm	Lucinoma annulatum	Intertidal to -750m	Sand and mud
119cm	Olivella baetica	Intertidal	Sand flats, sandy bays, and protected waters

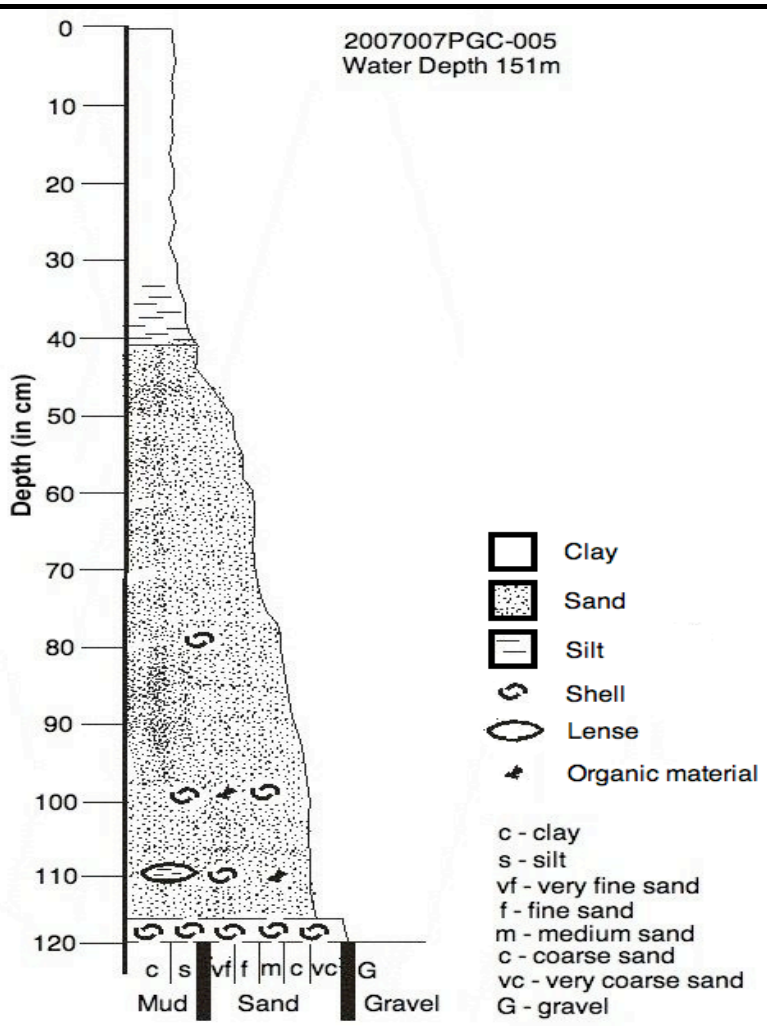

Figure 4.10 : Core shows fining upward sequence. Interlayered laminae of clayey silt are found throughout the core. A malacological study was performed on two sections of the core.

4.4 Hardy Bay

The main physiographic trend characterizing Hardy Bay is a depression that deepens northward toward Goletas Channel to a maximum depth of 300 m at its margin, which can be observed in Figure 4.11. The depression has high gradient walls defined by ridges, precipices and angular textures on the south and southeast walls. The walls of the depression in the western and southwestern portion of Hardy Bay have more gentle slopes and smoother textures.

Within the depression there are three smaller semi-confined inner basins bound by angular ridges (Figure 4.11). The small inner basins align and in a step-wise fashion progressively deepening northward toward Goletas Channel. Lowest relief ridge boundaries on each of the three small basins are located on northern embankments, at depths of 80 m and 140 m, and 200 m, respectfully. Below the lowest small basin Hardy Bay widens and opens to Goletas Channel.

Terrace

A terrace landform is of interest in Hardy Bay trending parallel to the coast along the 80 m isobath in the south and southeast extreme of the submarine valley (Figure 4.11). The distinct terrace geometry is recognized in multibeam by its low gradient shelf, slope break, and steep outer slope.

A slope break is notable where smooth, gradual gradients associated with an extensive shelf plateau increase sharply, dipping at high angles toward the submarine valley bottom. Four bathymetry profiles of the terrace oriented perpendicular to its slope break

are shown in Figure 4.12. The slope break can be observed between 70 m and 80 m isobath contours and traced for approximately 6 km along the submarine valley.

Bathymetric profiles show lateral variance in terrace geometry across Hardy Bay. Below the slope break, gradients are as high as ~ 6^{o} (10%), though in locations such as in Profile 3 from Figure 4.12 (c), the slope break is barely noticeable because of more gentle gradients. Small slope variations occur above and below the slope break in the other three profiles, however the slope break shows little variation in depth.

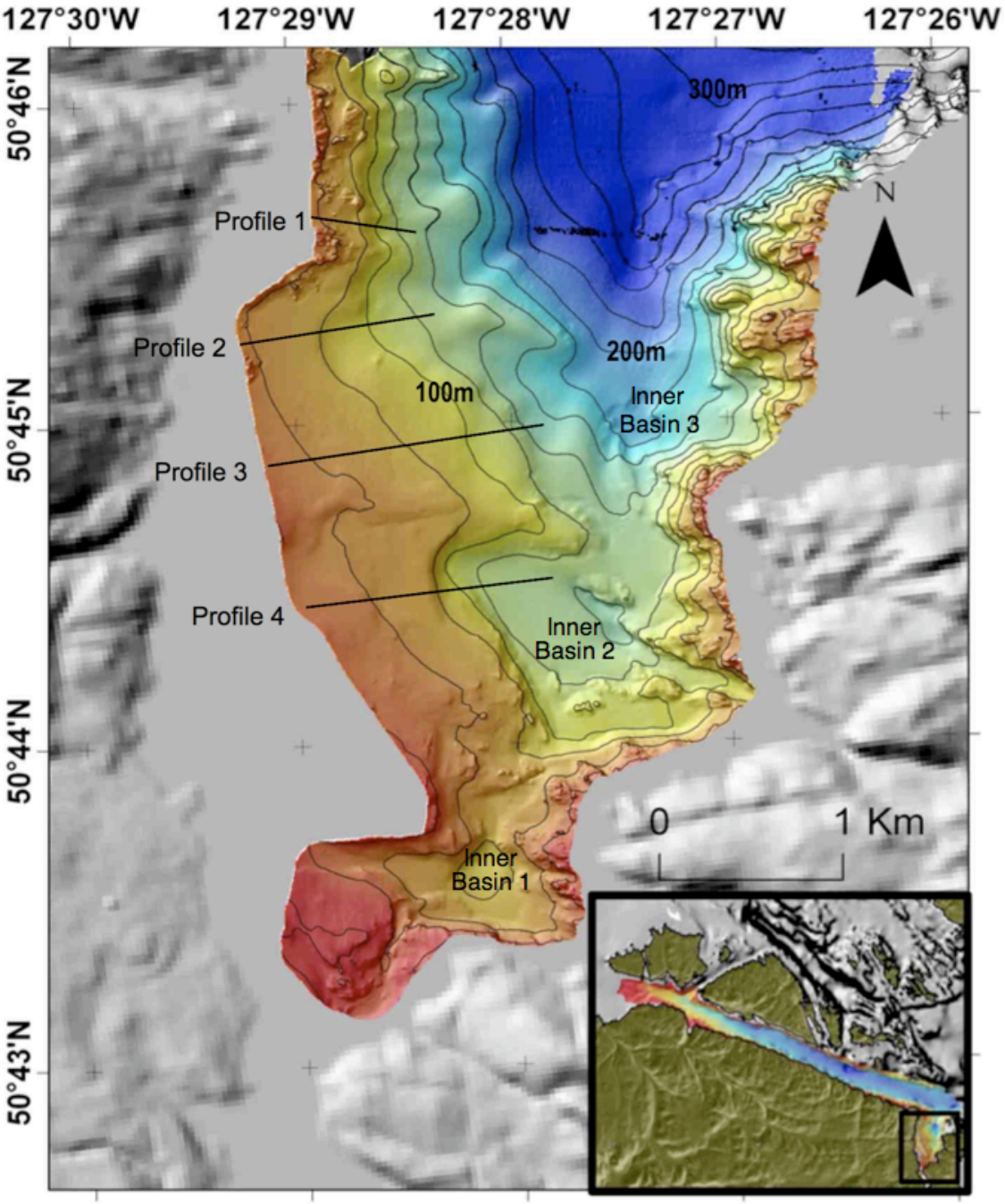

Figure 4.11 : Color shaded relief multibeam bathymetry map of Hardy Bay (isobaths are located 20 m apart). Note terrace along the 80 m contour with locations of Profiles 1-4 indicated.

(a)

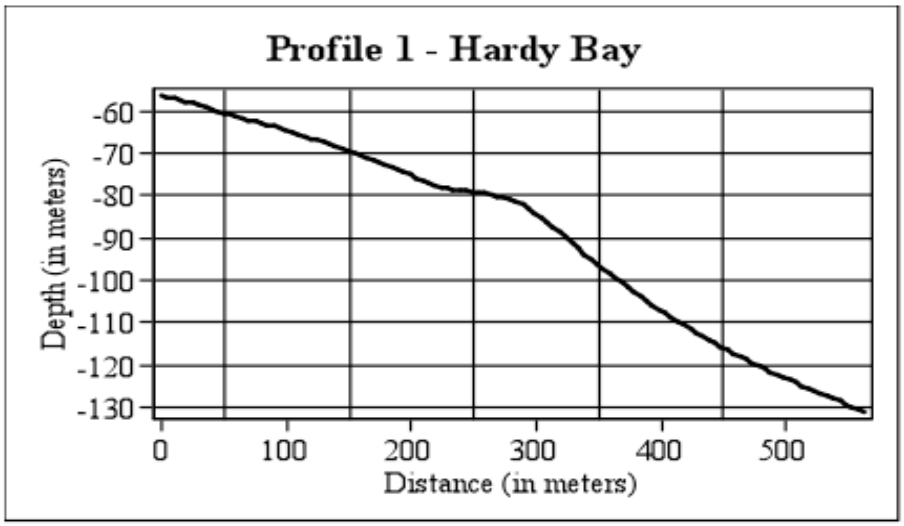
Profile 1 - Hardy Bay
Depth (in meters)
-60
-70
-80
-90
-100
-110
-120
-130
0
100
200
300
400
500
Distance (in meters)

(b)

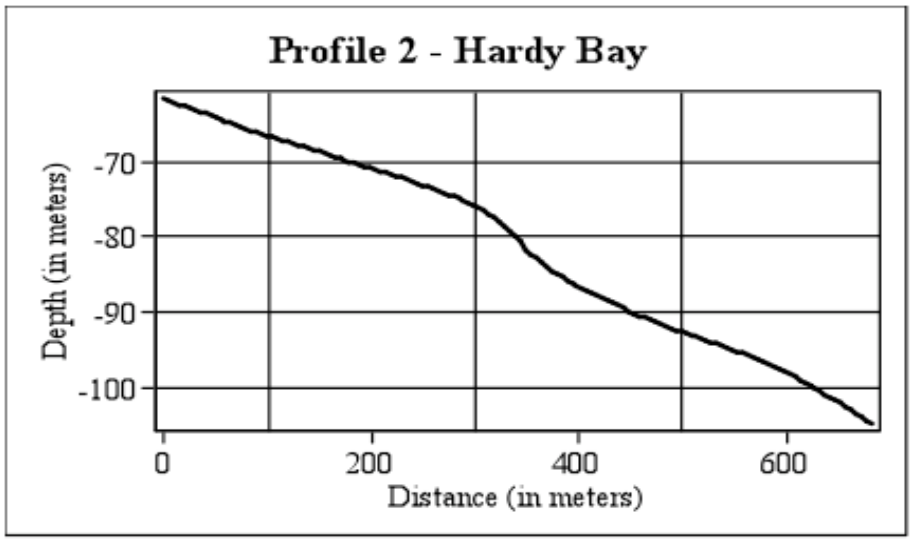
Profile 2 - Hardy Bay
Depth (in meters)
-70
-80
-90
-100
0
200
400
600
Distance (in meters)

(c)

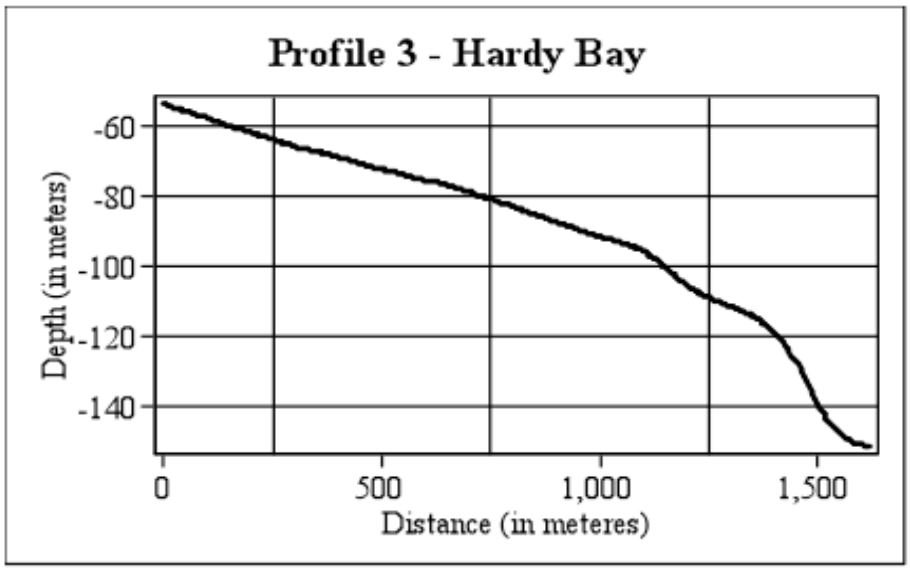
Profile 3 - Hardy Bay
Depth (in meters)
-60
-80
-100
-120
-140
0
500
1,000
1,500
Distance (in meteres)

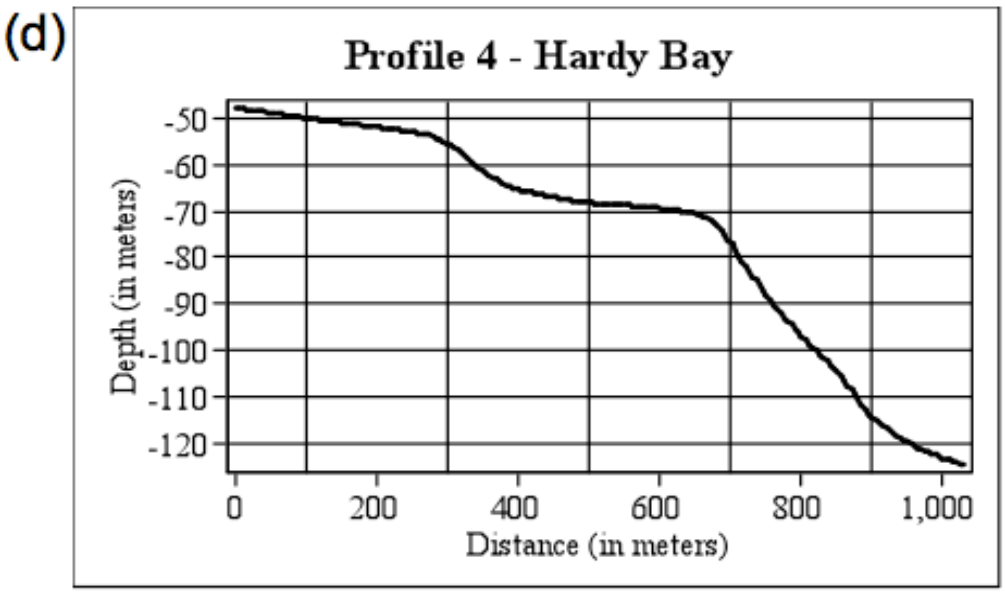

Figure 4.12 : Profiles 1 - 4 over terrace slope breaks located 70 - 80 m water depth in Hardy Bay. (Refer to Figure 4.11 for profile location information)

4.4.1 Shallow sediment architecture

A Huntec seismic survey of the Hardy Bay was conducted on the terrace, crossing two well defined sections of the terrace landform as shown in Figure 4.13. Seismic profiles c - c' and d - d' are shown in Figure 4.14 and Figure 4.15, respectfully.

Seismic profile c - c' (Figure 4.14) has a low gradient plateau, and a steeper grade below a slope break at 74 m water depth. The gradient decreases at 90 m water depth at the base of the high gradient slope where a small mound with ~ 2 - 3 m of relief is located. Facies B has a high amplitude acoustically turbid signature and some discontinuous convoluted bedding. The mound at the base of the slope appears to be acoustically turbid, with a similar signature as facies B. Facies C is ~ 2 m thick and continuous above the slope break, with high amplitude parallel bedding. Facies C thins below the slope break,

thickening again at the base of the terrace slope. The contact between facies B and C undulates slightly above the slope, with discontinuous parallel reflectors of facies C located between undulations associated with facies B.

Seismic profile d - d' (Figure 4.15) has a low gradient plateau, and steep profile below a slope break located at 80 m water depth. The high gradient slope decreases at 90 m water depth before increasing again below 95 m. The substructure contains lower facies A with a high amplitude turbid seismic signature, and areas where reflection is subdued and reflection free in places. Above the slope break, high relief undulations are noticeable in facies A where an unconformable relationship exits with overlying facies B and C. Facies C is 10 - 15 m thick above the slope break, with high amplitude parallel bedding. An unconformity is apparent within the facies above the slope break where bedding bifurcates into upper and lower limbs. The upper limb has continuous bedding across the entire profile, whereas the lower limb is discontinuous above the slope break. Also, above the slope break a narrow onlap sequence is recognizable between the limbs of the bifurcation, and is 5 m thick at maximum.

A clear contact interface does not exist between facies A and B because they have similar seismic reflection signature. Where facies A is recognized it forms precipices in the profile. It is possible that facies A is located where facies B has been interpreted in seismic profiles c - c' and d - d'.

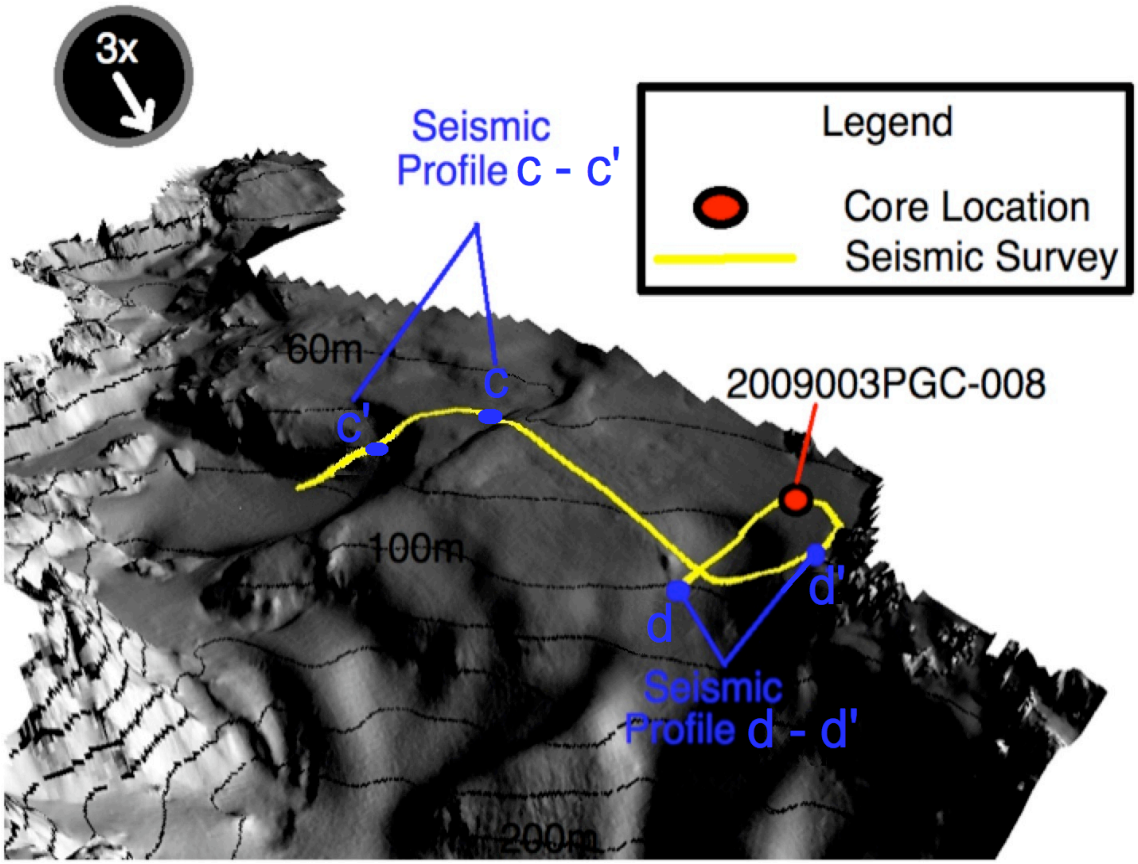

Figure 4.13 : Shaded relief 3-dimensional bathymetry map with core and seismic locations for Hardy Bay (isobaths are 20 m apart).Wheel diagram in upper left shows vertical exaggeration and view azimuth.

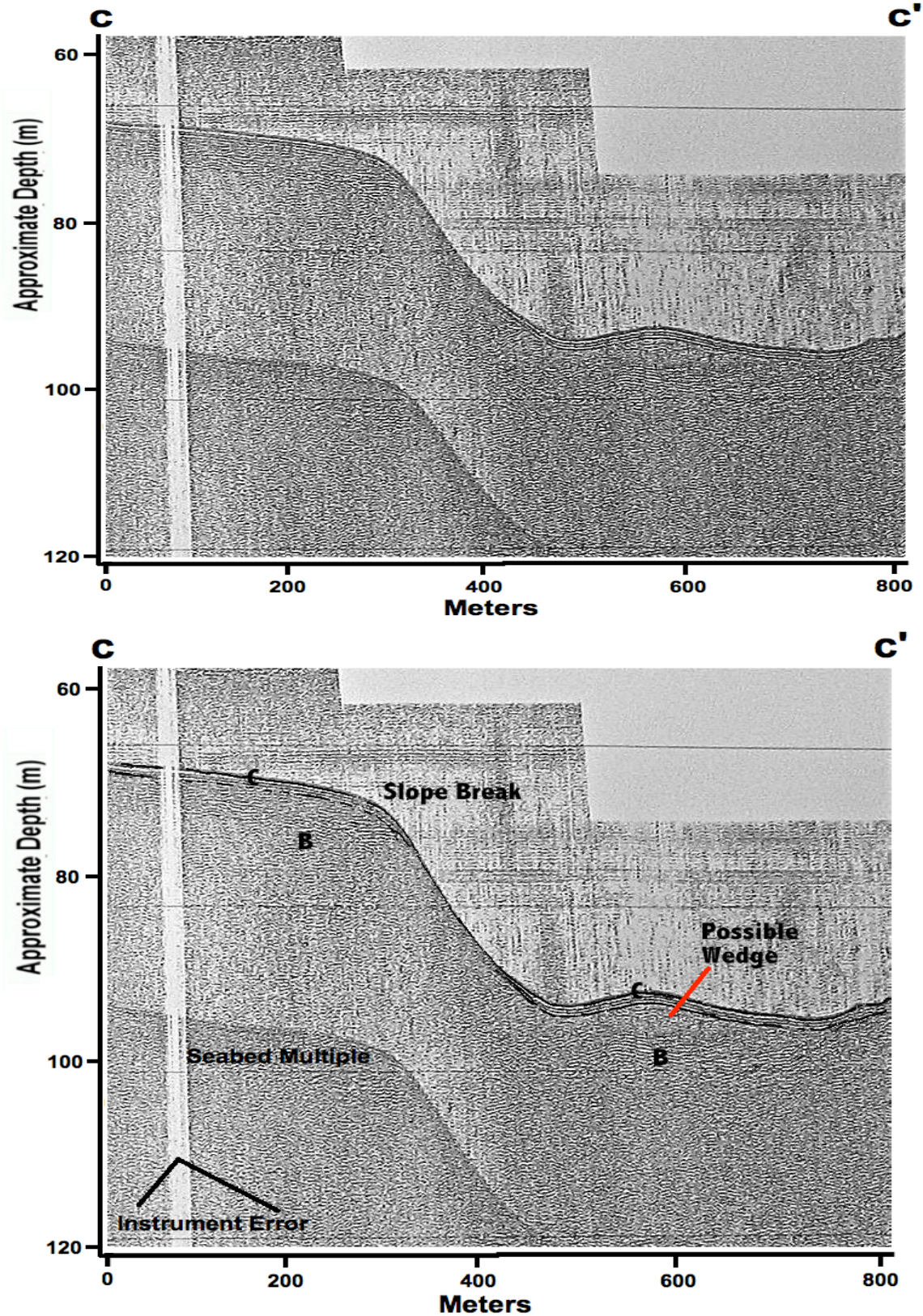

Figure 4.14 : Uninterpreted (Top) and interpreted (bottom) Huntec seismic profile c - c' from Hardy Bay. (Refer to 4.13 for location information)

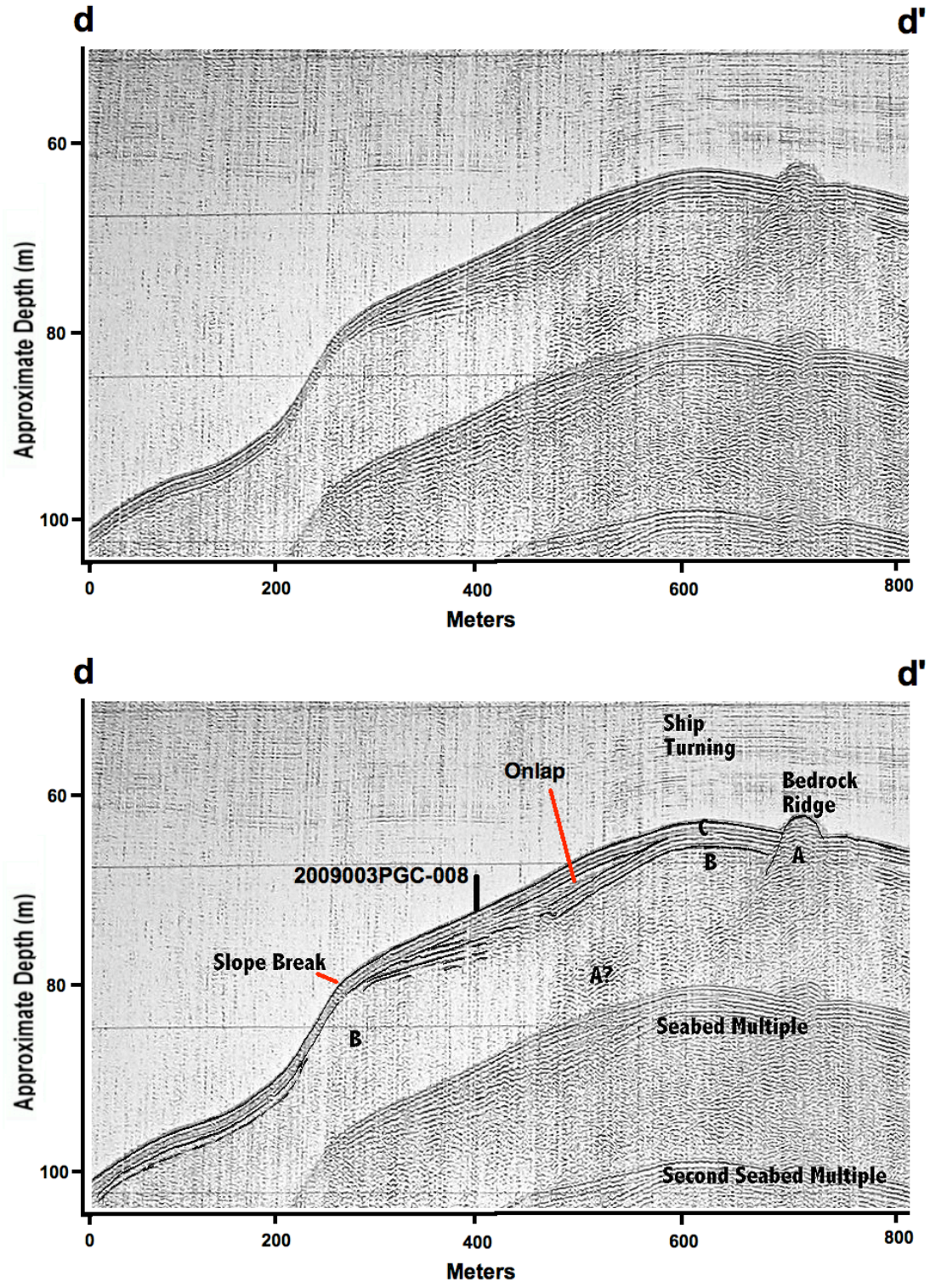

Figure 4.15 : Uninterpreted (top) and interpreted (bottom) Huntec seismic profile d - d' from Hardy Bay. (Refer to Figure 4.13 for location information)

4.4.2 Shallow sediment lithology

Piston core 2009003PGC-008, shown in core diagram Figure 4.16, recovered 3.6 m of sediment from 74 m water depth directly above the slope break on the terrace landform (see Figure 4.13 for core location). The core exhibits layers of well sorted fine to medium grained olive grey sand with interbedded dark olive grey clayey silt located between 65 cm and 160 cm between sand layers. The interbedded clayey silt occurs through 80 cm of the piston core with thicknesses ranging from 10 - 20 cm. A clayey silt bed at 100 cm contains a horizon of intact shells, otherwise small percentages (< 1%) of shell fragments are dispersed throughout the core, with less in the upper massive sand layer than in the layers below the clayey silt bedding. Trace coal fragments in the sequence were discovered at 120 cm in the core as indicated in Figure 4.16 (i.e. organic material).

An initial surface sample recovered from the site using the Petersen grab sampler contained bioturbated mud (Figure 4.17). This unit did not appear in the core sediments, and may indicate a hydrodynamic pressure front forced surface sediment to be displaced during initial penetration of the piston core during collection (see section 3.4).

Upon retrieval on deck of the CCGS Vector, the core showed some sign of being washed out, with high water content and lack of consolidation, which is conducive to vertical sediment mixing within core sleeve. Though some mixing is evident, much of the sediment core appears to have remained in sequence; therefore the description appears to be a valid representation of the main units associated with subsurface lithology. The interbedded clayey silt is more consolidated than sand layers and does not appear disturbed. However, the unconsolidated sands shows signs of segregation because of the

presence of thin clay (<1 cm) distributed on top of each core section, which likely originated from a clay matrix in the sand layers of the sediment column, and were washed out then redeposited by gravitational settling within the core sleeve after recovery.

Figure 4.16 : Core PGC2009003-008 has sand layers, interbedded with clayey silt units near mid-core.

Figure 4.17 : Grab sample collected from Hardy Bay. Note polychaete worm, an indication of bioturbation in the seafloor sample and oxygenated conditions.

4.5 Shusharti Bay

The main geometrical trend characterizing Shusharti Bay is a large scale depression that deepens toward Goletas Channel. Multibeam bathymetry in Figure 4.18 shows steep side walls along the periphery of the depression. Two plateaus are dominant within the depressed landscape with slope breaks located at 50 m and 60 m water depth. Below the upper slope break (50 m) there is an elevation drop of ~ 10 - 15 m to the lower plateau. Below the lower slope break (60 m) there is a steeply dipping slope that intersects with the basin floor of Goletas Channel ~ 100 m below. There are small scale undulations with smooth textures along the surface of the plateaus, slopes and slope breaks. The undulations take the form of meandering low relief (~ 2 - 5 m) ridges and mounds ~ 5 m wide in places.

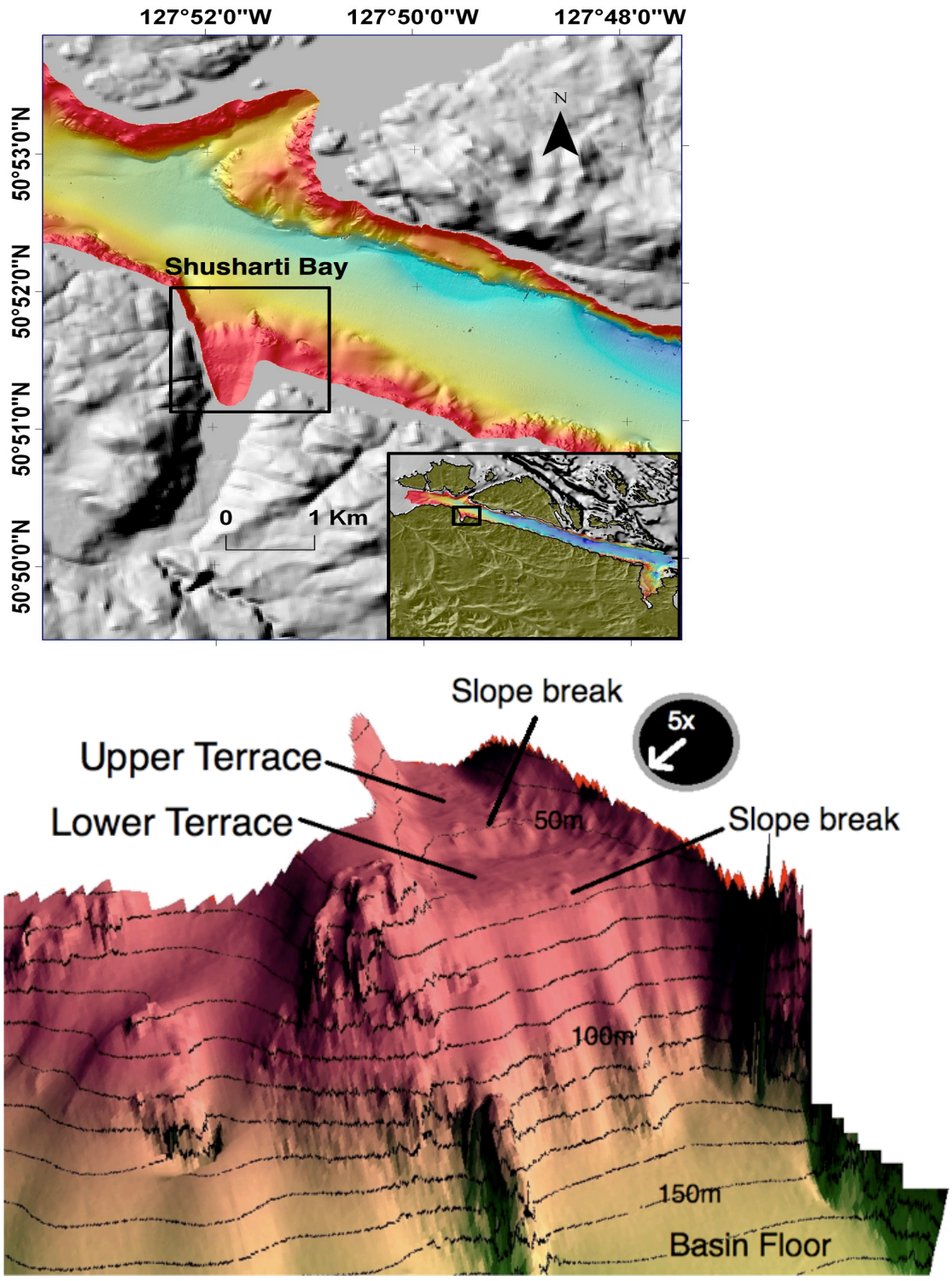

Figure 4.18 : Above - Color shaded relief location map of Shusharti Bay. Below - Oblique view looking southwest at Shusharti Bay with structures indicated. The shelf break of upper plateau is located along the 50 m isobath and the shelf break of the lower plateau is located at 60 m (isobaths are 10 m apart). Wheel diagram in upper right shows vertical exaggeration and view azimuth.

Chapter 5 - Interpretation

5.1 Goletas Channel

Goletas Channel can be broadly thought of as a fjord because of similarities to other deep embayments of sea along the adjacent coast with classification as fjord, characterized by great depth, steep and roughly parallel sides, frequent straight segments, and deep internal basins (Roberts and Rood, 1984). Goletas Channel is given a classification of "fjord-like trough", for its fjord-like structures and indicates possible geomorphologic origin. The morphology can only be regarded in a broad sense as a fjord, having morphologic elements that characterize a fjord, yet do not share all the physical characteristics.

The geomorphology of Goletas Channel is thought to be a product of glacial erosion along a tectonic trend (i.e. faulting, folding, geologic contacts), likely related to the geological contact of Vancouver and Bonanza Group Volcanics and Jurassic Island Intrusions, though the relationship is enigmatic. The conceptual view, similar to that of fjords, is that the overdeepened basin is located along structural trends more susceptible to erosion than surrounding rock (Holtedahl, 1967; Roberts and Rood, 1984). Since Goletas Channel structural trend is oriented northwest, similar to Nahwitti Lowland's structural trend (Armstrong et al., 1985; Rohr and Currie, 1997), selective erosion has likely been important to orientation. To the northwest, Goletas Channel opens onto Cook Bank and physiography becomes less confined. The shallow bathymetry is thought to be a bedrock threshold (sill), marking a location where ice that once flowed through Goletas Channel spread out, therefore having a less erosive effect. In addition to a bedrock

threshold, a glacial origin is supported by glacial striations found onshore (Dawson, 1886) and glacial deposits on Cook Bank (Luternauer et al., 1989a) and northern Vancouver Island (Hebda, 1983; Howes, 1981a,b, 1997).

During the Fraser glaciation the Cordilleran Ice Sheet flowed westward from the mainland, across southern Queen Charlotte Strait and then toward the northwest onto Vancouver Island (Howes, 1997). For the Cordilleran Ice Sheet or any previous ice sheet complex impinging on Queen Charlotte Strait, the least obstructed passage to the Pacific Ocean would have been through Queen Charlotte Strait, inferring a possible direct feed of ice to Goletas Channel during any prior glacial period. A thermochronologic study in the Coast Mountains suggests fjord erosion was highest during Late Pliocene onset of Northern Hemisphere glaciations, increasing by a factor of six during glacial periods in comparison to interglacial periods (Shuster et al., 2005). Similarly, it is likely that erosion in Goletas Channel has glacial origins, sustained directly by glaciers fed from ice sheets that once formed on the Coast Mountains.

The asymmetry in the transverse cross-sectional profiles of Goletas Channel basin walls (Figure 4.2) may be related to contrasting lithology or ice-flow conditions on each side of Goletas Channel. Transverse cross-sections show a contrast between slopes of the north facing basin walls (adjacent Vancouver Island) with the steeper south facing basin walls (adjacent Hope and Nigel Islands) and suggests a complex relationship between past ice streams and erosion. Two contributing factors to consider include ice flow direction and bedrock composition. Glacial striations on northern Vancouver Island suggest north

directed ice flow near Shusharti Bay and northwest directed ice flow adjacent Hardy Bay (Dawson, 1886). Lithology of north facing basin wall is igneous extrusive bedrock, contrasting with that of the south facing basin wall, composed of igneous intrusive bedrock. In general, igneous intrusive rocks are considered more resistant to weathering; however, resistance to weathering is also dependant on mineralogy, internal structure and post crystallization shearing, which have not been studied in the region. There are also a number of important factors that affect erosive efficiency of an ice stream including ice thickness and density, velocity of ice streams, rock fragment content and distribution within ice streams (Boulton, 1974). Due to the complexities of glacial erosion, evidence to provide explanation for the basin asymmetry is rather inconclusive.

5.2 Southeast Goletas Channel

The contrasting textures observed between basin walls and basin floor from Goletas Channel multibeam bathymetry are consistent with lithology contrasts. Rugged bathymetry along previously glaciated coasts is usually confined to coastal regions where basement rocks outcrop (Shaw, 2008). Where thin blankets of glaciomarine mud deposited from meltwater are present it often mimics the underlying relief. Offshore, bedrock is mantled by glacial and postglacial unconsolidated sediment, and relief is low.

As such, widespread rugged patterns in multibeam bathymetry of basin walls represent areas with little or no sediment accummulation, whereas smooth basin floor multibeam bathymetry indicates thicker sediment cover. In many locations sediments are draped into structural low relief pockets between higher relief, relatively sediment bare, bedrock

peaks that continue down slope through structural valleys onto the basin floor. The significance of this observation is likely related to lower ocean current velocities in structural valleys, leading to increased sediment deposition. Accordingly, undulating basin floor contourites (moats and mounds) are thought to be an indication of sedimentation transport processes. Shallow sediment lithology interpretation of Huntec seismic profiles collected from Goletas Channel elucidate more on the subject of basin floor sedimentation.

5.2.1 Shallow sediment lithology interpretation

Although there are no core samples from the basin floor of southeast Goletas Channel, Huntec seismic profiles help delineate lithology. In the interpreted profile shown in Figure 4.5, seismic facies B likely represents a massive organic mud unit based on its low amplitude reflection signature (Judd and Hovland, 1992). In seismic facies A, little structure can be distinguished because of acoustic turbidity, thought to be the product of scattering of acoustic energy by interstitial gas bubbles in the sediment. Gas charged sediments found in fjord environments are assumed to be of biogenic origin, usually caused by biogenic gas from bacterial degradation of organic material at low temperatures (Fleisher et al., 2001). Another derivation for the acoustically turbid character to be considered is lithology change, whereby a mud unit overlies a continuous gravel unit.

The discontinuous seismic reflections of increased intensity located throughout facies B are possibly enhanced reflectors caused by gas migration into a bedding interface. In

places, the enhanced reflectors can be observed to cut across acoustic turbidity of facies A (exemplified by the expanded portion of profile in Figure 4.5), thus indicating that the seismic signatures of facies A and facies B probably do not represent separate lithologies. The poorly defined transition between facies A and facies B is considered due to variable gas seepage in an organic rich mud unit and is not thought to be a stratigraphic horizon. There are no indication of pockmarks on the seafloor, suggesting gas seepage remains within the subsurface.

An alternative interpretation of the discontinuous beds (enhanced reflectors) originating from high-energy sediment transport processes, such as marine sediment gravity flows, seem unlikely and inconsistent with the setting. Most central areas of deep fjord basins are flat lying and exhibit smooth bathymetry, indicating low energy conditions associated with sedimentation originating from surface plumes.

Contourites

The geometry associated with the contourite patterns (mounds and moats) in Figure 4.3 are thought to be related to tidal current action within the basin. A possible explanation for the landforms may be related to channel constriction during ebb and flow of tides, which trap tidal edge waves at the basin wall causing wave refraction. In this way higher tidal amplitude along the edges of the basin walls are counter balanced by higher currents at the junction of the basin wall and basin floor, resulting in erosion of moats. The contourite landforms are conspicuously absent within 15 km of the basin mouth in northwest Goletas Channel, suggesting contrasting ocean dynamics between northwest and southeast basin.

Timing of formation of the contourite landforms cannot be constrained by seismic data alone. Subbottom structures in seismic profile are concealed by gas in a mud unit dispersed on the basin floor. Therefore, it is unknown whether the mud unit is a sediment fill for previously carved contourite structures or if contourite structures are carved directly into the mud unit.

5.3 Northwest Goletas Channel

A transition is observed in multibeam bathymetry of northwest Goletas Channel, with a gradual increase in sediment deposition from ~ 10 km south of the basin mouth (Figure 4.1). The transition to more sediment deposition on the flanks of the basin walls likely indicates proximity to sediment supply of Cook Bank. Scarps and channels of the basin mouth adjacent Cook Bank suggest dynamic sediment processes, and are also supplementary evidence of a nearby sediment source.

Mass sediment slides are apparent from basin mouth bathymetry, characterized by well-defined headwalls, defined by a steep slope rising at the head of each channel, with straight or slightly concave scarps and channel incisions (Lee et al., 2007). Whether a slide stops a short distance along a rupture surface or turns into a turbidity current which travels great distances is dependant on in-place stress, sediment properties, and morphology of the failed mass (Lee et al., 2007).

Morphologic elements, such as channels carved into the basin's headwalls and along the basin floor, and the absence of a sediment mass at the base of either headwall, suggest sediment from slides travelled as turbidity currents. Turbidity currents are completely turbulent, dilute mass concentrations of density driven sediment that continue movement by entrainment of seafloor sediment (Parson et al., 2007). As the turbidity currents moves downslope it loses sediment on the channel levees, increasingly confining itself with time (Kane et al., 2008).

The vertical v-shaped incisions identified as dendritic gullies in Figure 4.6 are characteristically defined by narrow leaf-like erosional patterns that intersect turbidity current channels at high angles (Parson et al., 2007). Headwalls are sharply defined, and are apparent as irregularities in the otherwise smooth basin wall, which is evidence of small-scale slides. Dendritic gullies are thought to form when turbidity currents flow through the channel thalweg undercutting basin slope sediments creating a slide, which also feeds sediment to the channel (Parson et al., 2007).

Channel Development

Multibeam bathymetry shows that the channels do not follow a straight line, but have complex patterns. The gradient of channel thalweg 1 changes in the downslope direction, with a transition at 160 m water depth, approximately 3 km along the channel profile (between section 2 and 3 in Figure 4.7) from a concave slope (decreasing slope) to a convex slope profile (increasing slope), which correlates with a decrease in sinuosity.

A possible explanation for the change of slope and sinuosity is notable from mutibeam bathymetry (Figure 4.6). The basin geometry is most narrow at the point where channel thalweg 1 slope and sinuosity changes, and may have acted as a bottleneck for sediment movement during turbidity current flows, thus impacting development.

Headwall development

Differences in character of each profile in Figure 4.7 likely reflect contrasting development processes across the mouth of Goletas Channel for each of the channels. Analysis of gradient for the headwall of each channel indicates poorly defined scarps and lower gradient channels through headwalls in channels 1 and 2 in contrast to channels 3 and 4. The lower gradients indicate an erosional episode, although is not evident whether slides caused headward erosion of slopes, or if erosion by river drainage when sea level was lower caused headwall erosion.

5.3.1 Shallow sediment architecture interpretation

Findings from piston core 2007007PGC-005 and seismic profile b – b' support the interpretation of a turbidity channel through the basin mouth of Goletas Channel. In the seismic profile, channel deposits can be recognized by high amplitude channel facies through each thalweg (Walker, 1992). Also, facies C has a high reflection amplitude and discontinuous non-parallel beds characteristic of sediment successions from lateral overflow onto the channel margin.

The sharply defined and irregular interface of facies B and C is discontinuous, likely representing an unconformity. The location of the unconformity correlates with the upper part of a possible "channel segment" in multibeam bathymetry (Figure 4.6), which is also denoted on the interpreted Huntec seismic profile of Figure 4.9, indicating that the unconformity may be representative of another turbidity current channel.

5.3.2 Shallow sediment lithology interpretation

Core 2007007PGC-004

Though validity of piston core 2007007PGC-004 is questionable, the massive sand unit may be representative of sediment deposition preserved on smooth bathymetric surfaces flanking basin walls in northwest Goletas Channel. The deposition of massive sand is consistent with paraglacial sediment deposition during waning ice conditions at the end of the last glaciation. Thick near shore successions are associated with higher yield river drainage during glacial retreat than at present, consistent with previous findings from Cook Bank (Luternauer et al., 1989a,b; Barrie, 1991). Isostatic rebound at the end of the last glacial cycle is associated with sea level regression and caused rivers to drain and disperse sediment onto the outer edge of Cook Bank. Subsequent sea level transgression caused further reworking of sediments distributed during low stand conditions.

Core 2007007PGC-005

Piston core 2007007PGC-005 is interpreted as a sediment succession representative of an environmental transition in the basin. The core location correlates with upper strata notable in Huntec seismic of channel margin facies C in seismic profile b - b' (Figure 4.9). The record indicates lateral turbidity current spill-out onto the channel margin as laminae of poorly sorted clayey silt, onto normally graded (fining upward) sediment.

-Normal graded sediment

The record of normal graded sediments in piston core 2007007PGC-005 is consistent with deposition during the paraglacial to postglacial transition. Thick near shore successions of sand in Queen Charlotte Sound and Cook Bank have been determined to represent higher yield river drainage during glacial retreat in a paraglacial environment during the Late Pleistocene – Holocene transition (Luternauer et al., 1989a,b; Barrie, 1991). Paraglacial deposition is also associated with isostatic rebound and sea level regression. With lower sea levels, rivers were forced to drain and disperse sediment onto the outer edge of Cook Bank. Subsequent sea level transgression is associated with reworking of sediment distributed during low stand.

The transition to mud observed in the upper part of core 2007007PGC-005 is thought to represent the transition to post-glacial conditions existing by early Holocene in Goletas Channel (Barrie, 1991). The unit represents an influx of organic rich muds, associated with hemipelagic sedimentation.

-Interlayered laminae and basal unit

The interlayered laminae observed in piston core 2007007PGC-005 are thought to represent turbidity current spill over of the channel margins. The basal bed of piston core 2007007PGC-005 may represent a larger turbidity current than represented by laminae of clayey silt found interlayered throughout the piston core. The basal unit contains poorly sorted sediment up to gravel grain size and the malacological assessment encompasses intact and fractured shells from a broad range of environments including assemblages that inhabit sandy and rocky regions of coast. A possible implication being that the basal unit represents a stronger, more voluminous, or less confined turbidity current than represented by the other laminae found in the core.

Channel overflow deposits are common with turbidity current channels and have been noted in channel margins on other parts of the British Columbia coast such as in Knight Inlet on the mainland coast (Ren et al., 1996). In Knight Inlet, submarine levees were found skirting the channels, representing occasional overflow of the channel margins. The margins contain muds and sandy mud laminae (layers from less than 0.25 cm to 1.5 cm thick) interstratified in 'normal' fjord muds. The findings in Goletas Channel are analogous, showing that occasionally coarser sediment of turbidity currents spilled out laterally from the channel onto the channel margins.

'Normal' sedimentation in piston core 2007007PGC-005 is thought to be a record of paraglacial to postglacial transition. The record indicates that turbidity current flows through the channel have been active since Late Pleistocene - Holocene and may have

been active previously. Channel overflow interruptions from 'normal' sedimentation are irregular through the sediment record, with an implication that millennia may pass between turbidity current overflow events.

5.3.3 Sediment processes

Potentially, there are a number of mechanisms that may have induced turbidity currents in Goletas Channel's history, involving high sediment deposition, sea level change, sediment redistribution by tidal currents and storm waves, and earthquakes. Because the environmental setting has changed through time in Goletas Channel, it has been more susceptible to slides at certain episodes of its history. The following scenarios deal with possible triggering mechanisms that may have caused sediment destabilization in Goletas Channel.

Scenario 1: Glacial Retreat

Ice is thought to have remained longer on Cook Bank than in surrounding waters, depositing thick beds of till in its wake (Luternauer and Murray, 1983). Research from the Antarctic has shown that during glacial retreat ice sheets are expected to retreat slower on banks than in adjacent troughs, with the effect of depositing thick accumulations of sediment on the higher ground (Thomas and Bentley, 1978). High sedimentation rates and glacial destabilization at the culmination of the last glacial cycle would have promoted sediment instability and slides for sediment near the basin mouth of Goletas Channel. Sediment from piston core PGC007007-005 does not exhibit glacial sedimentation; however, considering the relatively shallow penetration depth of PGC007007-005, it is possibile that the entire levee building history of Goletas Channel

is not exhibited by the core. Deeper core penetration may be necessary in order to discover if channels were active during glacial retreat.

Scenario 2: Sea level transition - physiographic change

A sudden and dramatic environmental change from a low energy embayment to high energy modern conditions affected northeast Goletas Channel during Late Pleistocene-Early Holocene sea level rise, with the implication of creating sediment instability. Figure 5.1 is a simulation of sea level transgression from a position of 100 m below present in the late Pleistocene to modern conditions, dating between ~ 10,500 ^{14}C yrs BP to ~ 8,000 ^{14}C yrs BP, whereby northeast Goletas Channel was transformed from an embayment to an open but constricted waterway to Queen Charlotte Sound. When sea level was < 10 m lower than present, Goletas Channel would have been an embayment with a boundary separating it from Queen Charlotte Sound. Sea level transgression over Cook Bank caused waves and tidal currents to sweep over Cook Bank causing erosion and reworking of sediments deposited during low stand conditions (Luternauer et al. 1989b) and possibly increasing susceptibility to sediment instability and slope failures.

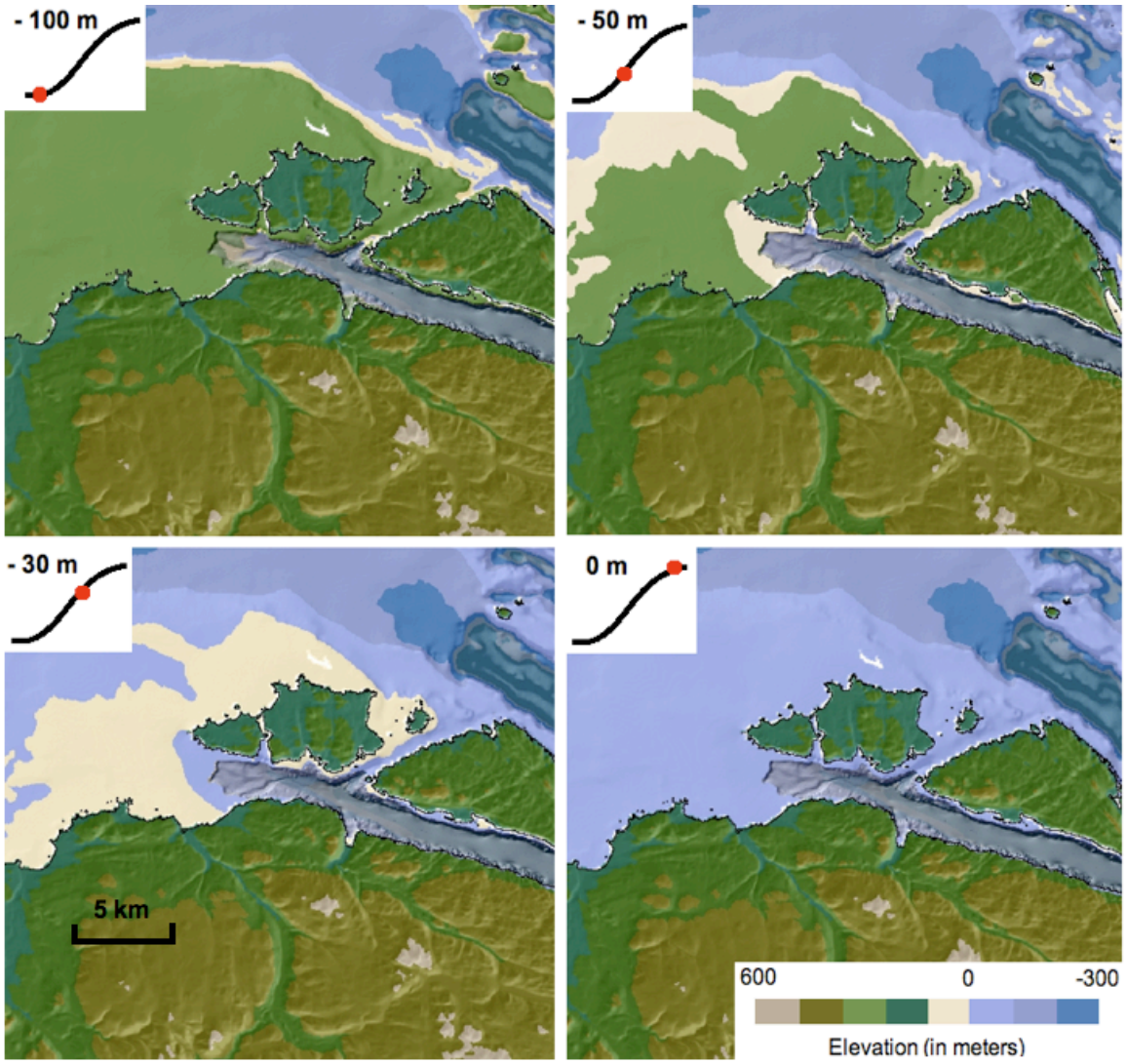

Figure 5.1 : A simulation of sea level progression in northwest Goletas Channel depicting transgression over Cook Bank ~ 10,500 ^{14}C yrs BP to ~ 8,000 ^{14}C yrs BP, from 100 m below present to modern sea level elevation. Sea level position from low stand to high stand is indicated in top left corner for each increment of the succession.

Scenario 3: Sea level low stand - narrow shelf sedimentation

During low sea level stand, rivers bypassed deposition to Cook Bank, instead depositing sediment to locations that are currently submersed and offshore, such as steep and narrow shelf locations (Luternauer et al., 1989a,b; Barrie, 1991), thus increasing susceptibility to slope failure. There is indication of relict river beds with a Cook Bank origin in the basin

mouth of Goletas Channel, evident from prominent headwall erosion in channels 1 and 2 (Figure 4.6). The combination of conditions, including low sea level stand, high sedimentation rates contiguous with a paraglacial environment, and steep unaccommodating environment for sediments at the basin mouth, may have contributed to sediment instability and slope failures.

Scenario 4: Sea level transitions - hydrostatic pressure changes

Sediments distributed on a slope are susceptible to instability during sea level transitions when hydrostatic pressure gradients of the ocean change, thereby effecting interstitial pore pressures (Lee et al., 2007). For sediment on a slope, shear resistance is reduced when hydrostatic pressure gradients are shifted as during a sea level transition, which is accompanied by pressure reorganization within the sediment column. Changing hydrostatic gradients during sea level transgression or regression can be a driving stress that triggers sediment failure and/or makes sediment more susceptible to any other driving stress.

Scenario 5: Sediment accretion

Reworked sands on Cook Bank have potential to accrete and lead to failures along its edges. This process may involve temporary stability as sediment accumulates along the shallow Nahwitti Bar at the basin mouth, followed by failure and a turbidity current event. Sediment redistribution is an ongoing post-glacial process, indicated by sand megaripples on Cook Bank with sediment migration away from the bank top (Barrie, 1991). Strong tidal currents (5.5 m/s) may be a catalyst for sediment redistribution across

Nahwitti Bar, which is a shallow sill ~ 9 m below present sea level (Triton Consultants Ltd., 2002).

An analogous process in Knight and Bute Inlet located along the central British Columbia coast involves temporary sediment accumuation in river mouth bars leading to intermittent turbidity current activity (Bornhold et al., 1994). Turbidity currents in Knight and Bute Inlet correlate with peak river discharge of the late summer months, attributable to high yield rivers fed by snow and glacier melting (Ren et al., 1996). In contrast, sediment yields for rivers into Goletas Channel are thought to be low (Barrie, personal communication, 2009). Intermittent turbidity currents into Goletas Channel may be related to tidal current and wave activity over Cook Bank analogous to Knight and Bute Inlet. This model requires monitoring of sediment accumulation and turbidity channels for further assessment.

Scenario 6: Earthquakes

An alternative possibility may involve earthquakes triggering mass sediment transport independent of sea level change. Though no major earthquakes have been recorded in the sediment record of central British Columbia, paleoseismic studies are ongoing in Frederick Sound located along the coast of Central British Columbia (A. Dallimore, personal communication, 2010). Earthquakes are thought to be related to sediment failures in the form of debris flows in Saanich Inlet on southern Vancouver Island (Stevens et al., 1997) and in Effingham Inlet on Vancouver Island (Dallimore et al.,

2007), and the potential exists for a similar relationship for initiation of turbidity currents in Goletas Channel.

5.4 Hardy Bay

The overall morphology of Hardy Bay is observed in multibeam by its depressed v-shaped geometry, which is a continuance of an onshore valley that deepens toward the northwest into Goletas Channel. The v-shaped geometry is given a non-genetic landscape classification of “submarine valley” because genetic terminology does not exist for such a structure. Since elongate depressions on land are referred to as valleys regardless of their mode of origin, it seems justifiable to use the term "submarine valley" in referring to the undefined types of elongate depressions that cut the continental shelf. The three smaller inner basins within the submarine valley likely have genetic affiliations related to glacial erosion along structural trends whereby erosion occurs along areas of weakness in the bedrock. Textures observed in multibeam bathymetry correlate with surface lithology just as in Goletas Channel. Angular geometries and textures suggest bedrock, and in general, smooth textures on gently sloping landscape represent areas with sediment cover.

Valley glaciers were prevalent on northern Vancouver Island during the Wisconsinan glaciation, and would have been dependant on ice sheets for sustenance (Howes, 1981a,b, 1997). Hardy Bay acted as a corridor for ice to Goletas Channel, and originated from some combination of structural trend or fault erosion by glaciers. During ice sheet recession, it is seems likely that any valley glacier would have become stagnant. As the rate of ice supply diminished or the rate of melting increased, snout recession would have resulted. The snout location, at the front of the valley glacier where supply and loss

counterbalance one another was displaced up-valley during recession until balance was achieved.

5.4.1 Shallow sediment architecture interpretation

The Huntec DTS seismic profiles c - c' (Figure 4.14) and d - d' (Figure 4.15), collected over the terrace landform, appear to contain features related to glacial and post-glacial environments, and provide important information for characterizing the terrace structure. Facies A is thought to represent bedrock because angular geometry associated with ridges were observed in multibeam that correlate with ridge location in seismic profile d - d' (Figure 4.15). Acoustically turbid facies A is perhaps related to Tertiary volcanics of the Vancouver and Bonanza Group previously mapped in the region (Armstrong et al., 1985).

Outcroppings of bedrock may be notable in the seismic survey by high amplitude acoustically turbid signature. One bedrock ridge breaks the surface in seismic profile d - d' (Figure 4.15). However, the boundary between bedrock and diamict are poorly defined because both produce acoustically turbid reflection signatures. Lower amplitude seismic signature and more gradual slopes are affiliated with diamict of facies B. Terrestrial deposits of glacial till are found on adjacent shores of northern Vancouver Island (Howes, 1981a,b) and are likely correlative to offshore Facies B, having genesis affiliated with direct deposition from a valley glacier.

5.4.2 Shallow sediment lithology interpretation

Facies C, as observed in Huntec seismic profile, is represented in piston core sample PGC2009003-008. The continuous bedding and high amplitude signature in seismic profile, is represented by sand and clay units from the core. This facies is capped by a modern mud unit, discovered in grab sample but not observed in seismic or core sample, indicating the mud unit is likely very thin.

The lithologies observed in piston core PGC2009003-008 likely represent environmental transitions, with diamict representative of glacial sedimentation, followed by continuous sediment deposition during glacial retreat and sea level change. The upper mud unit likely represents a transition to modern conditions, when river yields decreased due to limited terrestrial erosion, thus correlating with low sediment supply. The interpretation of sequence stratigraphy is better explained with respect to sediment processes.

5.4.3 Sediment processes

Glacial deposition

The terrace in Hardy Bay was likely formed by a grounded ice sheet during a glacial standstill. Glacial origin is supported by both seismic profiles c - c' (Figure 4.14) and d - d' (Figure 4.15) which indicate that the sediment facies associated with the terrace has a signature consistent with diamict. The formation of terraces on grounding lines of ice sheets have been examined on the glaciated shelf of western Antarctica (i.e. Grosswald, 1989). Terraces there are thought to represent sedimentation in front of the grounding line, where bed erosion exerted by the grounded ice sheet gives way to glaciomarine deposition. Interaction with warmer saline waters beneath the floating portion of ice

sheet, located seaward of the grounding line, causes deposition of glacial sediment load in the shape of a terrace (Figure 5.2). Within a stratified water column, when cold fresh water generated by ice overlies warmer saline ocean waters, circulation can be induced by internal gravity waves caused by tidal pumping of the ice sheet. Sea level was 30 m above present elevation after glacial retreat (Hebda, 1983) and implies that the terrace was submersed during formation, which is also common of this type of terrace.

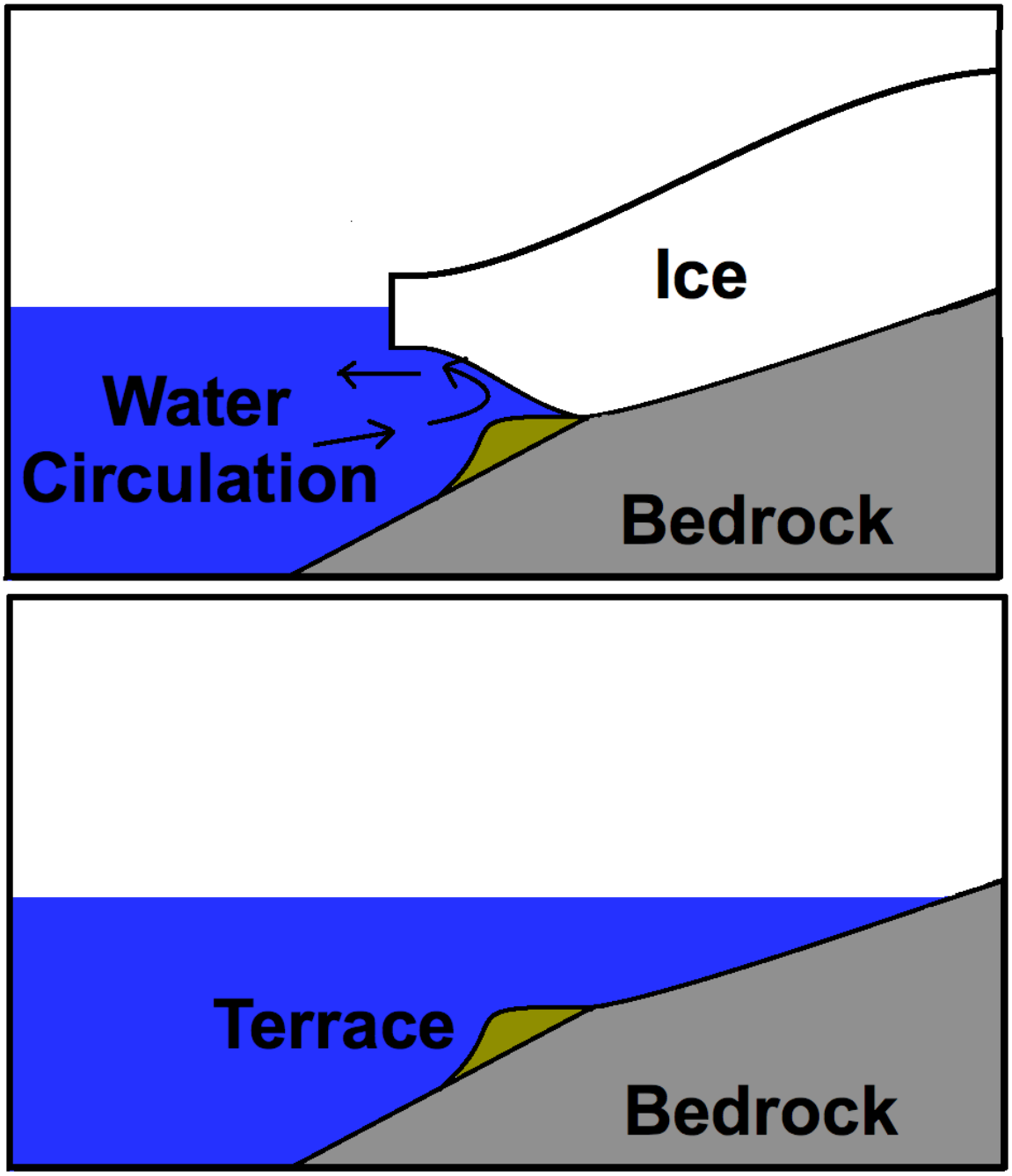

Figure 5.2 : Model of glacial deposition of terraces during rapid ice retreat from Hardy Bay. Upper: Circulation of warmer saline water in under the snout of a glacier replaces colder fresh water melting from ice sheet and results in sediment deposition at the ice grounding line. Below: Relict submarine terrace remains after glacial retreat at the beginning of the paraglacial environment stage (Modified from Grosswald, 1989).

Sea level change

In Hardy Bay, sedimentation overlying the terrace structure represents paraglacial and post-glacial environments. Sediment depositional variations within the sequence are consistent with a sea level change, as well as a singular erosional episode, which may indicate a meltwater outburst flood event.

In seismic profile d-d' (Figure 4.15) the sequence stratigraphy indicated by facies C represents sea level change in a paraglacial environment. Sea level change is represented by an onlap sequence within facies C, located between two limbs where sequence bifurcation is observed. Both limbs were deposited when sea level was higher than seismic collection depths, suggested by conformability and continuity into shallower waters. The onlap sequence represents a strata succession that discontinues shoreward with onlap onto the lower limb of facies C. Onlap positions are very good indicators of sea level still stand elevations (Vail et al., 1977) and suggests genesis during sea level rise from at least 74 m below present in Hardy Bay. The possibility that sea level may have been lower than suggested by the onlap sequence is negated by disruption of the sequence in the form of an unconformity that eliminated any evidence of a lower sea level boundary. The top bifurcation limb represents subsequent deposition after formation of the unconformity.

The sediment sequence in core 2009003PGC-009 may be representative of onlapping as seen in seismic profile d - d' (Figure 4.15) and reflect short-lived sea level still stands before sea level rise to modern elevations. The clay beds in core 2009003PGC-009

suggest deposition in a low-energy setting. Each clay bed is followed by sand, which represents environmental change from low-energy deposition back to high-energy deposition. In respect to an onlapping sequence, this section may be interpreted as a series of incremental sea level transgressions followed still stands. After each transgression a sand aggradation in deeper water would occur, resulting in shallowing, a lower energy environment, and a transition to clay deposition would be possible. This interpretation is viable if the rates of sea level regression caused by rapid isostatic rebound in response to deglaciation had slowed and were being surpassed by the rate of eustatic sea level rise. In other words, this sequence may represent a transition from isostatic sea level regression dominance to eustatic sea level transgression dominance. Hardy Bay had deglaciated prior to 13,630 C^{14} yrs BP (Hebda, 1983), which temporally corresponds with a eustatic sea level of at least 80 m below present, suggesting this hypothesis is compatible with previous findings.

The timing of sea level low stand can be estimated from interpreted stratigraphy. A rapid isostatic rebound in the range of 100 m in the first couple millennia after glacial retreat would have been necessary in order to explain the sea level regression. This corresponds with isostatic rebound rates discovered in other locations along the British Columbia coast (i.e. Clague et al., 1982). It must be noted that the dates eluded to in Figure 5.3 are not well constrained. For example, the terrestrial organic sample collected from 30 m above present sea level in Hardy Bay and dated to 13,630 C^{14} yrs BP represents initial terrestrial organic growth after glacial retreat, however there is no conclusive indication (ie. foram tests) that underlying silts were marine in origin. There is clear evidence to the

south that late-glacial sea levels were at least 53 m higher (Howes, 1981). Since the lowstand stratigraphy observed in seismic has not been radiocarbon dated, the timing is loosely constrained within 1-2 millennia of glacial retreat based on similar sea level curve trends on the British Columbia coast (ie. Clague et al., 1982). Also, the lowstand onlap strata is considered to represent a maximum sea level regression of 74 m since the wave base defining its deposition depth may have been as much as 10 m (J. Harper, personal communication). Accordingly, the additional low stand datum and sea level reconstruction for Hardy Bay is presented in Figure 5.3.

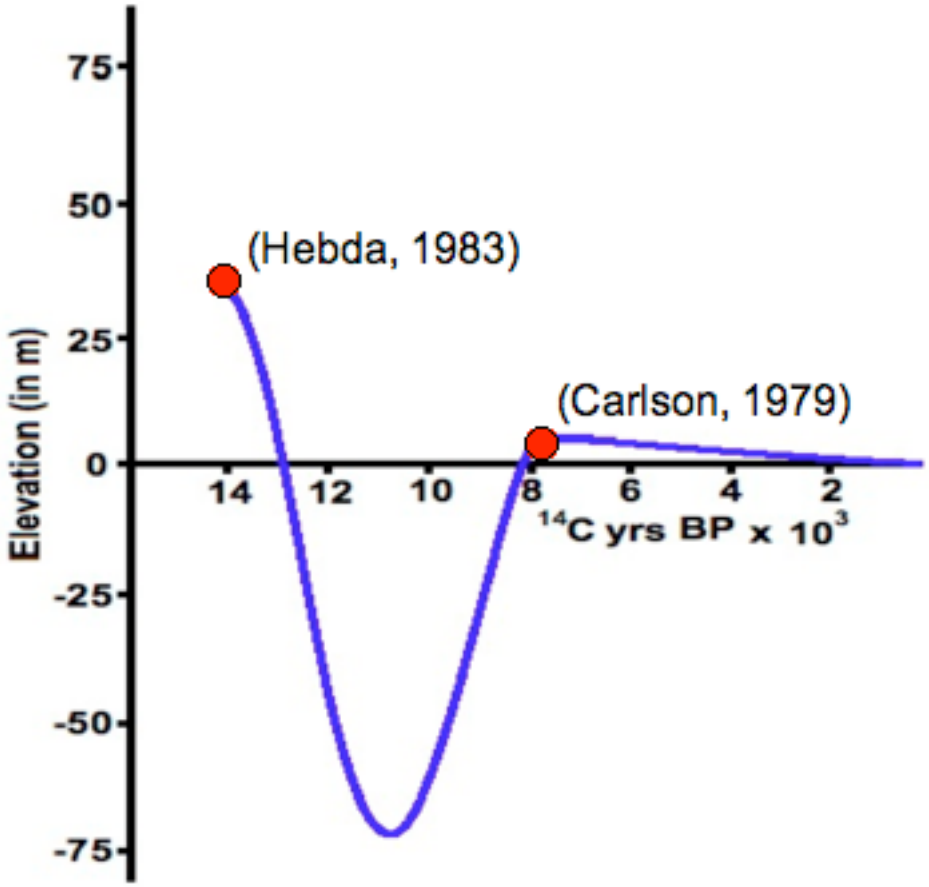

Figure 5.3 : Sea level reconstruction for Hardy Bay with high stand constrained by previous coastal research (i.e. Hebda, 1983; Carlson, 1979) and an interpretation of low stand from seismic data.

Meltwater Outburst

Though the relationship is ambiguous, an erosional event is apparent from seismic profiles and may have been widespread throughout Hardy Bay. The episode is evident from seismic profile d - d' (Figure 4.15) by a cross-cutting unconformity in stratigraphy across the discontinuous onlap sequence located above the slope break of the terrace structure. In seismic profile c - c' (Figure 4.14), located south (landward) of profile d - d', only the correlative strata from the upper limb of facies C is recognized, provoking the question, what happened to the onlap strata and lower limb of facies C in seismic profile c - c'? There are two possibilities: a) lower strata was not deposited or b) lower strata was eroded. Scenario a) is considered unlikely, as deposition should have been high in the vicinity of a downwasting valley glacier during a period of paraglacial sedimentation. Scenario b) indicates that erosion was more pronounced landward, resulting in complete erosion of strata above and below the terrace in profile c - c', whereas remnants of strata remained preserved in profile d - d'. One possible explanation for this erosion pattern is a meltwater outburst, with flooding focused near the inner reaches of Hardy Bay.

Since the unconformity is located above onlap stratigraphy, yet paraglacial sedimentation is observed above the unconformity, the timing of the event likely correlates with paraglacial conditions. Rapid isostatic rebound had slowed and rates of eustatic sea level rise were more prominent at the time. Valley glaciers were prominent on northern Vancouver Island, and though ice may have retreated from the Hardy Bay, inland glaciers may have existed for a number of millennia. From stratigraphy alone, the timing can only be speculated, but the event likely occurred within a couple millennia of initial

deglaciation 13,630 C^{14} yrs BP.

Glacial lake meltwater outbursts occur after the glacial walls containing a lake fail and abruptly release large volumes of water - this is a relatively common event in areas of glacial downwasting (i.e. Georgia Basin, British Columbia (Conway et al., 2001), Lake Missoula, Washington State (Wait, 1980). Previous research on Nahwitti Lowlands of northern Vancouver Island shows that the region exhibits kettle landforms (Hebda, 1983), fluvioglacial landforms which can result from ice calving and burial in sediment during flood events during sudden drainage of ice-dammed lakes (Rushmer, 2006). Kettle landforms can also form during in-place melting of ice blocks on a glacial outwash plain. Though evidence of kettles on northern Vancouver Island is consistent with a meltwater outburst event, further study is needed.

Oceanographic processes were considered as an alternative possibilities for the unconformities observed in sequence stratigraphy from Huntec seismic. Hardy Bay is an environment with low energy tidal processes because of the unrestricted connection to Goletas Channel, making it conducive to weak tidal currents. Wind waves are also not thought to be significant in Hardy Bay because its sheltered location also provides protection from dominant wind directions (R. Thomson, personal communication). Though there is tidal dominance in Hardy Bay, effects of oceanographic processes on sequence stratigraphy were likely not as dominant as allogenic processes, such as changes in river yield or sea level variation, during formation of the sequence stratigraphy observed in Hardy Bay.

5.5 Shusharti Bay

The elongate depression geometry of Shusharti Bay is a submarine valley, similar to Hardy Bay, however it is given a landscape classification of hanging submarine valley because of the high relief of the lower slope break above the basin floor of Goletas Channel (Vorren, 2003). Hanging submarine valleys are a product of tributary glaciers formed by ice streams smaller than the trunk glaciers. When the eroded trough fails to deepen to the depth of the main trough it forms an over-hanging valley. During retreat of the ice-stream an ice dam in the valley would have collapsed after losing support from the main trough ice stream and downwasted rapidly.

The upper plateau and upper slope break in Shusharti Bay has terrace geometry, however its origin is ambiguous and may or may not have a similar origin as the terrace in Hardy Bay. The landform is about 250 m wide, with a poorly defined discontinuous slope break, with separate small scale ridges formed on its crest and slope. Multibeam bathymetry is absent of angular textures associated with bedrock, though bedrock may be shallowly buried within the subsurface. As the landscape is considered to have a glacial origin, it is possible that the terrace landform, ridges and other mounds have a glacial origin, and may be a result of erosive spurs resulting from abrasion by a powerful ice tongue. Other possible origins for the terrace in Shusharti Bay include deltaic processes from sediment deposition in a paraglacial environment while sea level was lower, in which case the first slope break might represent the clinoform wedges formed on a beach during sea level rise, or a submarine fan delta (i.e. Mosher and Hewitt, 2004). Also the terrace could be a result of sediment draped over bedrock ridges, which would explain the discontinuous nature of the slope break. Terraces can form during various processes, and in the absence

of constraining data results remain inconclusive. Further study using ground truth methods would be useful in resolving seabed character and geomorphology in the area.

The submarine valley in Hardy Bay and the hanging submarine valley in Shusharti Bay have glacial origins similar to the fjord-like trough in Goletas Channel. Glacial environments in the past have undoubtedly had an impact on the marine valleys, based on sediment deposition and striations found in the adjacent landscapes (Dawson, 1886; Howes, 1981a,b, 1997; Hebda, 1983). While the valleys are considered to have acted as a corridor for ice to Goletas Channel, the origin of these valleys likely include some combination of structural trend erosion or faulting, fluvial erosion by oceanic processes or rivers, and glacier erosion.

Chapter 6 – Conclusions

1. Three of the main landforms from the study region have geometries and ground truth signatures common with mass sediment transport, contourites, and terraces. The landforms suggest that the physiography of Goletas Channel developed in a dynamic environment, influenced by changing sea levels, oceanographic processes, and varying rates of sedimentation during the transition from Fraser Glaciation to modern conditions during the Holocene. Table 6.1 provides an overview of landform structures of geological interest from each of the landscapes described.

Table 6.1 : Landscape, landform structures and morphologic elements for classification of Goletas Channel study region.

Landscape structure	Landscape Morphology	Landform structure	Landform Morphology
Fjord-like Trough (Goletas Channel)	U-shape, narrow, deep basin	Turbidite Channel	Gully, Scarp, Channel
		Contourites	Mounds and moats
Submarine Valley (Hardy Bay)	Seaward sloping depression	Terrace	Extensive shelf plateau, shelf break, and shelf slope
Hanging submarine Valley (Shusharti Bay)	Seaward sloping depression, intersects deeper basin above its floor	Terrace	Extensive shelf plateau, shelf break, and shelf slope

2. Goletas Channel likely formed as a glacial trough morphologically related to fjords on the inner coast. Large-scale geometries include a narrow and deep basin with a threshold located on the edge of Cook Bank. The basin has eroded during glacial activity, probably since the Late Cenozoic. Glacial ice may have followed a physiographical outlet to the

Pacific, which likely formed along a geological trend. Hardy Bay and Shusharti Bay appear to also have origins related to glacial erosion and tectonic trends. However, with each landscape studied an enigmatic relationship exists between geological trend locations and ice erosion.

3. There are contrasting sediment transport and deposition processes between northwest and southeast Goletas Channel. This is defined in the northwest by higher accumulation on basin walls and mass sediment transport, identified by channel landforms and turbidite sedimentation. In the southeast sediments are thinly distributed on the basin walls, and moat and mound landforms have formed on the basin floor. Difference in sediment distribution likely represents lower sediment supply in southeast Goletas Channel and contrasting ocean dynamics.

4. When turbidity current channels exist in fjords they are normally located at the head of the basin. However, in consideration of this perception of fjord dynamics the basin in Goletas Channel is reversed. It is a unique situation that the positions of the turbidity current channels are located at the mouth of the basin, at the margin where a sill separates the basin from the ocean. This is accomplished in spite of the absence of a high sediment yield river regime, reflecting complexity in the processes taking place, which had to change as the setting conditions evolved - a compulsory condition for explaining the sequences noticed in core samples. Mass sediment transport has been active near the basin mouth in Goletas Channel, triggering turbidity currents and resulting in channel landforms since Late Pleistocene. Likely triggers for sediment instability are high

sedimentation deposition rates at the basin mouth, sea level change, tidal currents, ocean waves, and earthquakes.

5. Turbidity current channels formed in paraglacial and post-glacial sediments of northwest Goletas Channel. Core 2007007PGC-005 from the channel margin suggest that sediment failures occurred during sea level rise over Cook Bank and imply millennium scale frequency of channel margin overflow. Frequency of turbidity current events may have been higher in the channels, since overflow deposition studied from the channel margin does not necessarily reflect event frequency inside the channel.

6. Tidal currents on the basin floor of Goletas Channel are likely responsible for the formation of contourite landforms. Postglacial sedimentation is associated with organic mud, forming interstitial subsurface gas observed throughout the Huntec seismic survey of the basin floor.

7. Sediment deposition in Hardy Bay provides an important record of sea level transition for northern Vancouver Island. Previous research of terrestrial deposition suggests that sea level was about 30 m above present prior to isostatic rebound 13,630 ^{14}C yrs BP (Hebda, 1983). Observations from seismic stratigraphy in profile d - d' (Figure 4.15) of this study shows that during isostatic rebound sea level regressed to at least 74 m below present in Hardy Bay. The timing of this sea level low stand needs to be constrained, but considering rates on other parts of the coast sea level low stand was likely reached within a millennium of ice dispersal from the coast. A eustasy dominant transgression

subsequent to isostatic rebound occurred prior to 8,020 ^{14}C yrs BP; thereafter, during mid to late Holocene, tectonic uplift has been a catalyst of sea level regression from ~3 m above present in the Hardy Bay region. (Sea level curve for Hardy Bay is shown in Figure 5.3.)

8. A grounded valley glacier in Hardy Bay is likely responsible for diamict sediment deposition and resulted in formation of the terrace landform. A terrace landform is also recognized in Shusharti Bay, however more evidence is needed in order to interpret its origin.

9. The stratigraphy observed in seismic profile from Hardy Bay includes an erosional unconformity. One possible explanation for the erosional event is meltwater outburst from downwasting ice on the Nahwitti Lowlands, however evidence is lacking. The unconformity is observed within the stratigraphy associated with sea level change, and appears to have interrupted a portion of the sequence. Best estimate for timing is within a few millennia after initial ice retreat from Hardy Bay, which occurred prior to 13,630 ^{14}C yrs BP (Hebda, 1983).

10. Implications of this study on other disciplines:

-Tectonic modeling: A sea level low stand of 74 m, from Hardy Bay is the only submarine sea level low stand estimation for over 250 km along the east coast of Vancouver Island between Cook Bank and Straight of Georgia. This sea level datum point provides information for lithosphere response to a load, which is important for

parameterizarion of the lithosphere in the region and may prove valuable for modelers of tectonics.

-Archaeology: Because subaerial ancient archaeology sites have been discovered on adjacent shores of Hardy Bay (dating to 8,020 ^{14}C yrs BP), the foregoing circumstance of a sea level transgression from 74 m below present implies relict coastlines existed on the coast in locations that have been submersed, which provides potential target information for finding undiscovered archaeology sites predating the known record in the area. Predating archaeology sites have the potential to provide artifacts from the earliest ancient cultures living on the coast of British Columbia.

-Infrastructure: Alternative energy assessments have discovered potential for tidal energy production over the Nahwitti Bar, on the edge of the basin mouth of Goletas Channel. Any future development should be aware of the record of sediment instability on the basin mouth evident from this studies observation of marine sediment gravity flows, suggesting further hazard assessments of sediment instability are required before infrastructure installation onto the seafloor.

Bibliography

Andrews, J.T. and Retherford, R.M. (1978) A reconnaissance survey of late Quaternary sea levels, Bella Bella/ Bella Coola region, central British Columbia coast; Canadian Journal of Earth Sciences, vol. 15, 341 - 350.

Armstrong, R.L., Muller, J.E., Harakal, J.E. and Muehlenbachs, K. (1985) The neogene Alert Bay vol.canic Belt of northern Vancouver Island, Canada: Descending-plate-edge vol.cansim in the arc-trench gap; Journal of Volcanology and Geothermal Research, vol. 26, 75 - 97.

Barrie, J.V. (1991) Contemporary and relict titaniferous sand facies, offshore British Columbia, Canada; Continental Shelf Research; vol. 11, 67 - 79.

Barrie, J.V. and Conway, K.W. (2002) Contrasting sedimentation processes and sea level changes in two adjacent basins on the Pacific margin of Canada; In: Glacier-Influenced Sedimentation on High-Latitude Continental Margin, edited by Dowdeswell, J.A. and O'Cofaigh, C., Geological Society of London, Special Publication, vol. 203, 181 - 194.

Bornhold, B.D., Ren, P. and Prior, D.B. (1994) High-frequency turbidity currents in British Columbia fjords; Geo-Marine Letters, vol. 14, 238 - 243.

Buckley, D.E., Mackinnon, E.G., Cranston, R.E. and Christian, H.A. (1994) Problems with piston core sampling: mechanical and geotechnical diagnosis; Marine Geology, vol. 117, 95 - 106.

Cannon, A. (2000) Settlement and sea-levels on the central coast of British Columbia: Evidence from shell midden cores; American Antiquity, vol. 65, 67 - 77.

Carlson, C. (1979) The early component at Bear Cove; Canadian Journal of Archaeology; vol. 3, 177 - 194.

Cherniawsky, J.Y. and Crawford (1996) Comparison between weather buoy and comprehensive ocean-atmosphere data set wind data for the west coast of Canada; Journal of Geophysics Research, vol. 18, 377 - 389.

Clague, J.J. and Bornhold, B.D. (1980) Morphology and littoral processes of the Pacific coast of Canada; In: The Coastline of Canada, edited by McCann, S.B., Geological Survey of Canada, Paper 80-10, pp. 339 - 380.

Clague, J.J. (1989) Quaternary geology of the Canadian Cordillera; In: Quaternary Geology of Canada and Greenland, edited by Fulton, R.J., Geology of Canada Series, No. 1, 17 - 96.

Clague, J.J. and James, T.S. (2002) History and isostatic effects of the last ice sheet in southern British columbia; Quaternary Science Reviews, vol. 21, 71 - 87.

Clague, J.J., Harper, J.R., Hebda, J.R., and Howes, D.E. (1982) Late Quaternary sea levels and crustal movements, coastal British Columbia; Canadian Journal of Earth Science, vol. 19, 597 - 618.

Dallimore, A., Enkin, R.J., Pienitz, R., Southon, J.R., Baker, J., Wright, C.A., Pedersen, T.F., Calvert, S.E., Ivanochko, T. and Thomson, R.E. (2008) Postglacial evolution of a Pacific coastal fjord in British Columbia, Canada: interactions of sea-level change, crustal response, and environmental fluctuations – results from MONA core MD02-2494; Canadian Journal of Earth Science, vol. 19, 1345 - 1362.

Dawson, G.M. (1886) On a geological examination of the northern part of Vancouver Island and adjacent coasts; Geological and natural history survey of Canada; Annual Report, Report B., 99 - 107.

Eyles, N. and Eyles, C.H. (1992) Glacial depositional systems. In: Facies Models, response to sea level change; edited by Walker, R.G. and James, N.P., Geological Association of Canada, chapter 5, 73 - 100.

Fairbanks, R.G. (1989) A 17,000 year glacio eustatic sea level record: influence of glacial melting rates on the Younger Dryas event and deep-ocean circulation; Nature, vol. 342, 637 - 642.

Fleisher, P., Orsi, T.H., Richardson, M.D. and Anderson, A.L. (2001) Distribution of free gas in marine sediments: a global overview; Geo-Marine Letters, vol. 21, 103 - 122.

Fluck, P. (2003) Contributions to the geodynamics of Western Canada; Doctoral Thesis, University of Victoria, Victoria, BC.

Friedrich, M., Kromer, B., Spurk, M., Hofmann, J. and Kaiser, K.F. (1999) Paleo-environment and radiocarbon calibration as derived from Late Glacial/Early Holocene tree-ring chronologies; Quaternary International, vol. 61, 27 - 39.

Galloway, J.M., Patterson, R.T., Doherty, C.T. and Roe, H.M. (2007) Multi-proxy eidence of postglacial climate and environmental change at Two Frog Lake, central mainland coast of British Columbia, Canada; Journal of Paleolimnology, vol. 38, 569 - 588.

Hebda, R.J. (1983) Late-glacial and postglacial vegetation history at Bear Cove Bog, northeast Vancouver Island, British Columbia; Canadian Journal of Botany, vol. 61, 3172 - 3192.

Hetherington, R. and Reid, R.G. (2003) Malacological insights into the marine ecology and changing climate of the late Pleistocene-early Holocene Queen Charlotte Islands archipelgo, western Canada and implications for early humans; Canadian Journal of Zoology, vol. 81, 626 - 661.

Hetherington, R., Barrie, J.V., Reid, R.G.B., MacLeod, R., Smith, D.J., James, T.S. and Kung,

R., (2003) Late Pleistocene coastal paleogeography of the Queen Charlotte Islands, British Columbia, Canada, and its implications for terrestrial biogeography and early postglacial human occupation; Canadian Journal of Earth Sciences, vol. 40, 1755 - 1766.

Hetherington, R. and Barrie, J.V. (2004) Interaction between local tectonics and glacial unloading on the Pacific margin of Canada; Quaternary International, vol. 120, 65 - 77.

Hetherington, R., Barrie, J.V., Reid, R.G.B., Macleod, R. and Smith, D.J. (2004) Paleogeography, glacially induced crustal displacement, and late Quaternary coastlines on the continental shelf of British Columbia, Canada; Quaternary Science Reviews, vol. 23, 295 - 318.

Holland, S.S. (1964) Landforms of British Columbia - a physiographic outline; Bulletin of the British Columbia Department of Mines and Petroleum Resources, No. 48, 138p.

Howes, D.E. (1981a) Terrain inventory and geological hazards: northern Vancouver Island; Province of British Columbia Ministry of Environment, Assessment and Planning Division, APD Bulletin 5, 105p.

Howes, D.E. (1981b) Late Quaternary sediments and geomorphic history of north-central Vancouver Island; Canadian Journal of Earth Sciences, vol. 18, 1 - 12.

Howes, D.E. (1997) Quaternary geology of Brooks Peninsula; In: Brooks Peninsula: An ice age refugium on Vancouver Island, edited by, Hebda, R.J., Haggarty, J.C., Heaton, T.H., Talbot, S.L. and Shields, G.F., British Columbia Ministry of Environment, Lands and Parks, Occasional Paper 5, Chapter 3, 1 - 19.

Hutchinson, I., James, T.S., Reimer, P.J., Bornhold, B.D. and Clague, J.J. (2004) Marine and limnic radiocarbon reservoir corrections for studies of late- and postglacial environments in Georgia Basin and Puget Lowland, British Columbia, Canada and Washington, USA; Quaternary Research, vol. 61, 193 - 203.

Intergovernmental Panel on Climate Change (IPCC) 4th assessment report (2007): Working group one, The Physical Science Basis; Cambridge University Press, Chapters 5 and 10.

Jones, D.L. and Silberling, N.J. (1977) Wrangellia a displaced terrane in northwestern North America; Canadian Journal of Earth Sciences, vol. 14, 2565 - 2577.

Josenhans, H.W., Fedje, D.W., Conway, K.W. and Barrie, J.V. (1995) Post glacial sea-levels on western Canadian continental shelf: Evidence for rapid change, extensive subaerial exposure, and early habitation; Marine Geology, vol. 125, 73 - 94.

Judd, A.G. and Hovland, M. (1992) The evidence of shallow gas in marine sediments; Continental Shelf Research, vol. 12, 1081 - 1095.

Kane, I.A., McCaffery, W.D. and Peakall, J. (2008) Controls on sinuosity evolution within submarine channels; Geology, vol. 36, 287 - 290.

Keary, P. and Brooks, M. (1991) Elements of Seismic Surveying; In: An introduction to geophysical exploration; Blackwell Science, chapter 3, 21 - 43.

Lambeck, K. and Chappell, J. (2001) Sea level change through the last glacial cycle; Science, vol. 292, 679 - 686.

Lee, H.J., Locat, J., Desgagnes, P., Parsons, J.D., McAdoo, B.G., Orange, D.L., Puig, P., Wong, F.L., Dartnell, P. and Boulanger, E. (2007) Submarine mass movements on continental margins; In: Continental Margin Sedimentation, edited by Nittrouer, C.A., Austin, J.A., Field, M.E., Kravitz, J.H., Syvitski, J.P.M. and Wiberg, P.L., Special Publication of the International Association of Sedimentologists, no 37, 213 - 274.

Lewis, T.J., Bentkowski, W.H. and Wright, J.A. (1991) Thermal state of the Queen Charlotte Basin, British Columbia: Warm; In: Evolution and Hydrocarbon Potential of the Queen Charlotte Basin, British Columbia, edited by Woodsworth, G.J., Geological Survey of Canada, Paper 90 -10, pages 489 - 506.

Libby, W.F. (1946) Atmospheric helium three and radiocarbon from cosmic radiation; Physical Review, vol. 69, 671 - 672.

Ludwin, R.S., Dennis, R., Carver, D., McMillan, A.D., Losey, R., Clague, J., Jonientz-Trisler, C., Bowechop, J., Wray, J. and James, K. (2005) Dating the 1700 Cascadia Earthquake: Great coastal earthquakes in native stories; Seismological Research Letters, vol. 76, 140 - 148.

Luternauer, J.L. and Murray, J.W. (1983) Late Quaternary Morphologic development and sedimentation, Central British Columbia Continental Shelf, Geological Survey of Canada, paper 83 -21, 1 - 38.

Luternauer, J.L., Clague, J.J., Conway, K.W., Barrie, J.V., Blaise, B. and Mathewes, R.W. (1989a) Later Pleistocene terrestrial deposited on the continental shelf of western Canada : Evidence for rapid sea-level change at the end of the last glaciation; Geology, vol. 17, 357 - 360.

Luternauer, J.L., Conway, K.W., Clague, J.J. and Blaise, B. (1989b) Late Quaternary geology and geochronology of the central continental shelf of western Canada; Marine Geology, vol. 89, 57 - 68.

Mathews, W.H., Fyles, J.G. and Nasmith, H.W. (1970) Postglacial crustal movements in southwestern British Columbia and adjacent Washington state; Canadian Journal of Earth Sciences; vol. 7, 690 - 702.

Mazzotti, S. and Adams, J. (2004) Near-term probabilities of a great earthquake on the Cascadia subduction zone; Bulletin of seismic society of America, vol. 94, 1954 -1959.

McKeown, D.L. (1975) Evaluation of the Huntec (‘70) hydrosonde deep tow seismic system; Bedford Institute of Oceanography Report Series, BI-R-74-4, 115p.

McLaren, D. (2008) Sea level change and archaeological locations on Dundas Island archipelago of north coastal British Columbia; Doctoral thesis, University of Victoria, Victoria, BC.

Mosher, D.C. and Hewitt, A.T. (2004) Later Quaternary deglaciation and sea-level history of eastern Juan de Fuca Strait, Cascadia; Quaternary International, vol. 121, 23 - 39.

Mosher, D.C. and Simpkin, P.G. (1999) Status and trends on marine high-resolution seismic reflection profiling: data acquisition; Geoscience Canada, vol. 25, 174 - 188.

Parson, J.D., Friedrich, C.T., Traykovski, P.A., Mohrig, D., Imran, J., Syvitski, J.P.M., Parker, G., Puig, P., Buttles, J.L. and Garcia, M.H. (2007) The mechanics of marine sediment gravity flows; In: Continental Margin Sedimentation, edited by Nittrouer, C.A., Austin, J.A., Field, M.E., Kravitz, J.H., Syvitski, J.P.M. and Wiberg, P.L., Special Publication of the International Association of Sedimentologists, no. 37, 275 - 337.

Ren, P., Bornhold, B.D. and Prior, D.B. (1996) Seafloor morphology and sedimentary processes, Knight Inlet, British Columbia; Sedimentary Geology, vol. 103, 201 - 228.

Roberts, M.C. and Rood, K.M. (1984) The role of the ice contributing area in the morphology of transverse fjords, British Columbia; Geografiska Annaler, Series A, Physical Geography, vol. 66, 381 - 394.

Robinson, S.W. and Thompson, G. (1981) Radiocarbon correction for marine shell dates with application to Southern Pacific Northwest Coast prehistory; Syesis, vol. 14, 45 - 57.

Rohr, K.M. and Currie, L. (1997) Queen Charlotte Basin and Coast Mountains: Paired belts of subsidence and uplift caused by a low-angle normal fault; Geology, vol. 25, 819 - 822.

Rushmer, E.L. (2006) Sedimentological and geomorphological impacts of the Jökulhlaup (Glacial Outburst Flood) in January 2002 at Kverkfjöll, Northern Iceland; Geografiska Annaler : Series A, physical geography; vol. 88, 43 - 53.

Ryder, J.M., Fulton, R.J. and Clague, J.J. (1991) The Cordilleran Ice Sheet and the glacial geomorphology of southern and central British Columbia; Geographie physique et Quaternaire; vol. 45, 365 - 377.

Shaw, J. (2008) Application of multibeam bathymetry to geological mapping; Proceedings of the Canadian hydrographic conference and national surveyors conference, Paper 8-3, 17p.

Shipp, R.C., Belknap, D.F. and Kelly, J.T. (1991) Seismic-stratigraphic and geomorphic evidence for a post-glacial sea-level low stand in northern Gulf of Maine; Journal of Coastal Research, vol. 7, 341 - 364.

Shuster, D.L., Ehlers, T.A., Rusmore, M.E. and Farley, K.A. (2005) Rapid glacial erosion at 1.8 Ma revealed by 4He/3He thermochronometry; Science, vol. 310, 1668 - 1670.

Souther, J.G., Armstrong, R.L. and Harakal, J. (1984) Chronology of the peralkaline, late Cenozonic Mount Ediza complex, northern British Columbia, Canada; Geological Society of America, Bulletin, vol. 95, 337 - 349.

Stanley, D.J. (1995) A global sea-level curve for the late Quaternary: the impossible dream? Marine Geology, vol. 125, 1 - 6.

Stevens, A., Clague, J.J. Bobrowsky, P.T. and Patterson, R.T. (1997) Late Holocene sedimentation in Saanich Inlet, British Columbia, and its paleoseismic implications; Canadian Journal of Earth Sciences, vol. 34, 1345 - 1357.

Stocker, T.F. and Wright, D.G. (1996) Rapid changes in ocean circulation and atmospheric radiocarbon; Paleoceanography, vol. 11, 773 - 795.

Stoker, M.S., Phesant, J.B. and Josenhans, H. (1997) Seismic methods and interpretation; In: Glaciated continental margins: an atlas of acoustic images, edited by Davies, T.A., Bell, T., Cooper, A.K., Josenhans, H., Polyak, L., Solheim, A., Stoker, A.S. and Stravers, J.A., part one, 9 - 26.

Stuiver, M., Quay, P.D. (1980) Changes in atmospheric carbon-14 attributed to a variable Sun; Science, vol. 207, 11 - 19.

Stuiver, M., Pearson, G.W. and Braziunas, T.F. (1986) Radiocarbon age calibration of marine samples back to 9,000 Cal B.P.; Radiocarbon, vol. 28, 980 - 1021.

Stumpf, A.J., Broster, B.E., and Levson, V.M. (2000) Multiphase flow of the late Wisconsinan Cordilleran ice sheet in western Canada; Geological society of America Bulletin, vol. 112,1850 - 1863.

Syvitski, J.P. (1991) Sediment deposition on glaciated continental margins; Continental Shelf Research, vol. 11, 897 - 937.

Thomas, R.H. and Bentley, C.R. (1978) A model for Holocene retreat of the West Antarctic ice sheet; Quaternary Research, vol. 10, 150 - 170.

Thomson, R.E., Bornhold, B.D. and Mazzotti, S. (2008) An examination of the factors affecting relative and absolute sea level in coastal British Columbia; Canadian Technical Report of Hydrography and Ocean Sciences 260, Fisheries and Oceans Canada, 49p.

Thomson, R.E. (1981) Oceanography of the British Columbia coast; Canadian Special Publication of Fisheries and Aquatic Sciences 56, 291p.

Thorsnes, T., Erikstad, L., Dolan, M.F.J. and Bellec, V.K. (2009) Submarine landscapes along the Lofoten-Vesterålen-Senja margin, northern Norway; Norwegian Journal of Geology; vol. 89, 5 - 16.

Triton Consultants Ltd. (2002) Green energy study for British Columbia, Tidal current Energy; BC Hydro Engineering, 69p.

Turcott, D.L. and Schubert, G. (1982) Geodynamics; John Wiley and Sons, New York.

Vail, P.R., Mitchum, R.M., and Thompson, S. (1977) Seismic stratigraphy and global changes of sea level, Part 3: Relative changes of sea level from coastal onlap; in Seismic stratigraphy: Applications to hydrocarbon exploration, edited by Payton, C.E., American Association of Petroleum Geologists memoir 7, 63 - 81.

Vorren, T.O. (2003) Subaquatic landsystems: Continental margins; In: Glacial Landsystems, edited by Evans, D.J.A., Oxform University Press, New York, 289 - 312.

Waitt, R.B. (1980) About forty last-glacial lake Missoula Jökulhlaups through Southern Washington; The Journal of Geology, Vol. 88, 653 - 679.

Walker, R.G. (1992) Turbidites and submarine fans; In: Facies Models: Response to Sea Level Change, edited by Walker, R.G. and James, N.P., Geological Association of Canada, 239 - 263.

Wentworth, C.K. (1922) A scale of grade and class terms for clastic sediments; Journal of Geology, vol. 30, 377 - 392.

Appendix

Piston Core 2009003-008

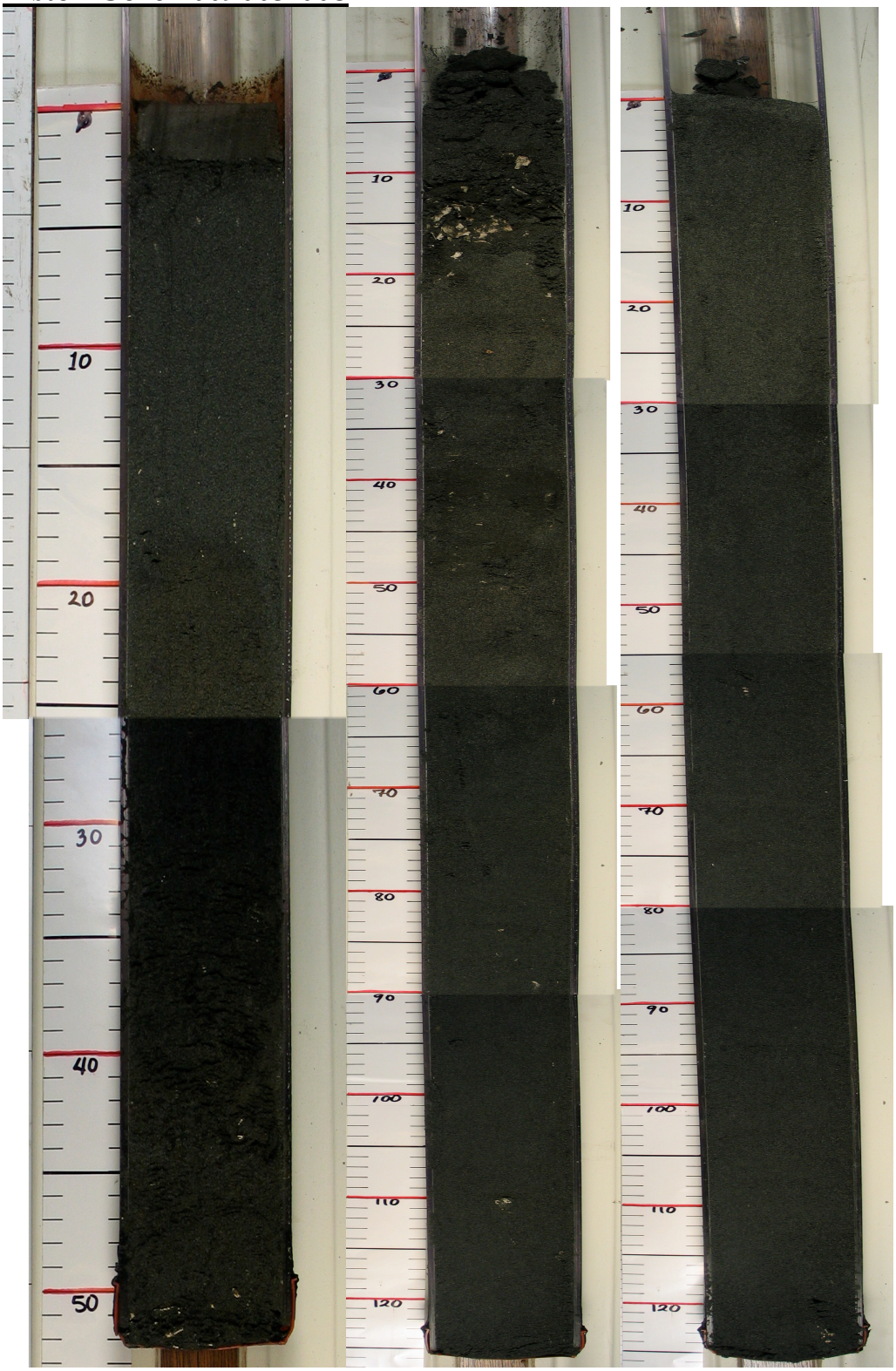

Core PGC2007007-004

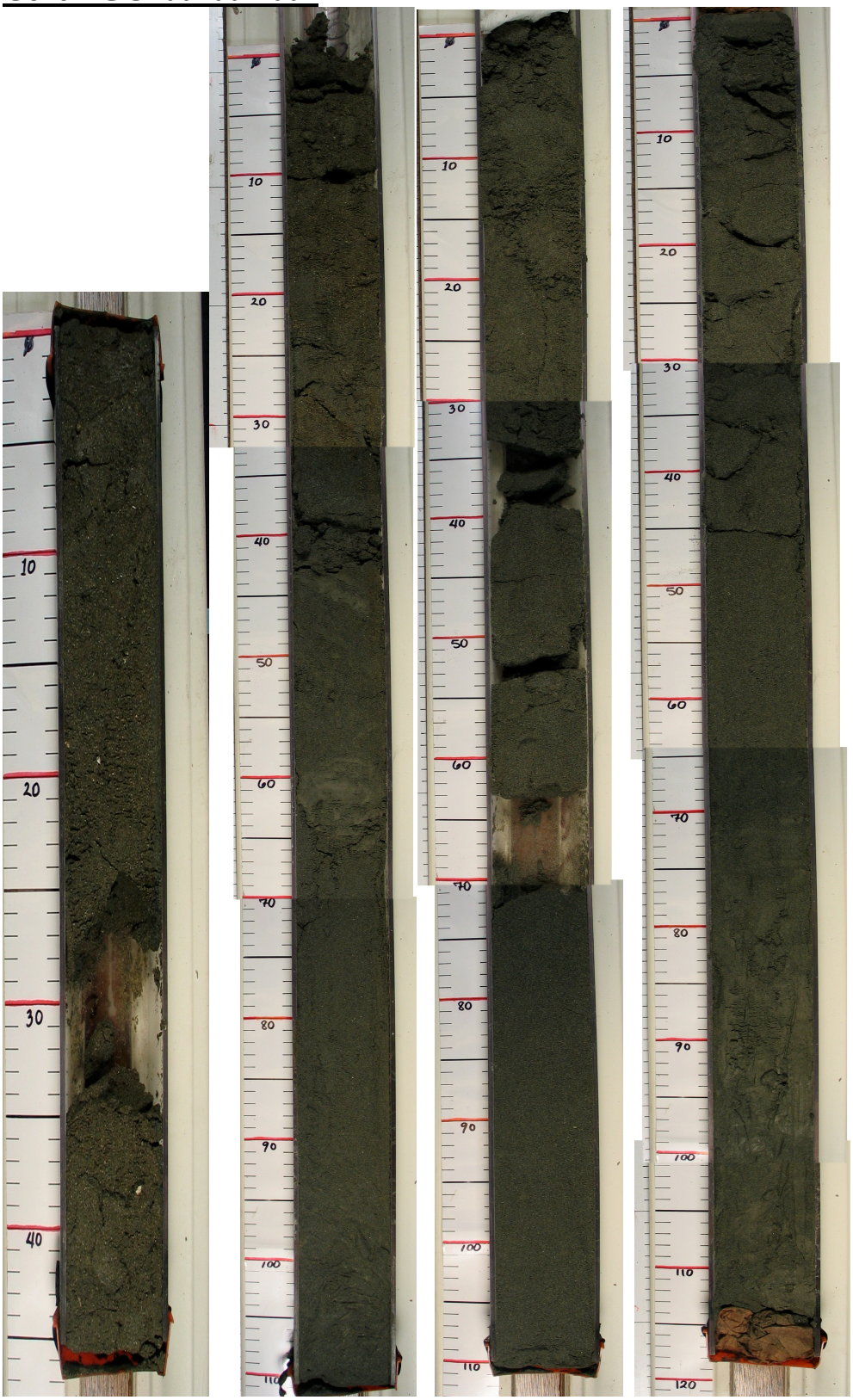

PGC2007007-005 piston core (left) - pilot gravity core (right).